

REPORT DOCUMENTATION PAGE			Form Approved OMB No. 0704-0188
<p>Public reporting burden for this collection of information is estimated to average 1 hour per response, including the time for reviewing instructions, searching existing data sources, gathering and maintaining the data needed, and completing and reviewing the collection of information. Send comments regarding this burden estimate or any other aspect of this collection of information, including suggestions for reducing this burden, to Washington Headquarters Services, Directorate for Information Operations and Reports, 1215 Jefferson Davis Highway, Suite 1204, Arlington, VA 22202-4302, and to the Office of Management and Budget, Paperwork Reduction Project (0704-0188), Washington, DC 20503.</p>			
1. AGENCY USE ONLY (Leave blank)	2. REPORT DATE 15 Dec 1994	3. REPORT TYPE AND DATES COVERED Final Report, December 1994	
4. TITLE AND SUBTITLE  Optimization of Filter and Electronics Prototypes for Respiratory Protection System (RESPO) 21		5. FUNDING NUMBERS  C - DAAA15-91-D-0002 Task 69	
6. AUTHOR(S)  Hofacre, K.C., Markham, R.L., Kimes, K.L.			
7. PERFORMING ORGANIZATION NAME(S) AND ADDRESS(ES)  Battelle Memorial Institute 505 King Avenue Columbus, OH 43201		8. PERFORMING ORGANIZATION REPORT NUMBER	
9. SPONSORING / MONITORING AGENCY NAME(S) AND ADDRESS(ES)  U.S. Army Chemical and Biological Defense Command Edgewood Area Aberdeen Proving Ground, MD 21010-5423		10. SPONSORING / MONITORING AGENCY REPORT NUMBER	
11. SUPPLEMENTARY NOTES  <b>19950403 171</b>			
12a. DISTRIBUTION / AVAILABILITY STATEMENT  Available for public release; Distribution Unlimited.		12b. DISTRIBUTION CODE	
13. ABSTRACT (Maximum 200 words)  The work reported is part of an overall effort to develop respiratory protection for the 21st century (RESPO 21). Two elements of the RESPO 21 project were investigated in this task: respirator filter development and blower and communication, electronic system development. The purpose of the filter task was to conceive, design, fabricate and optimize a filter element design concept. Filter development required continued evaluation of candidate media and to use these results to aid the filter design. The goal was to implement media that will result in a flexible filter element, unlike the current rigid metal canisters. The purpose of the electronics tasks was to design, miniaturize, and optimize the performance blower and communication systems for use with RESPO 21.			
14. SUBJECT TERMS RESPO 21, RESPIRATOR FILTER, COMMUNICATION SYSTEM BLOWER UNIT, INDIVIDUAL PROTECTION			15. NUMBER OF PAGES 136
			16. PRICE CODE
17. SECURITY CLASSIFICATION OF REPORT Unclassified	18. SECURITY CLASSIFICATION OF THIS PAGE Unclassified	19. SECURITY CLASSIFICATION OF ABSTRACT Unclassified	20. LIMITATION OF ABSTRACT SAR

# REPORT

---

FINAL REPORT

---

---

**OPTIMIZATION OF FILTER**

---

**AND ELECTRONICS**

---

**PROTOTYPES FOR**

---

**RESPIRATORY PROTECTION**

---

**SYSTEM (RESPO) 21**

---

To

---

**U.S. ARMY/ERDEC**

---

December 15, 1994

---

DISTRIBUTION STATEMENT A

Approved for public release;  
Distribution Unlimited



... Putting Technology To Work

# **DISCLAIMER NOTICE**



**THIS DOCUMENT IS BEST  
QUALITY AVAILABLE. THE  
COPY FURNISHED TO DTIC  
CONTAINED A SIGNIFICANT  
NUMBER OF PAGES WHICH DO  
NOT REPRODUCE LEGIBLY.**

## **FINAL REPORT**

**on**

### **OPTIMIZATION OF FILTER AND ELECTRONICS PROTOTYPES FOR RESPIRATORY PROTECTION SYSTEM (RESPO) 21**

**Task 69  
Contract No. DAAA15-91-D-0002**

**U.S. ARMY  
Chemical and Biological Defense Command**

**December 1994**

**by**

**K. C. Hofacre, R. L. Markham, and  
K. L. Kimes**

Accession For	
NTIS	CRA&I <input checked="" type="checkbox"/>
DTIC	TAB <input type="checkbox"/>
Unannounced <input type="checkbox"/>	
Justification _____	
By _____	
Distribution / _____	
Availability Codes	
Dist	Avail and / or Special
A-1	

**BATTELLE  
505 King Avenue  
Columbus, Ohio 43201-2396**

## EXECUTIVE SUMMARY

The work reported is part of an overall effort to develop respiratory protection for the 21st century (RESPO 21). Two elements of the RESPO 21 project were investigated in this task: respirator filter development and blower and communication electronic system development. The purpose of the filter task was to conceive, design, fabricate, and optimize a filter element design concept. Filter development required continued evaluation of candidate media and to use these results to aid the filter design. The goal was to implement media that will result in a flexible filter element, unlike the current rigid metal canisters. The purpose of the electronics tasks was to design, miniaturize, and optimize the performance of blower and communication systems for use with RESPO 21.

Samples of candidate media were evaluated to assess the feasibility of using these media in a filter and if feasible use the results to design and optimize a filter element. Tests were conducted for the following: airflow resistance, 0.3  $\mu\text{m}$  aerosol filtration efficiency, and for carbon media, the sorptive capacity of dimethyl methylphosphonate (DMMP) vapor or cyanogen chloride (CK). The design criteria for the filter element required that (1) the airflow resistance not exceed 25 mm H<sub>2</sub>O at 85 lpm, (2) the aerosol filtration efficiency exceed 99.99 percent for 0.3  $\mu\text{m}$  particles at 32 lpm, (3) the DMMP gas life exceed 110 min when it was challenged with 3000 mg/m<sup>3</sup> of DMMP vapor at 32 lpm, and (4) the CK gas life exceed 30 min when challenged with 4000 mg/m<sup>3</sup> under simulated breathing conditions corresponding to 25 lpm. These performance tests were also conducted on filter elements to assess their performance relative to the design specifications.

Based upon performance results of the above tests, a two-sided, 0.85 in.-thick demonstrator filter element with outer dimensions of 4.5 x 6.5 in. and available filter media dimensions of 3.75 x 5.25 in. was fabricated with the following media:

- 1 layer electrostatic filtration media
- 4 layers carbon loaded fabric
- 1 layer electrostatic filtration media
- 1 layer spacer material
- 1 layer electrostatic filtration media
- 4 layers carbon loaded fabric
- 1 layer electrostatic filtration media

These media were integrated with an airflow transition piece (AFTP) in an encapsulation molding process to seal the media into a filter element. The AFTP is a novel design whereby the air that enters both sides of the filter into the center of the filter can be transported through a manifold into air ducts that lead to the mask. This AFTP also served as the filter frame and aided the filter production process. Molds were designed to fabricate both the AFTP and the filter element. A search and evaluation was conducted to identify polymeric materials to fabricate the AFTP and the edge sealant for encapsulation molding. Materials were selected based upon their softness, flexibility, adhesion properties and curing properties required by the filter element design.

Ninety demonstrator filter elements were fabricated, and their performance was evaluated for comparison against the design criteria. The demonstrator filter elements were not fully capable of meeting the design requirements. The airflow resistance of 25 mmH<sub>2</sub>O at 85 lpm was achieved, but the 0.3 μm aerosol penetration averaged 0.44 percent; the CK gas life averaged 22 min; and the DMMP gas life averaged 79 min. Additional demonstrator filters were fabricated with five and six layers of carbon material. The aerosol penetration was still higher than specifications, but DMMP and CK gas life was adequate. The additional layers of material increased the airflow resistance to 30 and 32 mmH<sub>2</sub>O for five and six layer carbon filters, respectively.

The demonstrator filter elements show that the design concept is viable and promising for the RESPO 21 filter element. The filter design has been optimized within the size constraints and for the filtration media available. However, for the filter to achieve the design performance specifications, improvements in the media performance are needed or additional area must be made available.

Brassboard demonstration systems of communication and blower systems were further developed as part of this task. The development effort focused on enhancements and refinements of the system to miniaturize components, improve efficiency of power consumption, and improve performance.

The communications systems were to achieve an 85 percent voice transmission, operate for over 12 hr at room temperature with a lithium battery power source occupy less than 6.5 in.<sup>3</sup>, and weigh less than 225 g.

The enhancements to the final design were not quite sufficient to meet all of the design criteria. Qualitative voice transmission tests were performed by Battelle before units were sent to ERDEC for quantitative testing. Good voice transmission was achieved. An evaluation of the power requirements of the communication system indicate that the unit should be capable of operating for >20 hr at room temperature when powered by a lithium battery. The communication unit has a volume of 8.5 in.<sup>3</sup> and a weight of ~150 g. Most of the feedback noise was eliminated and the units performed well at low and high volume settings. The units were designs to interface with other RESPO 21 mask concepts that were being produced. This involved the design and fabrication of custom connectors for adaption to the mask in a collaborative effort with ERDEC.

The blower systems were to be capable of delivering 2 cfm of airflow against 30 mmH<sub>2</sub>O pressure head, operate for 12 hr at room temperature with a lithium battery power source, occupy less than 6.5 in.<sup>3</sup>, and weigh less than 225 g.

The enhancements to the blower system design were not quite adequate to achieve the design requirements. The blower is capable of delivering 2 cfm against 30 mmH<sub>2</sub>O pressure head, per manufacturing specifications. When operated against no pressure head, the battery life was sufficient (at room temperature). The volume of the blower unit (blower control circuitry, not the blower itself) was 8.5 in.<sup>3</sup> and weighed ~190 g. Four power

settings are available: off, low, medium, and high so the user can select the level of assisted breathing that is desired. The unit is also equipped with a low battery power indicator.

Although the final designs for both the communications and blower subsystems did not achieve the desired design requirements, significant enhancements to the size and operating performance were made. Improvements could be made to reduce noise in the communications units by reevaluating the circuit design. The primary improvement that could be made with the blower system is with packaging. Refinement of the enclosures could improve durability and water resistance of the unit.

## TABLE OF CONTENTS

	<u>Page</u>
I. INTRODUCTION . . . . .	1
1.1 Background . . . . .	1
1.1.1 Filter . . . . .	1
1.1.2 Electronics . . . . .	2
1.2 Objective . . . . .	2
1.2.1 Filter . . . . .	2
1.2.2 Electronics . . . . .	3
1.3 Scope . . . . .	3
2.0 DESIGN CRITERIA . . . . .	4
2.1 Filter Element . . . . .	4
3.0 TECHNICAL APPROACH . . . . .	7
3.1 Filter Design and Fabrication . . . . .	7
3.1.1 Edge Sealant Evaluation . . . . .	8
3.1.2 Airflow Transition Piece (Filter Frame) . . . . .	10
3.1.3 Encapsulation . . . . .	11
3.2 Filtration Media Assessment . . . . .	11
3.2.1 Airflow Resistance . . . . .	11
3.2.2 Aerosol Filtration Efficiency . . . . .	12
3.2.3 DMMP Gas Life Testing . . . . .	13
3.2.4 Cyanogen Chloride Gas Life Testing . . . . .	14
4.0 FILTRATION MEDIA PERFORMANCE . . . . .	15
4.1 Airflow Resistance . . . . .	15
4.2 Aerosol Filtration Efficiency . . . . .	18
4.3 DMMP Gas Life . . . . .	19
4.4 CK Gas Life . . . . .	21
5.0 FILTER DESIGN . . . . .	24
5.1 Edge Sealing . . . . .	24
5.1.1 Required Characteristics . . . . .	24
5.1.2 Materials Selection . . . . .	25
5.2 Airflow Transition Piece . . . . .	27
5.2.1 Design Concepts . . . . .	27
5.2.2 Mold Design . . . . .	28
5.2.3 Performance Assessment . . . . .	30

**TABLE OF CONTENTS**  
**(Continued)**

	Page
5.3 Encapsulation . . . . .	31
5.3.1 Design Concepts . . . . .	31
5.3.2 Mold Design . . . . .	33
5.4 Mock-up of Filter Elements . . . . .	35
5.4.1 Filter Design Concept Definition . . . . .	35
5.4.2 Concept Validation . . . . .	35
6.0 MODEL FILTER ELEMENTS . . . . .	36
6.1 AFTP Fabrication . . . . .	36
6.2 Filter Fabrication . . . . .	38
6.3 Performance Evaluation . . . . .	43
6.3.1 Airflow Resistance . . . . .	48
6.3.2 DMMP Gas Life . . . . .	49
6.3.3 CK Gas Life . . . . .	50
6.3.4 Aerosol Filtration Efficiency . . . . .	51
6.3.5 Thickness . . . . .	52
6.4 Qualitative Assessment . . . . .	52
6.5 Optimization . . . . .	53
6.5.1 Improvements . . . . .	53
6.5.2 Area Effect . . . . .	54
7.0 ELECTRONIC SYSTEMS . . . . .	58
7.1 Communications Assist Subsystem Refinements . . . . .	58
7.1.1 Feedback Elimination . . . . .	58
7.1.2 VOX Circuit . . . . .	60
7.1.3 Noise Filtering . . . . .	60
7.1.4 Volume Adjust . . . . .	62
7.1.5 Communications Output Compatibility . . . . .	63
7.1.6 Microphone Compatibility . . . . .	63
7.1.7 Component Selection Analysis . . . . .	64
7.1.8 Circuit Miniaturization . . . . .	65
7.1.9 Performance Characteristics . . . . .	66
7.2 Miniature Blower Subsystem Refinements . . . . .	68
7.2.1 Blower/Airflow Study . . . . .	68
7.2.2 Improved Blower Drive Circuit . . . . .	69
7.2.3 Component Selection Analysis . . . . .	70
7.2.4 Circuit Miniaturization . . . . .	71
7.2.5 Performance Characteristics . . . . .	71

**TABLE OF CONTENTS**  
**(Continued)**

	<u>Page</u>
7.3 Power Source Subsystem Refinements . . . . .	75
7.3.1 Battery Study . . . . .	75
7.3.2 Mission Power Considerations . . . . .	76
7.3.3 Power Source Testing . . . . .	77
7.4 Integration and Fabrication of Prototype System . . . . .	78
7.4.1 Custom Packaging Considerations and Design . . . . .	78
7.4.2 Package Evaluation and Testing . . . . .	81
7.4.3 Subsystem and System Integration . . . . .	81
7.5 Production of Prototype Units . . . . .	82
7.6 Evaluation and Testing of Prototype System . . . . .	84
7.6.1 Communications Subsystem . . . . .	87
7.6.2 Miniature Blower Subsystem . . . . .	88
8.0 CONCLUSIONS AND RECOMMENDATIONS . . . . .	89
8.1 Filter Elements . . . . .	89
8.2 Electronic Systems . . . . .	90
9.0 REFERENCES . . . . .	91
 APPENDICES	
A. FILTER DESIGN CONCEPT GENERATION . . . . .	A-1
B. MATERIAL SUPPLIERS . . . . .	B-1
C. ENGINEERING DRAWINGS OF FILTER PARTS AND MOLDS . . . . .	C-1
D. FILTER FABRICATION PROCEDURES . . . . .	D-1
E. MECHANICAL DRAWINGS, ELECTRONIC SCHEMATICS, AND PERFORMANCE DATA OF ELECTRONIC SUBSYSTEMS . . . . .	E-1

## LIST OF TABLES

	<u>Page</u>
Table 1. RESPO 21 Design Criteria for Filter Elements . . . . .	4
Table 2. RESPO 21 Design Criteria for Communications Subsystems . . . . .	5
Table 3. RESPO 21 Design Criteria for Miniature Blower Subsystem . . . . .	6
Table 4. Airflow Resistance Correlation and Comparison to Design Specification . . . . .	15
Table 5. Percent Penetration of 0.3 $\mu\text{m}$ PSL Through 13.2 $\text{cm}^2$ of Media at a Flow Rate of 1.5 lpm . . . . .	18
Table 6. DMMP Gas Life and DMMP Sorptive Capacity of Carbon Media . . . . .	20
Table 7. CK Gas Life and Sorption Capacity of Carbon Media . . . . .	22
Table 8. Definition of Filter Concept . . . . .	41
Table 9. Performance Results of the Model Filter Elements . . . . .	44
Table 10. Summary Statistics of the Airflow Resistance of Demonstrator Filter Elements . . . . .	49
Table 11. Summary Statistics of the DMMP Gas Life of Demonstrator Filter Elements . . . . .	50
Table 12. Summary Statistics of the CK Gas Life of Demonstrator Filter Elements . . . . .	50
Table 13. Summary Statistics of Aerosol Penetration of Demonstrator Filter Elements . . . . .	52
Table 16. Battery Life at Room Temperature as a Function of Continuous Operating Time in a V461LS Blower . . . . .	79
Table 17. Weight of Communications and Blower Subsystems . . . . .	86

## LIST OF FIGURES

	<u>Page</u>
Figure 1. Correlation of Airflow Resistance vs AirFlow Rate for Various Filtration Media .....	16
Figure 2. Schematic of an AFTP .....	29
Figure 3. Photograph of the Encapsulation Mold with AFTP for Producing Filter Elements .....	34
Figure 4. Photograph of a Representative AFTP .....	37
Figure 5. Photograph of a Representative Filter Element .....	39
Figure 6. Cross-Sectional Diagram of Filter Element .....	40
Figure 7. Photograph of Communications (left) and Blower Controller Systems .....	85

## I. INTRODUCTION

### 1.1 Background

The Edgewood Research, Development and Engineering Center (ERDEC) is entering development of the next generation of respiratory protection, Respiratory Protection System 21 (RESPO 21). RESPO 21 is intended to replace the current M40 series mask and is being designed to maintain protection, reduce mission degradation, and improve compatibility with current and future equipment.

Concept studies have been completed for all RESPO 21 component systems. The task reported here documents the efforts to support model development of the respirator filter and electronics (communication system and blower unit) concepts. The resulting demonstrator units will then be used in an advanced technology demonstration.

#### 1.1.1 Filter

Current filter elements for the M40 series of respirators are housed in rigid, metal canisters that contain media for aerosol filtration and adsorption of gases or vapors. The aerosol filtration media are often pleated for increased surface area. Certain harmful gases are removed by adsorption to activated carbon that has been treated with hexavalent chromium or zinc metal cations. These cations provide active sites to chemisorb certain poison gases. The carbon is generally present as a coarse granular bed, but can also be present in a fine granular form incorporated in a fabric, as in C-18 core material of the M13A2 filter element.

The goal of the new filter design will reduce breathing resistance and the bulk of the current filtration system, yet maintain or improve its filtration performance. The new design is also intended to be flexible and will therefore incorporate pliable particulate aerosol filtration and gas adsorption media with a safe, flexible edge seal.

The work reported in this "Filter System" volume is a continuation of previous efforts to identify and evaluate potentially useful materials to develop demonstrator filter elements for RESPO 21.<sup>(1,2)</sup> This report describes the activities performed to (1) select

materials for edge sealing, (2) assess filtration media performance, and (3) fabricate and evaluate demonstrator filter elements.

### **1.1.2 Electronics**

As part of the system concept for a multi-layer protective mask, electronic subsystems are being developed to support the blower assist, communication, and control unit features of the design. Battelle has played a major role in several phases of this development effort. Early concept studies were performed by Battelle to assess various methods for the control unit and communication functions. Battelle was responsible for the development of a brassboard demonstration system which included a multi-layer mask, communications assist, blower assist, power and control subsystems. An effort was needed to further develop and enhance the brassboard systems.

## **1.2 Objective**

The overall objective of this task was to optimize the size and performance of the RESPO 21 filter and electronics concept models. Once optimized, demonstrators of the concepts were to be fabricated to support an advanced technology field demonstration for the RESPO 21 development program.

### **1.2.1 Filter**

The overall objective of this effort was to optimize the size and performance of the respirator filter model to be used in RESPO 21. Specifically, the objective of this effort was to evaluate aerosol filtration and gas adsorption media and to identify an edge sealing and airflow transition approach for use in a filter. From these evaluations, filter design concepts were formulated and demonstrator filters representative of a selected concept were fabricated and assessed for their ability to meet a set of design criteria.

### **1.2.2 Electronics**

The objective of this effort was to develop and implement design enhancements to the early versions of brassboard electronic systems. Once an improved system design was achieved, this effort also led to the development of prototype units for delivery to ERDEC.

### **1.3 Scope**

This report describes the work performed to design, optimize, and fabricate models of the concepts for RESPO 21 filter elements and electronic components.

## **2.0 DESIGN CRITERIA**

### **2.1 Filter Element**

The RESPO 21 filtration system is intended to provide performance comparable to or exceeding that of the existing rigid, metal housing canisters. Design requirements have been established for the following parameters: (1) airflow resistance, (2) aerosol filtration efficiency, (3) gas life, (4) surface area, and (5) thickness.

The performance criteria for these parameters (established by ERDEC in their Statement of Work for this project) are shown in Table 1.

Table 1. RESPO 21 Design Criteria for Filter Elements

<b>Characteristic</b>	<b>Requirement</b>
DMMP Life	$\geq 330,000$ Ct; 110 min, $3000 \text{ mg/m}^3$ , 32 lpm
CK Life	$\geq 120,000$ Ct; 30 min, $4000 \text{ mg/m}^3$ , 25 lpm intermittent flow
Particulate Filtration	$\leq 0.01\%$ penetration, maximum for $0.3 \mu\text{m}$ diameter particles at 32 lpm
Airflow Resistance	$\leq 25 \text{ mm H}_2\text{O}$ at 85 lpm, desired $\leq 45 \text{ mm H}_2\text{O}$ at 85 lpm, required
Filter Size	Maximum size 4.5 in. x 6.5 in. (11.4 x 16.5 cm)
Surface Area	$\sim 40$ to $50 \text{ in.}^2$ ( $260$ to $320 \text{ cm}^2$ )
Thickness	Minimized, $< 2.5 \text{ cm}$ required

Integration and compatibility with other components of the RESPO 21 system were implicit in the design process. The logistics of implementing a design and human factors considerations were also part of the design process. As a result, the filter was expected to be located near the chest, and the available space for locating the filter was estimated to be approximately 4.5 x 6.5 in. (11.4 x 16.5 cm).<sup>(3)</sup> With this space constraint, the filter required a two-sided design because it provided the most surface area within this space claim.

The process for selecting materials for the filter's edge seal and for assessing the performance of the filtration media that meet the above criteria is presented in Section 3.0.

## **2.2 Electronic Components**

The RESPO 21 electronics system consists of a communications subsystem and a blower subsystem.

The communications subsystem is a voice amplification system that consists of a microphone, amplifier, noise reduction filter, feedback elimination circuit, volume control circuit, power source, low battery warning circuit, output speaker, and field radio and mask interfaces.

The blower subsystem provides airflow inside the mask which reduces breathing resistance for the mask wearer, helps to eliminate internal moisture build-up which can obstruct vision, and provides positive mask pressure for added protection. It consists of a blower, blower control unit, and a power source.

The power source subsystem consists of a battery pack and a low battery indicator circuit. The power source subsystem is required to provide regulated, DC power to the communications and blower control circuits.

The performance goals given for the communications and blower subsystems are given in Tables 2 and 3, respectively.

Table 2. RESPO 21 Design Criteria for Communications Subsystems

Characteristic	Requirement
Performance (voice transmission)	85% voice transmission per the Modified Rhyme Test (with and without blower unit running)
Life	$\geq 12$ hr at room temp with lithium battery source $\geq 6$ hr at -25°F with lithium batteries $\geq 6$ hr at room temp with alkali batteries
Size/Weight	$\leq 6.5$ in <sup>3</sup> and $\leq 225$ g
Special Features	Low voltage indicator, high and low setting

Table 3. RESPO 21 Design Criteria for Miniature Blower Subsystem

Airflow	2 cfm ( $\pm$ 5% at 30 mm H <sub>2</sub> O head pressure
Life	$\geq$ 12 hr at room temp with lithium battery source $\geq$ 6 hr at -25°F with lithium batteries $\geq$ 6 hr at room temp with alkali batteries
Size/Weight	$\leq$ 6.5 in <sup>3</sup> and $\leq$ 225 g
Special Features	Low voltage indicator, high and low setting

## **3.0 TECHNICAL APPROACH**

### **3.1 Filter Design and Fabrication**

The general approach taken to develop a flexible filter was to (1) provide information to select materials and processes for preparing demonstrators for this project and for high-volume production of filters, (2) prepare a mock-up of filter for performance evaluation, (3) fabricate a suitable mold for the demonstrators, and (4) prepare evaluation samples and demonstrator filters.

The search for edge sealants and the preparation of a suitable design proceeded concurrently. Materials were sought through literature searches, discussions with suppliers of suitable materials, and interactive sessions with Battelle staff with relevant knowledge and experience. Samples were obtained of promising candidates and the materials were cured in contact with the selected filter media to determine if the impregnation by and bonding with the sealant was adequate. The cure time and temperature were varied to determine what might be the optimal curing conditions. The aerosol filtration material being considered was an electrostatic medium. Such media are sensitive to heat; therefore, it was necessary to keep its temperature below 150°F so its filtration efficiency would not be jeopardized. This temperature sensitivity became a significant limitation in adjusting the curing cycles of polymers used for the edge seal to shorter times.

Concurrently, a mold for adding the edge seal to the filter stack was designed. This effort required a design of an airflow transition piece to route air from the filter to the mask connection. Several idea generation sessions were held with engineers and polymer scientists, resulting in a number of potentially viable ideas for the transition design.

The molds were designed and fabricated, and the candidate edge sealants were used to prepare filter elements in a final confirmation of the suitability of the material and the transition and mold designs. A procedure was then devised for production of filter elements. This procedure was applied in producing the filters required for delivery to ERDEC.

### 3.1.1 Edge Sealant Evaluation

The filter being designed and developed for RESPO 21 comprises a stack of filtration media on each side of a two-sided filter. To assure that there is no leakage of contaminated air around this stack, it is necessary to seal the edges. Several characteristics are required for this sealant including:

- Adhesion to the filter media
- Low viscosity to assure impregnation of the edges of the filter media to accomplish physical attachment to the media
- Adequate resistance to chemical agent permeation at the thickness selected for the edge seal to prevent contamination through the edge seal
- Softness and flexibility so that the wearer of the filter will not be injured when falling on the filter
- Strength and durability to withstand the service environment
- Producibility, including short molding cycle times and low reject rates in production
- Adhesion to airflow transition piece.

After several material/process combinations were considered, information to select several candidates was gathered from the literature and from consultation with Battelle staff who have experience regarding relevant polymers. Companies that supply appropriate materials were identified, and samples were requested for materials with a relatively low (40 to 60) Shore A hardness (i.e., soft and flexible). Additionally, consideration was given to producibility of edge seals using the materials and designs selected from the beginning of filter development to ensure that the end product can be produced efficiently and cost effectively in the longer term.

The goal was to identify a sealant that could be demolded (cured) after no more than 30 min at a temperature of 150°F or less (because of the temperature sensitivity of the aerosol filtration medium). This limitation was required only for the encapsulation molding that included the filter media. The filter frame (airflow transition piece) could be molded at any temperature since that operation did not include the filter media.

Evaluation of Curing Conditions. Candidates were mixed according to the supplier's recommendations and poured into aluminum containers. Surface tack and time till demolding were monitored at room temperature and at selected temperatures up to 160°F. The shortest time to demolding was determined by both the amount of surface tack and actual demolding of samples.

Evaluation of Adhesion/Impregnation of the Sealant to the Filter Media. Adhesion and/or impregnation of the filter media by the edge sealant was necessary to assure a seal so that contaminated air is forced through the filter media. To test the adhesion between the filter media and the candidates for the sealant, small sections were molded in the full-sized mold from the previous RESPO 21 study.

The sealants were mixed and poured into the mold and cured at the prescribed temperature and time. The samples were examined for state of cure, impregnation of the filter media, and indications of lack of cure in the vicinity of the filter media.

Evaluation of Adhesion of Encapsulating Sealant to Filter Frame Sealant. One of the major concerns with the design approach of sealing material to a filter frame is the need for adhesion between the frame and the edge sealant used for encapsulation molding. This might best be accomplished if the two materials are similar but of different hardness, the transition piece being a stiffer grade. Adhesion tests were conducted using two different hardnesses of one type of material or two different materials.

To evaluate adhesion, one polymer was prepared, vacuum degassed, and cast in a small aluminum cup according to supplier's directions and allowed to cure until it could be demolded, about 30 min. After demolding, the sample was cut in half with scissors and again placed in an aluminum cup.

The second material in the evaluation was then prepared as above and cast against the cured sample of the first material in the cup and allowed to cure until it could be demolded, about 30 min.

If the two pieces could be pulled apart by hand at the interface without much difficulty, it was judged that there was not adequate molecular bonding at the interface of the two materials. If the two materials could not be pulled apart by hand, it was judged that

bonding between the two materials was adequate for use together in the filter frame and encapsulation.

### **3.1.2 Airflow Transition Piece (Filter Frame)**

An important part of the filter design and development was devising a means to transfer the filtered air from the filter to the mask: an airflow transition piece (AFTP). This requires some type of transition that will permit air to flow from the inner space of the filter to the ducts leading to the mask. It is important that this transition allow the use of the maximum filter area. The filter design proposed in the previous RESPO 21 program involved a two-stack design in which both sides of the filter element acted as intakes for the air and the filtered air was drawn from the space between the two stacks. The model filters from the previous RESPO 21 effort used a transition that passed through one side of the two-sided filter, but the new designs being considered included a transition on the side of the filter so that there would be no loss in filter surface area.

The transition piece must:

- Add minimal resistance to air flow during breathing
- Maximize the space available for effective surface area
- Be soft and flexible enough that there would be little likelihood of injury if the wearer fell on the filter
- Seal well to the edge sealant to assure no leakage of contaminated air during breathing
- Be producible in a high volume, high-quality production process.

The design of the AFTP evolved from brainstorming sessions that included designers, polymer experts, and filtration experts. The diverse team assured that all critical aspects of the AFTP, as it is incorporated into the filter elements, performs as required.

After qualitative evaluation of design concepts, parts of a single concept were produced using stereolithography (SLA) technology. The SLA parts were evaluated independently to assess the feasibility of the design (primarily airflow resistance). Modifications to the design were then made in an effort to optimize its performance. The AFTP design was optimized by a tradeoff study of minimum airflow resistance versus

maximum space available for effective filter area. The SLA parts also permitted the evaluation of mock-up filter elements, which were used to demonstrate validity of the filter design concept.

### **3.1.3 Encapsulation**

The encapsulation process was the process whereby the filter element was produced. Encapsulation incorporated the AFTP, filter media, and edge sealant to form the final filter element.

The approach taken to design the encapsulation mold followed closely with that of the AFTP and was very much dependent upon the AFTP design. In fact, the design of both the AFTP and encapsulation mold progressed simultaneously. After the AFTP design was finalized and a limited number of AFTP were produced, the final specifications to the encapsulation mold were made.

## **3.2 Filtration Media Assessment**

Four major performance tests were conducted to qualify media for consideration in a design concept and to verify its performance: airflow resistance, aerosol filtration efficiency, dimethyl methylphosphonate (DMMP) gas life, and cyanogen chloride (CK) gas life. The procedures implemented for these tests are summarized in the following sections. Details of the test procedures can be found in a prior RESPO 21 report.<sup>(1)</sup> In principle, the same test procedures were used to evaluate the media and to evaluate demonstrator filter elements. However, due to geometric differences, slight variations in the test apparatus and procedures were required.

### **3.2.1 Airflow Resistance**

Airflow resistance (pressure drop) tests were conducted on single and multiple layers of aerosol filtration and gas adsorption materials. These data were then used to predict the performance of the filter element. Additionally, consideration was given to the number of

layers required based upon gas adsorption performance and filtration efficiency. Identical tests were conducted on model concepts to demonstrate their ability to meet the pressure-drop requirement. The test method used followed that described in American Society for Testing Materials (ASTM) F778-88<sup>(4)</sup>. Modification and deviations were made as necessary to meet our specific needs.

Test coupons 4.5-in. diameter were loaded into a test rig. When secured in the specimen holder, a 4-in. diameter opening (12.6 in.<sup>2</sup>) was available for air to pass through. Tests were conducted at various flow rates, ranging from 10 to 50 lpm. For a given material, single or multiple layers were evaluated using at least three different flow rates. A pressure tap located downstream of the test specimen was connected to an inclined manometer to measure the pressure differential relative to atmospheric pressure. Airflow resistance ( $\Delta P$ ) was then correlated with flow rate (Q). The correlation was assumed to be linear and is written as  $\Delta P = \alpha Q + \beta$  where  $\Delta P$  has units of mm H<sub>2</sub>O, Q has units of lpm, and  $\alpha$  and  $\beta$  are constants obtained from a linear regression of  $\Delta P$  vs Q data. This correlation was then used to predict resistance at a flow equivalent to 85 lpm through the filter design area.

A similar test was performed with the demonstrator filter elements. Air ducts were connected to the AFTP ducts and joined in a Y to a common duct. This common duct had a pressure tap to measure vacuum relative to atmospheric pressure. The contribution of the system was subtracted to get airflow resistance of the filter.

### **3.2.2 Aerosol Filtration Efficiency**

Aerosol filtration efficiency tests were conducted on demonstrator filter elements using monodisperse 0.3- $\mu\text{m}$  polystyrene latex particles (PSL, Duke Scientific, Palo Alto, CA). In principle, these tests were conducted following the procedures established in ASTM F1215-89<sup>(5)</sup>. The method has been modified, as necessary, to meet our specific needs.

A nebulizer aerosol generator atomized a water suspension containing 0.3- $\mu\text{m}$  PSL particles. These particles mixed with a drying airstream and then passed through a charge neutralizer into an upstream plenum. Inserted in this plenum was a transport line that was attached to a test filter element. On the downstream side of the filter, a sampling port was

located in the airline to measure the aerosol penetrating the filtration media. A sampling port in the plenum was used to measure the upstream particle concentration filtered by the filter medium. A laser aerosol spectrometer (LAS-X, Particle Measuring Systems, Boulder, CO) was used to measure the upstream (U) and downstream (D) aerosol concentration.

Filtration performance was quantified in terms of percent penetration ( $P\%$ ) which is determined as follows:  $P\% = D/U \times 100\%$ . Filtration efficiency ( $\eta\%$ ) was calculated as follows:

$$\eta\% = 100 - P\%.$$

### **3.2.3 DMMP Gas Life Testing**

Performance of carbon-containing materials was assessed by determining the gas life against a simulant challenge vapor of dimethyl methylphosphonate (DMMP). The carbon media (supplied by ERDEC) contained untreated, activated charcoal, and some samples contained whetlerized charcoal. The DMMP gas life test followed those conditions established in the C2 canister purchase description EA-C-1322C Amendment 6.<sup>(6)</sup>

The target challenge DMMP concentration was  $3,000 \pm 200 \text{ mg/m}^3$ . The challenge vapor was generated by bubbling 1.5 lpm of air through pure liquid DMMP maintained at  $\sim 110^\circ\text{F}$ . The exiting DMMP vapor-laden air entered a condenser/liquid trap maintained at  $68^\circ\text{F}$ , resulting in a saturated DMMP vapor stream. From vapor-liquid-equilibrium data this results in a DMMP vapor concentration of  $\sim 3,100 \text{ mg/m}^3$ <sup>(7)</sup>. Challenge vapor-laden air flowed through a 41 mm diameter test coupon at a rate of  $\sim 1.5 \text{ lpm}$ , which is equivalent to 32 lpm through  $290 \text{ cm}^2$  (45 in.<sup>2</sup>). Note that the actual test sample was 47 mm in diameter, but the edge seal in the holder resulted in flow through only a 41-mm-diameter section. The concentration of DMMP in the effluent stream was continuously monitored with a phosphorus analyzer (PA260, Columbia Scientific Instruments Corp., Austin, TX). The PA260 is capable of detecting concentrations of 1 ppb, which is well below the breakthrough concentration of  $0.04 \text{ mg/m}^3$  (8 ppb). The test was performed until the DMMP concentration exceeded the breakthrough concentration or until the 110-min gas-life criterion was met.

A similar system was implemented to evaluate demonstrator filter DMMP gas life. The entire filter was exposed to the challenge vapor by placing it in a test chamber. DMMP vapor-laden air was constantly pulled through the filter at 32 lpm. The phosphorus analyzer sampled from a port located in the downstream air duct to quantify the concentration of DMMP penetrating the filter.

### **3.2.4 Cyanogen Chloride Gas Life Testing**

For media that contain treated carbon (either type ASC or ASZM), the CK gas life was determined using the conditions specified in the M13A2 filter MIL-SPEC.<sup>(8)</sup>

A test system was constructed capable of generating a 4,000 mg/m<sup>3</sup> CK challenge concentration at environmental conditions of 75 ± 5°F and 80 ± 5% RH. Filter elements were tested using a simulated respiration rate of 25 breaths/min and a tidal volume of ~0.85 l/breath. Because small test coupons could not be tested under simulated breathing conditions, tests were conducted using a constant flow of 1.5 lpm through 41-mm-diameter disks. These results were useful to compare media performance and to provide an initial approximation of the media's sorptive capacity. Breakthrough concentration was defined as 8 mg/m<sup>3</sup>.

A gas chromatograph equipped with a flame ionization detector (GC/FID) was used to measure CK concentration. Preliminary tests were conducted to find the optimum GC operating parameters for separation and sensitivity. A calibration curve was established at a concentration range covering the breakthrough concentration. The challenge concentration was diluted by a factor of 200 before it was injected into the GC. Air samples downstream of the filter were collected about every 5 min and injected directly into the GC. Breakthrough time was recorded when the downstream concentration exceeded 8 mg/m<sup>3</sup>.

## 4.0 FILTRATION MEDIA PERFORMANCE

The results presented here pertain to the performance evaluation of filtration media that serve as a basis for defining the model design. The data were used to assess media performance, determine the suitability of the media for use in design concepts, and determine the quantity of material needed.

### 4.1 Airflow Resistance

Table 4 presents results from the airflow resistance correlations for selected media. These data are for multiple layers of M-ASZM carbon material and Omega Web® media used in the filter elements. Figure 1 presents these data in graphical form.

Table 4. Airflow Resistance Correlation and Comparison to Design Specification

Medium	Layers	Correlation <sup>(a)</sup>		$\Delta P^{(b)}$ (mmH <sub>2</sub> O)
		$\alpha$	$\beta$	
Omega Web®	1	0.054	-0.17	1.3
Omega Web®	2	0.15	-0.31	3.6
Omega Web®	3	0.26	-0.58	6.4
M-ASZM	6	0.60	-0.68	15.5
M-ASZM	7	0.68	-1.0	17.4
M-ASZM	8	0.73	-0.73	18.9

<sup>(a)</sup>Correlation equation has the form  $\Delta P = \alpha Q + \beta$  where Q (lpm) and  $\Delta P$  (mm H<sub>2</sub>O) through 80 cm<sup>2</sup> of material.

<sup>(b)</sup>At flow rate equivalent to 85 lpm through 39.4 in.<sup>2</sup> (255 cm<sup>2</sup>) of material.

The test rig used to measure airflow resistance as a function of flow rate had an open area of 80 cm<sup>2</sup> for airflow through media. The final filter design has an effective area of 255 cm<sup>2</sup> (127 cm<sup>2</sup> on each side of the filter). The airflow resistance specification for the filter element is for 85 lpm. Since pressure drop is a function of the face velocity through

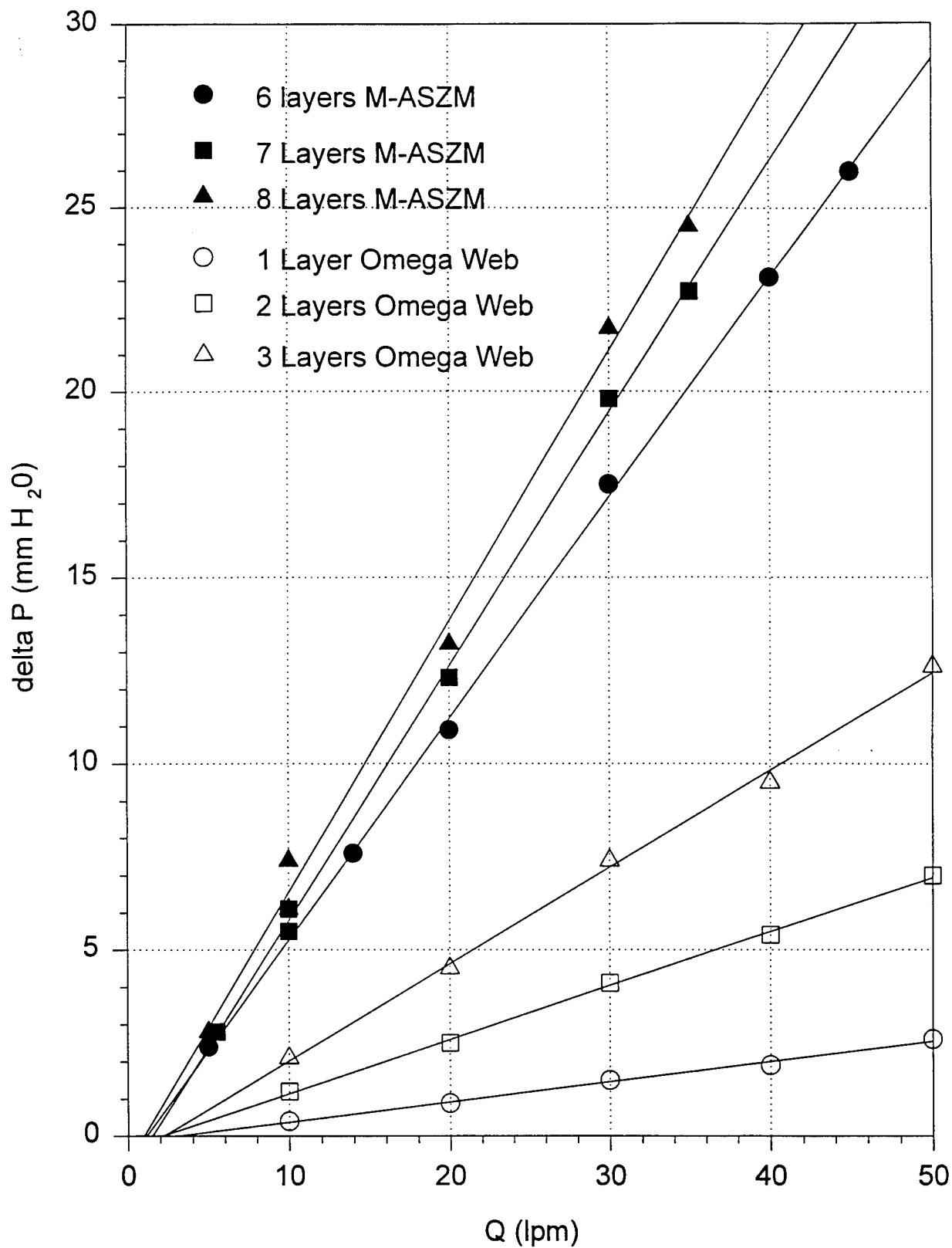


Figure 1. Correlation of Airflow Resistance vs AirFlow Rate for Various Filtration Media

the material, the test rig results can be used to predict airflow resistance of the filter as follows:

$$\frac{Q_{test}}{80 \text{ cm}^2} = \frac{85 \text{ lpm}}{S_{filter}} \quad (1)$$

where  $Q_{test}$  is the airflow rate (lpm) in the test rig and  $S_{filter}$  is the available surface area ( $\text{cm}^2$ ) of filtration media in the filter. For the filter elements produced,  $S_{filter} = 255 \text{ cm}^2$ , therefore  $Q_{test} = 27 \text{ lpm}$ . The equation has been cast in this form so that the effect of filter area can be assessed.

At a flow rate equivalent to 85 lpm through a filter element, each additional layer of carbon media (on each side of the filter) will increase the airflow resistance  $\sim 2.0 \text{ mmH}_2\text{O}$ . Likewise, each additional layer of Omega Web<sup>®</sup> will increase airflow resistance by 1.5 to 2.0  $\text{mmH}_2\text{O}$ . The results for the Omega Web<sup>®</sup> agree well with those reported<sup>(9)</sup>. The reported pressure drop across a single layer of Omega Web<sup>®</sup> at a flow rate equivalent to 34 lpm in this test rig is 2.5  $\text{mmH}_2\text{O}$ , and the measured resistance at 34 lpm would give  $\sim 2.3 \text{ mmH}_2\text{O}$ .

These results indicate that a filter element with two layers of Omega Web<sup>®</sup> and seven layers of M-ASZM in each stack will result in a filter element that has an airflow resistance of  $\sim 28 \text{ mmH}_2\text{O}$ . The filtration media will contribute  $\sim 20 \text{ mmH}_2\text{O}$  to the resistance and the AFTP will add another  $\sim 8 \text{ mmH}_2\text{O}$ . Filter elements with more layers of material were expected to exceed the pressure drop specification. (It is originally believed that the filter airflow resistance requirement was 30  $\text{mmH}_2\text{O}$ , but this includes the duct work and interface with the mask, which has  $\sim 5 \text{ mmH}_2\text{O}$  pressure drop. After this analysis, the filter resistance was to be reduced to 25  $\text{mmH}_2\text{O}$ .)

These preliminary data were used as the basis for definition of the AFTP and encapsulation mold. These results appeared to be further corroborated by the production of hand-made model filter elements with SLA AFTP and the measured airflow resistances corresponded to those predicted. When initial model filter elements were produced using the molds, the airflow resistance was at least 25% higher than predicted.

## 4.2 Aerosol Filtration Efficiency

Results from 0.3  $\mu\text{m}$  PSL aerosol penetration tests are presented in Table 5.

Although the Omega Web® is an electrostatic filtration medium, it is not a highly efficient filtration material. The M-ASZM carbon material filters fewer than half of the 0.3  $\mu\text{m}$  particles and is expected to be very inefficient. The reported filtration efficiencies are highly variable, which may be a result of the apparent nonuniformity of the Omega Web® material. The reported penetration (for 0.3  $\mu\text{m}$  dioctylphthalate particles at a velocity of 7.1 cm/s) is 24 percent.<sup>(9)</sup> The data reported in Table 3 are for a face velocity of 1.9 cm/s. Particle penetration efficiency will decrease with decreasing flow rate.

Table 5. Percent Penetration of 0.3  $\mu\text{m}$  PSL Through 13.2  $\text{cm}^2$  of Media at a Flow Rate of 1.5 lpm

Medium	Layers	Percent Penetration
Omega Web®	1	2.5
Omega Web®	1	7.2
Omega Web®	1	1.2
Omega Web®	1	21
Omega Web®	2	0.030
Omega Web®	2	0.77
Omega Web®	3	0.0064
M-ASZM	5	11
M-ASZM	6	8.3
M-ASZM	7	5.5
M-ASZM	8	3.6

The airflow resistance results indicated that approximately seven layers of carbon material could be included in the filter element, along with two layers of Omega Web®. Using an average penetration through a single layer of Omega Web® of ~4 percent (excluding the 21 percent penetration value) and the penetration through seven layers of carbon is ~5.5 percent, the predicted filtration efficiency of the filter element is

0.01 percent. This would just meet the design specification. Based upon these results, it was determined to proceed with the Omega Web® as the filtration media.

Previous work indicated that 3M Filtrete® material (e.g., G0120) would have a lower airflow resistance and higher filtration efficiency than Omega Web®, but the Filtrete® is more sensitive to degradation by heat because the Filtrete® has a much higher charge density than Omega Web®. Sensitivity to heat was considered critical because of the high-temperature molding process anticipated. The Omega Web® could withstand 150°F for 24 hr with degradation. Also, because the Omega Web® material has a lower charge density, it would also be less susceptible to degradation due to humidity and particulate loading.

#### 4.3 DMMP Gas Life

Results of the DMMP gas life tests are presented in Table 6. This table also includes the mass of DMMP adsorbed, the mass of carbon in the test specimen available for adsorption of vapor, and the ratio of DMMP mass adsorbed to carbon mass. The ratio is intended to indicate the effectiveness of the carbon to adsorb DMMP and standardize the results to permit comparison between materials. The quantity of carbon contained in the sample assumes a 41-mm-diameter sample (assumes the 3-mm-wide edge of the sample does not contribute to DMMP adsorption because of the edge seal) and relies upon manufacturer-supplied data regarding the carbon loading in a material. The table includes selected results from the previous RESPO 21 study.<sup>(2)</sup> The medium tested for this study was the new M-ASZM (3M Corporation, St. Paul, MN) carbon fabric procured for this project.

Results for the M-ASZM carbon material used in the filter elements were consistent with previous results of similar material. The C-18 core material used in the M13A2 filter has a DMMP capacity very close to that of the M-ASZM material. The average ratio of mg DMMP to mg carbon for M-ASZM ( $\xi$ ) medium was 0.21, compared to that of 0.19 measured in a single test for the C-18 core material. Based on a single test, it is not clear whether the 0.36 mass ratio for M-ASZM for the earlier RESPO 21 study is accurate; it appears high. The mass ratio for the low profile filtration system produced and evaluated by Battelle was 0.33.<sup>(10)</sup>

Table 6. DMMP Gas Life and DMMP Sorptive Capacity of Carbon Media

Sample	Layers	Life <sup>(a)</sup> (min)	Cumulative DMMP Loading	Carbon <sup>(b)</sup> Mass (mg)	(mg DMMP/mg carbon)	Ratio
C-18 core	4	45	270	1400		0.19
M-ASC	5	100	370	2000		0.19
M-ASZM <sup>(c)</sup>	5	160	730	2000		0.36
M-ASZM	3	39	180	1200		0.15
M-ASZM	4	60	270	1600		0.17
M-ASZM	5	98	440	2000		0.22
M-ASZM	6	140	430	2400		0.26
M-ASZM	6	106	476	2400		0.20
M-ASZM	8	160	720	3200		0.23

<sup>(a)</sup>Standardized for a challenge concentration of 3000 mg/m<sup>3</sup>.

<sup>(b)</sup>Calculated from the carbon loading reported by the manufacturer.

<sup>(c)</sup>M-ASZM material from previous RESPO 21 task<sup>(2)</sup>.

These results were also used to estimate the gas life (assuming scale-up is linear with area and effective area is 100 percent of the open area) of a filter element. The average DMMP gas life per layer of carbon medium was calculated to be 18 min for the six tests. Therefore, at least six layers of carbon medium would be needed to provide the required 110 min gas life. The effects of scale-up (geometry, flow distribution, etc.) were unknown when these data were used to predict performance in a filter element. Therefore, the initial filter model was designed based upon seven layers of carbon material for a safety factor.

The mass ratio ( $\xi$ ) can be cast in an equation as a function of breakthrough time ( $\tau$ , min), number of layers in each filter stack ( $\eta_l$ ), and the filter's surface area ( $S_F$ ,  $\text{cm}^2$ ) open for airflow through the filtration media. The mass ratio can be calculated as:

$$\zeta_{DMMP} = \frac{96 * \tau}{30 * \eta_l * S_F} = 3.2 \frac{\tau}{\eta_l * S_F} \quad (2)$$

where 3.2 is a constant obtained by  $32 \text{ l/min} \times 3 \text{ mg/l CK challenge divided by } 30 \text{ mg/cm}^2$  (carbon mass loading on the fabric). Equation (2) can be solved for any one of the variables,  $\tau$ ,  $\eta_l$ , or  $S_F$  by specifying two of the three and taking  $\xi_{DMMP} = 0.21$ .

#### 4.4 CK Gas Life

Results from the CK tests are presented in Table 7. Multiple layers of the M-ASZM medium used in the filter elements were evaluated and compared to the previous years M-ASZM sample and the C-18 core material. The table is interpreted in the same manner as the DMMP gas life data in Table 6. The reported gas lives have been standardized for a  $4000 \text{ mg/m}^3$  CK challenge concentration. Difficulties were encountered with maintaining a reproducible GC calibration, so the challenge concentration is based upon known pure CK flow rate and dilution flow rate. (Subsequent tests showed that CK challenge concentrations measured using a calibrated GC were within  $\pm 15$  percent of those predicted based on calibrated flows.)

Table 7. CK Gas Life and Sorption Capacity of Carbon Media

Medium	Layers	Life <sup>(a)</sup> (min)	Mass of CK Adsorbed (mg)	Mass of Carbon <sup>(b)</sup> (mg)	Ratio (mg CK/mg carbon)
M-ASZM <sup>(c)</sup>	5	18	108	2000	0.054
C-18 core	5	11	66	1600	0.041
M-ASZM	4	20	120	1600	0.075
M-ASZM	4	23	140	1600	0.088
M-ASZM	6	29	170	2400	0.071
M-ASZM	6	29	170	2400	0.071
M-ASZM	8	46	280	3200	0.088

(a) Standardized for a challenge concentration of 4000 mg/m<sup>3</sup>.

(b) Based upon carbon loading reported by the manufacturer.

(c) M-ASZM material from previous RESPO 21 study<sup>(2)</sup>.

Materials were compared by comparing the ratio of mass of CK adsorbed to the mass of carbon available. The new M-ASZM medium had an average mass ratio of 0.079, which was higher than that measured for any material previously tested. The single test conducted for C-18 core material resulted in a ratio of 0.0041. Using the M-ASZM results to scale up for design of a filter element, a minimum of six, and preferably seven, layers of M-ASZM media would be used as the basis for the initial filter design.

Previous filter design studies were reviewed to assess whether the 0.079 ratio was reasonable. The work performed by MSA in the late 1960s to characterize the C-18 core material indicated that six layers of material (open area of 100 cm<sup>2</sup> per layer) tested under conditions of 12.5 lpm, 4000 mg/m<sup>3</sup> CK challenge concentration had an average gas life of 20.4 min.<sup>(11)</sup> The basis weight of the material is ~220 lb/3000 ft<sup>2</sup> (~36 mg/cm<sup>2</sup>) with ~70 percent carbon by weight, which yields ~25 mg/cm<sup>2</sup> of carbon. MSA's analysis of effective area for this test system resulted in only 62 percent of the open area effective. Using the above data, the ratio of mass CK adsorbed to mass of carbon utilized is 0.11. If it is assumed that 100 percent of the carbon in the open area is effective, then the mass ratio is 0.068. It is very unlikely that the available area is 100 percent effective; therefore, the actual mass ratio is likely to be somewhat greater than 0.068.

Battelle's work to develop the low profile filter generated similar results.<sup>(10)</sup> The low profile filter contained the C-18 core material discussed above. One of the six filters tested to ensure that the required CK gas life was met was permitted to run until breakthrough. A breakthrough time of 97 min was measured when the filter was tested against a CK challenge concentration of 780 mg/m<sup>3</sup> and 25 lpm intermittent flow. The filter element effective area was reported to be 170 cm<sup>2</sup> and four layers of C-18 material were used. Using the above data, the mass ratio of CK adsorbed to carbon available was 0.082. A single test with swatches of C-18 core material yielded a mass ratio of 0.041. Additional filter and swatch tests would need to be conducted to determine whether the swatch test results and filter results are significantly different. Both of these filter studies lend credence to the mass ratio value measured for the M-ASZM material.

The mass ratio  $\xi_{CK}$  can be used to either determine the number of layers ( $\eta_l$ ), breakthrough time ( $\tau$ ), or surface area ( $S_F$ ) if two of the three are fixed. This calculation is identical to that in Eq. (2) except the coefficient is 3.33 (25 l/min\*4 mg/l ÷ 30 g/cm<sup>2</sup>).

$$\zeta_{CK} = 3.33 \frac{\tau}{\eta_l * S_F} \quad (3)$$

## 5.0 FILTER DESIGN

### 5.1 Edge Sealing

#### 5.1.1 Required Characteristics

The most important characteristics of the edge seal that guided the material selection process were (1) adhesion/penetration of the filter media, (2) softness, (3) durability, and (4) producibility.

The edge sealant must adhere exceptionally well to the filtration media to prevent airflow from channelling past the filtration media. Adhesion and sealing are improved if the sealant can partially penetrate the filter layers. The edge seal should be soft so that it is comfortable to the wearer during impact. The edge seal should also be flexible so that the filter can flex and form to the body of the wearer. The edge sealant must also be durable enough to withstand wear on it during typical field situations. Although not considered in this study, the susceptibility of the edge seal to agent permeation needs to be considered in future efforts.

To prepare a few demonstrator filters, it is more cost effective to use material/process combinations amenable to low-cost molds and easy design modifications, even though the materials may be costly, the molding cycles long, and the process sometimes cumbersome. However, the production of large numbers of parts offers the potential for using lower-cost materials in processes that yield a much higher volume of parts within a given time. Often these material/process combinations produce higher quality parts that are more uniform. If the anticipated number of parts is in the thousands, this approach is usually preferred. The cost of production is a major portion of the cost of a part. Two important factors in production costs are (1) the processing time per part and (2) the number of parts made from one set of tooling. Producing a large number of parts on one tool during a short

processing cycle significantly lowers the cost per part. Emphasis was given to materials and processes for the production of limited demonstrators from which information on the process could be learned.

### **5.1.2 Materials Selection**

Several types of materials were identified as particularly interesting for the short-term goal of producing demonstrators, and two types of materials were considered for the edge seal: silicones and polyurethanes. An idea generation session was held with a team of senior scientists from the Battelle Polymer Center. The objective was to assure that all candidate materials were identified and considered for use in the edge sealing system of the filter. Appendix A lists the raw ideas. At the stage at which the list was prepared, no evaluation had been made of the ideas. Each material was eventually evaluated for its suitability in the project.

Twelve materials were obtained and evaluated in the laboratory. Included were:

- Dow Corning Silicone 3110 with catalyst 4
- Polytek Poly-Fast 72-40 RTV Liquid Rubber
- BJB Enterprises LS-40 A/B Polyurethane Elastomer
- BJB Enterprises F-60 Polyurethane Elastomer
- BJB Enterprises F-40 Polyurethane Elastomer
- Smooth-On PMC-724 Flexible Polyurethane Molding Compound
- Smooth-On PMC-744 Flexible Polyurethane Molding Compound
- Dow Corning Sylgard 186 - silicone with platinum catalyst
- Dow Corning 3112 RTV - silicone with tin catalyst
- GE RTV 630 - silicone with platinum catalyst
- Conap TC 640 polyurethane
- Conap TC 660 polyurethane

Company names, addresses, phone numbers, and Battelle's contact at each supplier are provided in Appendix B.

Almost all materials evaluated in this study could be used to prepare an edge seal of the design selected for this project. The differences were in the time and temperature required for curing, adhesion to itself or another material in the encapsulation process, and the presence of small molecules after the cure is complete that had potential to interfere with the function of the carbon.

Each material listed above was tested by curing at a variety of time/temperature combinations to determine the potential for use in molding with the electrostatic materials in a mold. The target was to achieve demolding within 15 min after injection of the two part mixture in the mold.

Each material that cured below 150°F with demolding in less than 40 min was also evaluated for adhesion to itself and to other candidates. Materials that would be used in the transition piece would not have to be cured at low temperatures but did have to adhere to a candidate for use in the encapsulation.

Materials that provided a strong odor after curing were also avoided. For example, some candidate silicones release acetic acid during the curing process. It is possible that this compound would poison the activated charcoal, and so they were rejected.

Since molding the AFTP (filter frame) does not involve any temperature sensitive materials and impregnation of the filter media is not required, it was possible to injection mold the transition piece from a thermoplastic polyurethane. Adhesion trials were conducted to determine if any of the candidate edge sealant materials will bond to Pellethane, an injection moldable grade of thermoplastic polyurethane. The only material which showed any promise was the Shore A 75 material from BJB Enterprises. Another trial was conducted to test the adhesion of the F-60 to itself. Uncured F-60 was molded against cured material. There were several areas in which adhesion did not occur, it did occur however across the midline of both samples. Adhesion was good at the fresh surface created by cutting the cured piece and at the surface exposed to air during curing. There was no adhesion at the surface that was in contact with the aluminum cup during curing.

The materials that met all the criteria were SP-180 polyurea-urethane for the transition piece and F-70 polyurethane, both from BJB Enterprises. These were the materials used to produce demonstrator filter elements.

## 5.2 Airflow Transition Piece

### 5.2.1 Design Concepts

Due to the limited surface area available for the RESPO 21 filter element, it had been determined that a two-sided filter element would be needed. To integrate into the mask facepiece that ERDEC was designing, dual ducts from the filter were desired. Each duct would lead to an inlet port located near each cheek of the mask. A single duct on the filter would require the airflow to be split before entering the mask. These baseline parameters served as the starting point for generation of AFTP design concepts. Details of the design concepts generated are given in Appendix A.

The most difficult aspect in the design of the overall filter was how to move the filtered air from the point at which it exited the surface of the filter media to the ducts leading to the mask. Assuring that this "transition" minimizes air flow restriction while also assuring that the parts will have no leakage of contaminated air into the filtered air stream was the essential element in the design process. Assuring a leak-free situation would require that the filter media be clamped against the transition piece with sufficient pressure to prevent leakage of the low-viscosity edge sealant into the active area of the filter media.

Design of the transition was focused on the specifics of how the premolded transition piece can be sealed into the edge seal. The problems are in (1) achieving a tight seal around the edge of the transition piece to prevent flow of the sealant into the active area of the filter during the molding process and (2) assuring adhesion of the parts of the filter system to prevent leakage of contaminated air. In the most obvious approach, the mold would be designed to clamp the filter media against the transition piece to prevent flow. This is not practical with most of the designs considered. There must be a space between the media and the transition, and that juncture is not amenable to high clamping pressure that was anticipated to keep the edge sealant from leaking between layers of media.

Two idea generation sessions were held with Battelle mechanical and design engineers to identify approaches and concepts for the air flow transition for the filter, and the results were reported in a letter to the Government<sup>(12)</sup>. The objective of the sessions was to devise a specific design and carry the design through a consideration of how the concept

would be produced, both in early evaluation experiments and in production. Appendix A includes the list of raw ideas from the sessions. Please note that this list of ideas is in its original form.

These concepts were qualitatively assessed to select a single design to further develop. Resources did not permit multiple designs to be investigated by model production due to the high cost of mold design and fabrication. A single AFTP was devised and the design concept was transferred to Pro Engineer Software to further enhance/define the design.

From these sessions came the general concept that was eventually developed for the preparation of filter elements. In that design, a part would be molded that would incorporate (1) the manifolds and connectors that lead to the mask and (2) a frame upon which would be mounted stacks of filter material.

Some modifications were made to this general concept because of the limitations of preparing a small number of parts in a laboratory. In particular, the design incorporated an encapsulation of two filter stacks mounted in a filter frame that incorporates the air flow transition from the space between the filter stacks to the tubes/ducts leading from the filter element to the mask. This encapsulation obviates the need for adhering each layer of filter media to its neighbors.

The Client approved Battelle's recommended design for the air flow transition element during a review meeting held at Battelle<sup>(13)</sup>. Battelle proceeded with the evaluation of the design and of the filter media combinations needed to meet the Army's specifications.

The transition piece (also called the filter frame) was designed and acrylic parts were prepared by stereolithography. Although the SLA parts were not flexible, they provided considerable information as the design team considered the structure and producibility of the filter.

### **5.2.2 Mold Design**

A detailed engineering drawing of the final design concept selected is presented in Appendix C, and Figure 2 illustrates a schematic of the AFTP. The final AFTP mold design

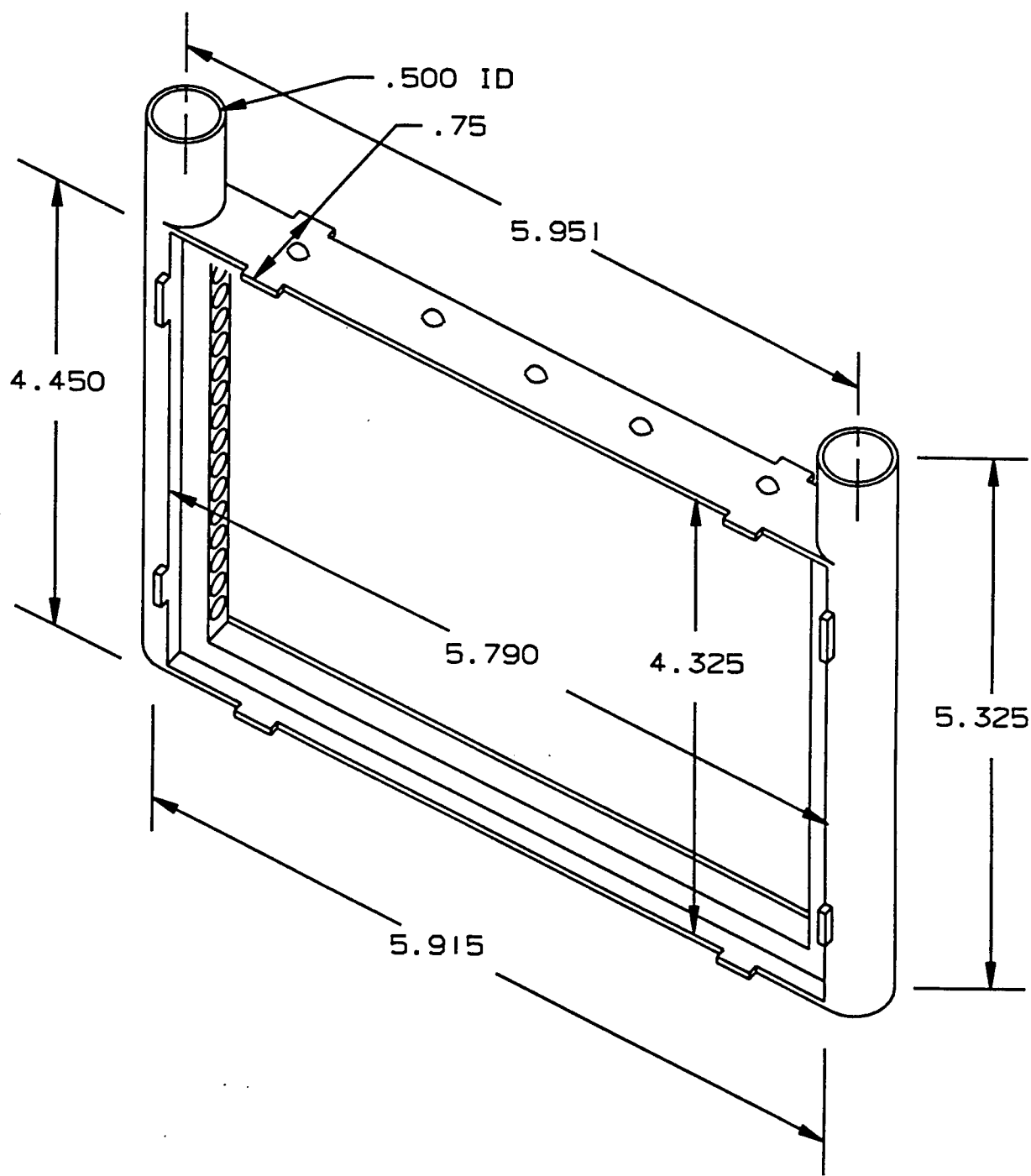


Figure 2. Schematic of an AFTP (All dimensions in inches)

was not made until after semiquantitative and quantitative assessment of the design was made. An engineering estimate of the necessary gap between the top and bottom filter stacks was made. The gap between the two filter media stacks was optimized to permit airflow to the filter ducts with minimal resistance (large gap) with minimal contribution to filter thickness (narrow gap). Although an extremely narrow gap between the two filter stacks would minimize filter thickness, the resulting narrow channel for airflow through the filtration media to the air duct would significantly increase airflow resistance.

In seeking additional designs for the air flow transition, a number of ideas were identified that raised questions about the restriction of flow due to the space between the two stacks of filter media. Of particular concern was that uniform flow be attained through as much of the filter surface area as possible. Uneven flow through the filter would mean that the entire available surface area is not effectively utilized.

A model of the airflow within the space between filter stacks was developed. It was assumed that the spacer material would add no restriction to flow. It was projected that if the spacer is 1/4-in. thick, there should be less than one percent nonuniformity in the flow rate across all areas of the filter. This approximation is based on a simple model. However, the results indicate that a significant change due to modifications to some assumptions would still seem to provide very little airflow nonuniformity.

### **5.2.3 Performance Assessment**

The SLA parts were used to assess the airflow resistance of the AFTP. Several SLA parts were made with slight modifications to the design. The variations included the number of holes along the filter support ridge that permitted air to flow from the filter media to the air duct and the geometry of the air duct. The number of manifold holes were varied to ensure adequate opening for the air to pass with minimal resistance, yet maintain structural integrity of the ridge so that it would support compression during encapsulation molding. The duct geometry was varied to maximize the available area for filtration media. The cross section of the air duct was either completely open (circular duct) or was half open (semicircular duct). If the ducts are full circles, then airflow resistance through the ducts is reduced, but this reduces the area available for filter media. (The outside width of the filter

was to be less than 6.5 in., so when the air duct was changed from circular to semicircular, the width of available filter media was increased.)

The airflow resistance measured for the AFTP that was used in the final design was  $\sim 8 \text{ mmH}_2\text{O}$ , nearly 33 percent of the target  $25 \text{ mmH}_2\text{O}$  airflow resistance. This AFTP had the semicircular ducts. The variations of the number of holes, over the range tested, did not significantly affect airflow resistance. Engineering judgment was used to select the final hole size and distribution. Changing air duct geometry significantly affected airflow resistance. When the air duct was changed from semicircular to circular, the airflow resistance dropped from  $\sim 8 \text{ mmH}_2\text{O}$  to  $\sim 4 \text{ mmH}_2\text{O}$ . Justification for the final design selection is given in Section 5.4.1.

### 5.3 Encapsulation

#### 5.3.1 Design Concepts

Encapsulation was the process whereby the filter elements were produced. It is termed encapsulation because the filter media and AFTP are encapsulated by the edge sealant.

The design of the encapsulation technique followed the design of the AFTP because encapsulation depended upon the AFTP design. Two main approaches were taken. First, the layers of media could be adhered together then sealed into the AFTP. This approach would eliminate the need to pinch the filter media with the AFTP during production. Second, the filter media would be sealed to the AFTP during an injection molding process, which would require the material to be pinched.

Description of the Concept. During idea generation sessions for air flow transition designs, an idea was presented for providing a different type of edge seal from the ones presently used with filters. In this concept, the edges of the individual layers would be adhered and sealed to one another with an adhesive/sealant placed between layers of the filter media. By using the proper viscosity of sealant, the sealant would impregnate the media providing a barrier to agent. In this concept, there would be no need for the large roll of

sealant around the edge. Elimination of the roll has potential for extending the length and width of the "active" area of the filter and thus increasing the life of the filter. This may also lower the profile of the filter and would "soften" the impact of the filter on the wearer if the wearer fell heavily upon it. The filter also would be more flexible and, therefore, would conform more closely to the curve of the body.

Confirmation Experiments. To confirm the potential for this design, a preliminary experiment was carried out in which a sealant was spread between each layer of filter media and the sealant in the full filter stack was cured. The resulting filter stack was then potted into the SLA-generated filter frames.

Several filter elements were constructed using eight layers of carbon-loaded fabric (M-ASZM) between single layer (top and bottom) of aerosol filtration medium (Filtrete and/or Omega) and Lumite spacer material. The edges of the filter elements were glued with several different types of adhesives including:

- Silicone Sealant
- Elmer's Glue
- PolyFast 72-40 RTV

The adhesives were changed to obtain more suitable characteristics of the sealed area in the filter stacks. The rubber gasket adhesive was too stiff, the silicone sealant gave off acetic acid upon curing which may have poisoned the charcoal, and the Elmer's glue was too stiff. The PolyFast material performed the best.

The media held together well and the filter was soft and flexible. Two filter stacks were laid together with the spacer and the SLA-generated filter frame between so that a complete filter was produced. Several filter stacks were assembled in this manner. The feasibility of the concept described above was confirmed.

Some other materials were suggested for use as the edge sealant in this process. Included were Scotch-Grip 847 Rubber and Gasket Adhesive and Permatex Gasket Sealant. A 3M representative was also consulted and he suggested trying the following materials:

- 4693 Plastic Adhesive
- Jet Weld TE 031 Thermoset Adhesive
- Jet Weld TE 100 Thermoset Adhesive

The above approach was feasible on a bench scale operation, and it was useful to produce hand-made filter elements with an SLA AFTP. The SLA AFTP could not withstand the pressure required to pinch the filter stack. This method was used to confirm the filter design but was not used for production.

For production of demonstrator filter elements, the approach of pinching the filter stack and encapsulating the entire AFTP and edge of the stack was employed. Because the amount of pressure applied to the area as the mold closes and the media are clamped is critical to the assembly process, mechanisms that would allow changes in the clamping pressure were sought. This was also desirable since the number of layers of filter media needed to meet the performance specifications for the filter was not known at the time the mold had to be designed and fabricated. The final design allows for rapid and inexpensive changes to the dimensions of the clamping ring and for shimming the part to increase and reduce the clamping pressure.

The original concept for the encapsulation process did not include encapsulation of the air ducts on the sides of the filter. It was believed that variations in the dimensions of the filter frame would cause considerable variation in the placement of the frame in the cavity of the encapsulation mold, resulting in leakage and compression of the manifold. An extensive study of the dimensions of many filter frames was carried out. The results indicated that the variations can easily be accommodated in the mold design. Thus, it was decided to encapsulate all of the filter frame including the manifold.

### **5.3.2 Mold Design**

The final mold design captured the filter media as well as the entire AFTP, including the ducts. It also had provisions to adjust the pinch gap by the use of shims. The ability to adjust the pinch gap permitted the flexibility to accommodate various numbers of layers of filtration media and optimization of the pinch pressure. Adequate pinch is required to ensure sealant does not penetrate the media beyond the pinch point, yet does not overcompress, which could damage or deform the media or AFTP.

Figure 3 illustrates the components of the encapsulation mold. A detailed schematic of the mold design is provided in Appendix C.

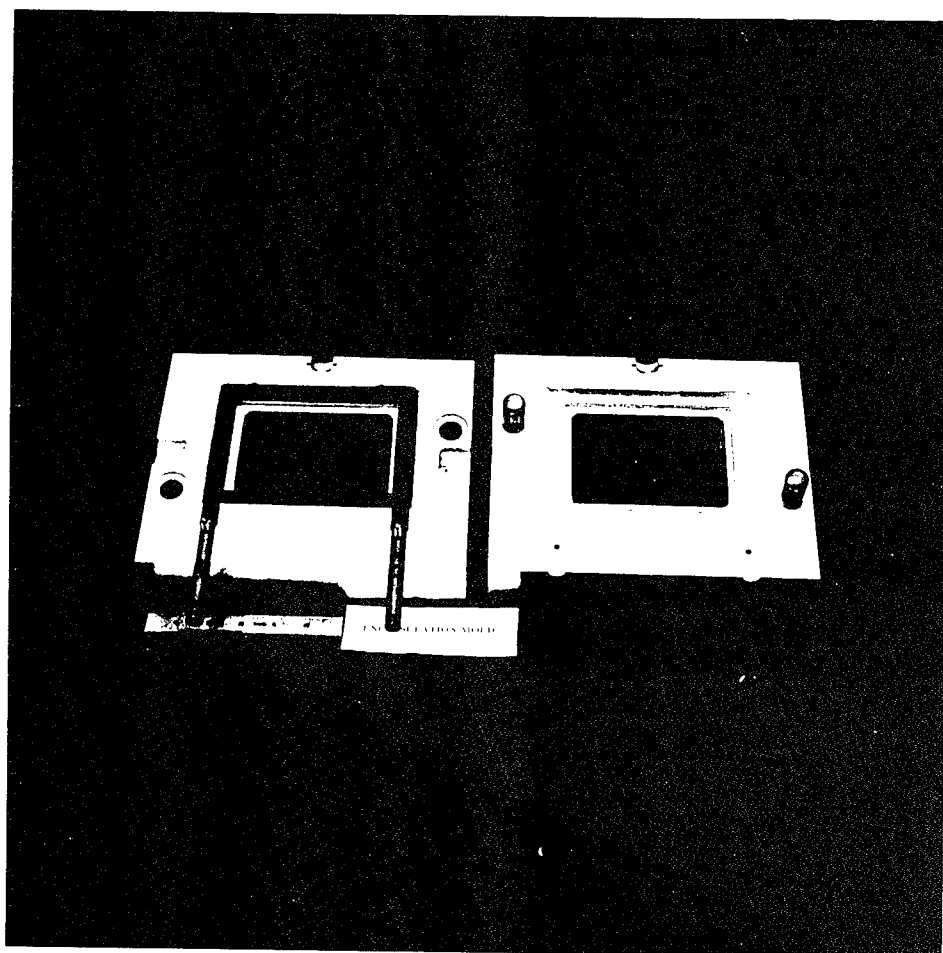


Figure 3. Photograph of the Encapsulation Mold with AFTP for Producing Filter Elements

## **5.4 Mock-up of Filter Elements**

### **5.4.1 Filter Design Concept Definition**

The results from material performance evaluations and the airflow resistance data for the AFTP were used to define the filter concept.

The AFTP piece selected for inclusion in the filter was the one with semicircular air ducts, even though it had a higher airflow resistance than the alternate design with full circular ducts (8 mmH<sub>2</sub>O versus 4 mmH<sub>2</sub>O). The reasons this AFTP design was selected over the alternate design that offered a lower airflow resistance is because the reduced filter area associated with the alternate design causes an increase in airflow resistance through the filtration media.

The open area available for filtration media is 255 cm<sup>2</sup> for the semicircular duct design and 230 cm<sup>2</sup> for the full circular duct design. The 25 cm<sup>2</sup> is the area "lost" per each layer of filtration media; therefore, if seven layers are included in each stack of media, 175 cm<sup>2</sup> of carbon medium area is not available. This means that an additional layer of carbon material is required to compensate for the reduced area. (Consequently, to maintain gas life, eight layers in a media stack would be required in the available area of 230 cm<sup>2</sup>. The additional layer of carbon material and the increase in air velocity through the media would result in a ~5 mmH<sub>2</sub>O airflow resistance. Hence, the 4 mmH<sub>2</sub>O reduction in airflow resistance with the full circular duct design is offset by an increase of 5 mmH<sub>2</sub>O resistance through the filter media. Based upon this analysis, the AFTP with the semicircular duct was selected because it maximized the area available for filtration media. This analysis assumes that all of the open space for filter media will be used effectively, which may not hold in an actual filter element.

### **5.4.2 Concept Validation**

An attempt was made to validate the filter concept defined in the previous section. SLA parts of the AFTP were used to make hand-made filter elements were intended to be representative of the filter design, which would permit accurate quantitative evaluation of the

concept. The main concern was that tests of material swatches would not be an accurate indicator of material performance in a filter element because of scale-up problems (geometry effects, flow dynamics, compression) that could not easily be predicted.

Limited success was achieved with the mockup filter elements. Only a few were fabricated because they were labor intensive to produce and difficulties in production caused the process to be very inefficient. Only two workable mockups were produced, and they were only successfully evaluated for airflow resistance. The measured airflow resistance agreed with that predicted based upon the swatch data. Attempts to measure aerosol penetration and gas life were not successful. It was not clear whether there were leaks in the filter or the filter (AFTP) was porous and easily penetrated. Because of limited resources, no additional attempt was made to confirm the usefulness of this design with mockup filter elements.

## **6.0 MODEL FILTER ELEMENTS**

The material performance and filter design results were used as the starting point for production and evaluation of model filter elements. This section discusses the findings regarding fabrication of AFTP and filter elements and evaluation of the filter elements.

### **6.1 AFTP Fabrication**

The procedure used to fabricate an AFTP is summarized below and details are provided in Appendix D. A photograph of an AFTP is given in Figure 4.

Components of the mold were cleaned to remove residual polymer from the previous run and surfaces were coated with a soap solution to ensure easy release of the AFTP from the mold. The components of the mold were then assembled and placed in a heated press. The two-part polymer was simultaneously mixed and injected into the mold. The polymer then cured in the mold for 15 min at a temperature of 150°F. The mold was removed from the press and the AFTP was recovered. During the demolding process, care was given to reduce the chance of tearing the AFTP. The AFTP was especially susceptible to tears in the duct.

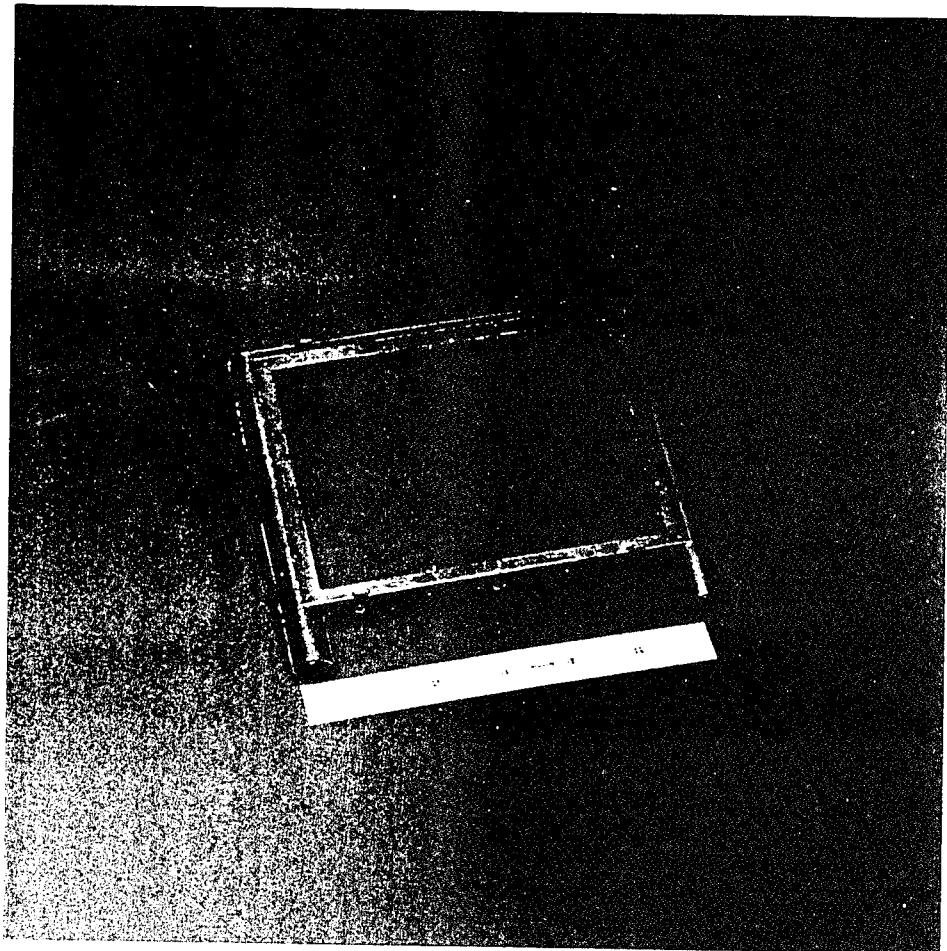


Figure 4. Photograph of a Representative AFTP

Several preliminary trials ("shots") were performed to establish this procedure. Initial attempts to fabricate an AFTP were unsuccessful because of improper quantity of polymer and incomplete filling. The result was air pockets or an incomplete part. These problems were anticipated and easily corrected. The addition of strategically located air vents solved the air pocket problem. The AFTP is not rugged by itself and was susceptible to tearing when the piece was being removed from the mold. Other problems that were occasionally encountered included improper mixing during injection and excessive adhesion to the mold. There were a significant number of AFTP that had weak spots at the end of the air duct. It is not clear what caused this weak area. It is suspected that the polymer did not fully cure or was not a good mix. Removal of the pin during the demold operation further weakened (sometimes tearing) the duct. About 80 percent of the AFTP produced were of satisfactory quality for use in a filter element.

## 6.2 Filter Fabrication

Filter production using the encapsulation mold is summarized here, and additional step-by-step details are given in Appendix D. A photograph of a filter element is given in Figure 5. A cut-away view of a filter is illustrated in Figure 6. This figure depicts the filter media that comprise the filter element. A description of the filter is given in Table 8. When describing these filters, the number of layers in a stack are given. Two stacks, the top and bottom, form a complete filter.

The aerosol filtration medium, Omega Web® (3M Corporation, St. Paul, MN), is a melt-blown polypropylene, electrostatic material. The carbon medium for gas filtration is also made by 3M. The carbon granule is sprayed onto a polyurethane substrate. The thickness of the carbon medium is 0.051 in. per layer and a basis weigh weight of 200 g/m<sup>2</sup>, with a 300 g/m<sup>2</sup> carbon loading.

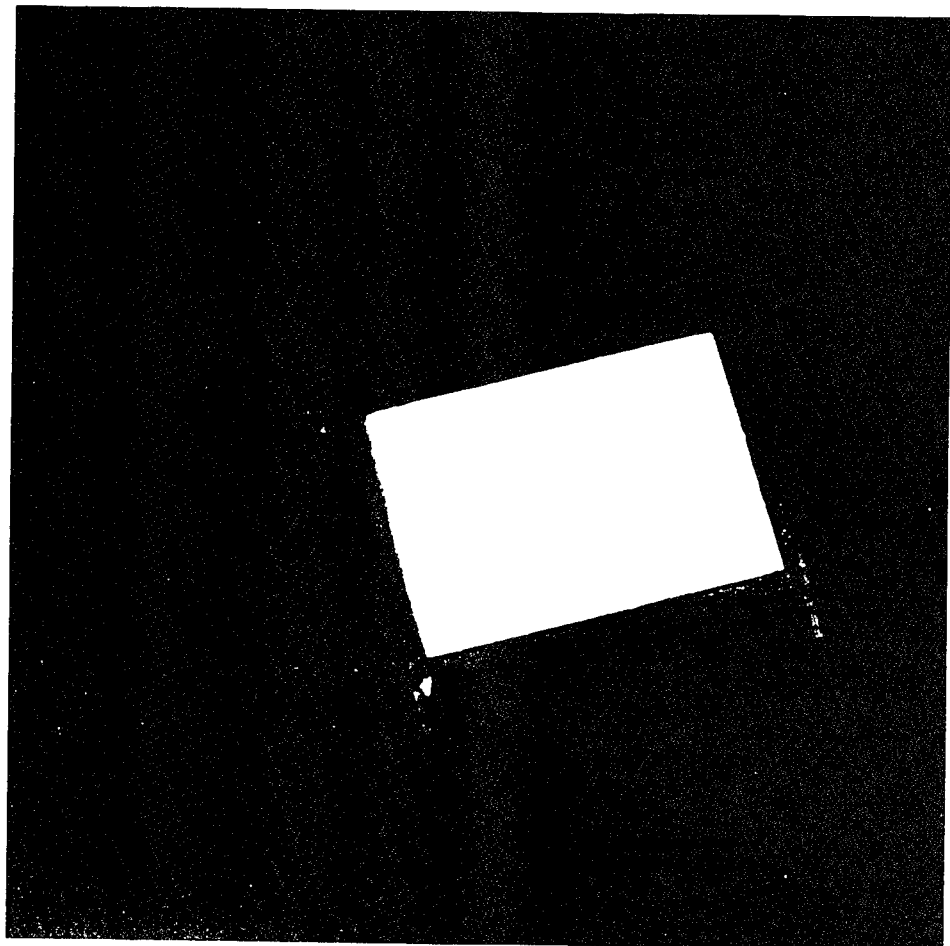


Figure 5. Photograph of a Representative Filter Element

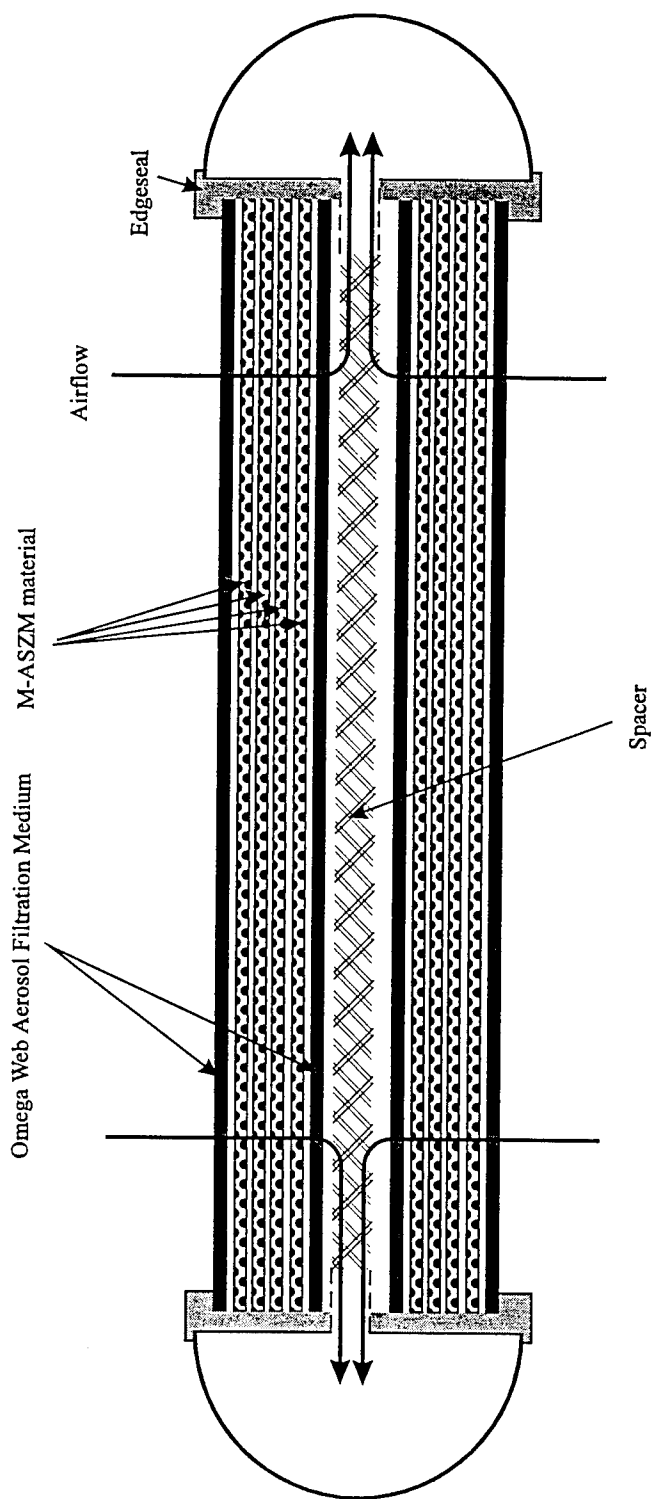


Figure 6. Cross-Sectional Diagram of Filter Element

Table 8. Definition of Filter Concept

Filter Characteristic	Definition
Size (overall)	4.5 x 6.5 in. rectangle
Media	M-ASZM carbon (gas adsorption) Omega Web® (aerosol filtration)
Filter Stack	1 layer Omega Web® 4 layers M-ASZM 1 layer Omega Web® 1 layer spacer 1 layer Omega Web® 4 layers M-ASZM 1 layer Omega Web®
Filter Media Area	3.75 x 5.25 in.
Air Ducts	1/2-in. diameter semicircle
Air Flow	Dual sided
Edge Sealant	F-70 polyurethane
Spacer	Lumite Style 60617000
AFTP Material	SP-180 polyurea-urethane

The filter media stack (one for each side) is prepared by cutting the media using a die and press. Not only are the media cut, but they also are somewhat crimped together around the cut edge. This crimp provides some stability to the filter stack and aids with the alignment of the filter stacks in the encapsulation mold. The bottom filter stack is positioned into the bottom half of the encapsulation mold followed by the AFTP and insertion of a spacer. The top filter stack is laid upon the AFTP and the top half of the cavity is placed atop the composite filter components. Alignment of components is verified before and during compression of the assembly in the heated press. Once in the heated press, the two-part polymer is simultaneously mixed and injected into the mold cavity. The polymer is allowed to cure in the heated mold for 15 min, and then the filter is removed from the mold. The mold is cleaned and prepared for another run. Filter elements are cured at ambient temperature for 7 days and placed in a vacuum for 2 hr to help remove any residual monomer.

Several trials were required to characterize the performance of the mold. Shakedown production runs were required to properly vent the mold to eliminate air bubbles, determine volume of polymer required in a "shot", determine proper pinch gap and establish proper filter alignment, and release of the part from the mold.

Inherent in any injection molding procedure is the formation of air bubbles. Air bubbles can form primarily due to the inability of air to escape as the polymer fills the voids or due to improper balance of the polymer as it flows. Both problems were encountered with the use of this mold. Minor modification to the mold were made (air vents incorporated) that successfully eliminated the air pockets.

The optimal volume of polymer was determined by trial and error. Too much polymer would cause a high pressure within the mold and potentially cause the polymer to penetrate the filter media beyond the pinch point, rather than flow out through the small vents. Too little polymer would result in a short "shot", leaving voids and if too little, an incomplete seal.

It was not possible to determine the clamping pressure required to prevent impregnation of the active areas of the filter media before the mold was prepared. The mold was designed to allow adjustment of the distance between the two edges of the clamping rings on top and bottom on the mold. The closer the clamping rings, the higher the pressure on a given number of layers.

Initial evaluations of the filter media indicated that about seven layers of M-ASZM filter media between an electrostatic aerosol filter would be needed to meet the performance specifications for the filter. The first trials were made with this array of filter media on each side of the AFTP. In nearly every case, at least one side of the filter would slip inside the clamping rings allowing the sealant to enter the layers of media within the active filtration area. Several iterations were carried out, and it was confirmed that the pinch gap was too narrow for this quantity of material.

Four layers of the filter media and one layer of Omega electrostatic filter were easily encapsulated by the edge sealant. A few filters were made with five and some with six layers of M-ASZM media on each side. The gap between the clamping rings was adjusted (increased) by use of 1/32 and 1/16-in. shims on each side of the mold.

Another criterion for a suitable transition piece is adhesion of the edge sealant for the encapsulation to the material of construction for the transition piece. It was expected that the same material for both would assure this adhesion, but this did not prove to be true. One of the main deterrents to adhesion to the transition piece surface was the residual mold release that interfered with the bonding of the two materials. Several different mold releases were tried in small sample moldings. Cleaning the surface of molded parts with solvent or etching the surface with various strengths of acid were also tried without success. The best mold release system used Permalease 2040, a white coating that is applied directly to the surface of the mold cavity. It has proven to provide easy demolding for more than 30 injections before it needed to be renewed.

In a few cases, small areas of the parts stick to the mold which may result in tearing the part. This can be remedied on a short-term basis by applying a Dupanol soap solution directly to the area to which the part sticks.

Only minor modifications to the mold were made primarily for air venting and pinch gap adjustment which was expected. The mold performed well and the success rate was 90%. There were a few filters that occasionally had an air gap or slight penetration of sealant beyond the pinch point.

### 6.3 Performance Evaluation

A randomly selected subset of the model filter elements were evaluated to determine whether they achieve the performance requirements established in Table 1. The performance of initial filter elements are not representative of the final production process. The first four 4C-XX, 5C-0, and 6C-0 filters were made using a narrow pinch gap, which increased airflow resistance. It is believed that excessive compression altered either the flow behavior through the media and/or distorted the AFTP. The results of the performance evaluation tests are presented in Table 9.

Table 9. Performance Results of the Model Filter Elements

Filter ID	Pressure Drop (mmH <sub>2</sub> O)	Aerosol Penetration (%)	DMMP Gas Life (min)	CK Gas Life (min)
4C-1	28.4			
4C-2	28.4		91	
4C-3	29.4			(a)
4C-4	29.4			
4C-5	26.3			(b)
4C-6	26.3			28
4C-7	27.3	0.58	93	
4C-8	27.3	0.46		(c)
4C-9	25.7			27
4C-10	26.3			
4C-11	24.7	0.63	65	
4C-12	27.8			
4C-13	24.2			
4C-14	23.6			
4C-15	26.3			
4C-16	27.8			
4C-17	27.8		68	
4C-18	28.9			
4C-19	26.8			
4C-20	25.7			
4C-21	(d)			
4C-22	24.7			
4C-23	25.7			
4C-24	24.7			
4C-25	24.7			
4C-26	24.7			
4C-27	24.7			
4C-28	24.7			
4C-29	24.7			
4C-30	24.7			

Table 9. (Continued)

Filter ID	Pressure Drop (mmH <sub>2</sub> O)	Aerosol Penetration (%)	DMMP Gas Life (min)	CK Gas Life (min)
4C-31	25.7			
4C-32	26.8			
4C-33	25.7			
4C-34	25.7			
4C-35	24.7			
4C-36	(d)			
4C-37	26.8			
4C-38	31			
4C-39	25.7			
4C-40	25.7			
4C-41	24.2			
4C-42	25.2			
4C-43	24.2			
4C-44	27.3			
4C-45	25.2			
4C-46	24.2			
4C-47	23.1			
4C-48	24.2			
4C-49	25.2			
4C-50	26.3	0.12		15
4C-51	24.2			
4C-52	27.3			
4C-53	27.3			
4C-54	26.3			
4C-55	25.2			
4C-56	26.3			
4C-57	27.3			
4C-58	28.4			
4C-59	29.4			
4C-60	23.1			

Table 9. (Continued)

Filter ID	Pressure Drop (mmH <sub>2</sub> O)	Aerosol Penetration (%)	DMMP Gas Life (min)	CK Gas Life (min)
4C-61	26.3			
4C-62	25.2			
4C-63	26.3			
4C-64	26.3			
4C-65	25.2	0.41		24
4C-66	25.2			24
4C-67	25.2			
4C-68	27.3			
4C-69	24.2			
4C-70	24.2			
4C-71	24.2			
4C-72	29.4			
4C-73	24.2			
4C-74	24.2			
4C-75	(d)			
4C-76	(d)			
4C-77	23.1			
4C-78	(d)			
4C-79	24.2			
4C-80	24.2			
4C-81	24.2			
4C-82	23.1			
4C-80b	24.2			15
4C-81b	25.2			
4C-82b	25.2			
4C-83b	25.2			
4C-84	25.2			
4C-85	25.2			
4C-86	26.3			

Table 9. (Continued)

Filter ID	Pressure Drop (mmH <sub>2</sub> O)	Aerosol Penetration (%)	DMMP Gas Life (min)	CK Gas Life (min)
5C-0	32.6			
5C-1	29.4			29
5C-2	28.9			
5C-3	33.1			(c)
5C-4	31	0.22	116	
5C-5	31	0.22	110	
5C-6	30.5			14
5C-7	28.4			13
5C-8	29.4			
5C-9	31			31
6C-0	41			
6C-1	31.5	0.083		53
6C-2	31.5	0.092		49
6C-3	31.5			31
6C-4	33.6			
6C-5	34.7			
6C-6	31.5			

- (a) Interferant peak.
- (b) Breathing machine failed.
- (c) Connector leak.
- (d) Filter too poor a quality to test.

### 6.3.1 Airflow Resistance

All filter elements were tested to measure the airflow resistance at a constant flow rate of 85 lpm. Results are contained in Table 9 and are segregated by the number of carbon layers in the stack (e.g., 5C-XX filters have five layers of M-ASZM in each filter stack, and two such stacks comprise a filter element). A summary of these data are provided in Table 10.

The average ( $\bar{x}$ ) airflow resistance for the 4C-XX filters was 25.6 mmH<sub>2</sub>O with a standard deviation (sd) of 1.6 mmH<sub>2</sub>O; the minimum and maximum were 23.1 and 31 mmH<sub>2</sub>O, respectively. For filters with five carbon layers in a stack, the average pressure drop measured was 30.2 mmH<sub>2</sub>O with a standard deviation of 1.6 mmH<sub>2</sub>O. Filter elements with six carbon layers had an average pressure drop of 32.4 mmH<sub>2</sub>O and a standard deviation of 3.5 mmH<sub>2</sub>O.

Based on the airflow resistance results for the filter media (Section 4.1), these airflow resistances are ~20 percent higher than expected. The average airflow resistance of five AFTP was ~8 mmH<sub>2</sub>O, as predicted based on the SLA model AFTP. Therefore, the airflow resistance through the media is higher in the filter than predicted. Each layer of M-ASZM carbon material is expected to increase the airflow resistance by ~2.5 mmH<sub>2</sub>O. The increase in airflow resistance was ~4 mmH<sub>2</sub>O when the layers of carbon were increased from four to five; the resistance increased about another 2 mmH<sub>2</sub>O when a sixth layer was added. The pinch gap of the encapsulation mold was not increased when a fifth layer was added because removal of the shim opened the gap too much, causing the polymer to penetrate past the pinch point. Filters made with six layers had a wider pinch gap and the compression of material was reduced. Earlier shakedown trials indicated that airflow resistance increased significantly more than expected if there was excessive pinching. (See results for 4C-1 through 4C-4, 5C-0 and 6C-0, all produced without shims.)

The design of the filter element was driven by the need to meet the airflow resistance requirement. Therefore, as directed by the Government, filter elements were made with the maximum number of layers (four) of M-ASZM material which would still meet the airflow resistance specification. Layers of M-ASZM were removed even though it would mean the gas life requirements would not be achieved.

Table 10. Summary Statistics of the Airflow Resistance of Demonstrator Filter Elements

Number of Carbon Layers	Filter Count	Air Flow Resistance		
		$\bar{x}$ (mmH <sub>2</sub> O)	sd (mmH <sub>2</sub> O)	Predicted ΔP (mmH <sub>2</sub> O)
4	80 <sup>(a)</sup>	25.6	1.6	22
5	9 <sup>(b)</sup>	30.3	1.4	25
6	6 <sup>(c)</sup>	32.4	3.5	27

<sup>(a)</sup>Excludes filters 4C-1 through 4C-4 because they were manufactured with excessive pinch pressure.

<sup>(b)</sup>Excludes filter 5C-0 because it was manufactured with excessive pinch pressure.

<sup>(c)</sup>Excludes filter 6C-0 because it was manufactured with excessive pinch pressure.

### 6.3.2 DMMP Gas Life

DMMP gas life tests were performed on arbitrarily selected filter elements with four, five, and six layers of M-ASZM. Measured filter lives are presented in Table 9, and a summary is given in Table 11. The average DMMP gas life is compared to the predicted gas life. Predicted gas life assumed 100 percent effective filter area and was calculated from Eq. (2). There is close agreement between the measured and predicted gas life. Each layer of carbon material added about 21 min to the gas life, 3 min higher than predicted. The standard deviation for filter elements with five and six carbon layers is very small. Because only two tests were performed, little confidence can be associated with the accuracy of the average and standard deviation.

The swatch tests were a good predictor of media performance in the filter element. The mass ratio of DMMP to carbon is consistent with the swatch data, but somewhat higher. These results suggest that all of the carbon available is being utilized, which is surprising. Edge effects were anticipated, but were either too small or the edge effect was greater in the swatch test than in a filter element.

Table 11. Summary Statistics of the DMMP Gas Life of Demonstrator Filter Elements

Number of Carbon Layers	Filter Count	DMMP Gas Life			mg DMMP/mg carbon (-)
		$\bar{x}$ (min)	sd (min)	Predicted (min)	
4	4	79	15	72	0.25
5	2	110	4.2	90	0.28
6	2	130	0	108	0.27

To assure the DMMP gas life specification of 110 min is met, six or more layers of M-ASZM material are required in this filter design.

### 6.3.3 CK Gas Life

CK gas life tests were performed on arbitrarily selected filter elements with four, five, and six layers of M-ASZM. Measured filter lives are presented in Table 9, and a summary is given in Table 12.

Table 12. Summary Statistics of the CK Gas Life of Demonstrator Filter Elements

Number of Carbon Layers	Filter Count	CK Gas Life			mg CK/mg carbon (-)
		$\bar{x}$ (min)	Sd (min)	Predicted (min)	
4	6	22	5.6	24	0.072
5	4	22	9.6	30	0.058
6	3	44	12	36	0.096

The average CK gas life was compared to the predicted gas life. The predicted gas life assumes 100 percent effective filter and was calculated from Eq. (3). There is close

agreement between the measured and predicted gas life for filter elements with four carbon layers. The measured CK gas life of filter elements with five carbon layers in a stack is significantly lower than predicted. The average measured CK gas life of filters with five carbon layers is the same as filters with four carbon layers. The 5C-XX filters had a wide variation in measured gas life. Filters with six carbon layers had a significantly longer gas life than predicted: 44 min versus 36 min. Again, significant scatter was present in the data. In all cases, the filters with the lowest CK gas life were tested about 2 months after production and storage in polyethylene bags. Whether storage had an effect on gas life is unknown.

The mass ratio of mg CK adsorbed to mg carbon available for the four carbon layer filter elements is consistent with those values in Table 7 (Section 4.4). The mass ratio for the five and six layer carbon filters differ by nearly a factor of two, but are still consistent with those reported for the C-18 core material used in the M13A2 filter.

To assure the CK gas life specification of 30 min is met, six or more layers of M-ASZM material are required in this filter design.

#### **6.3.4 Aerosol Filtration Efficiency**

A portion of the filters evaluated for CK or DMMP gas life were also evaluated for penetration of  $0.3 \mu\text{m}$  PSL particles at a constant air flow rate of 32 lpm. A summary of these results are presented in Table 13 and are compared to predicted results. Filters tested included those with four, five, and six layers of carbon material.

Aerosol penetration was significantly higher (over an order of magnitude higher) than the specification given in Table 1. The average aerosol penetration was  $\sim 0.44$  percent for the 4C-XX filters, compared to a predicted penetration of 0.029 percent. Based on swatch tests, the predicted aerosol penetration specification would not be met. It is not clear why the measured value is so much higher than that predicted. Because the results are reproducible, a leak in the filter or connection is unlikely. Also, if there was a leak, it would have been detected during gas life tests.

Table 13. Summary Statistics of Aerosol Penetration of Demonstrator Filter Elements

Number of Carbon Layers	Filter Count	Aerosol Penetration		
		$\bar{x}$ (%)	sd (%)	Predicted (%)
4	5	0.44	0.20	0.029
5	2	0.22	0	0.019
6	2	0.088	0.006	0.012

Because the aerosol penetration was significantly higher than predicted and significantly higher than the specification in Table 1, another layer of filter medium is required. One additional layer of particle filtration media is predicted to be sufficient to achieve the penetration requirement.

#### 6.3.5 Thickness

All filter elements, whether they contained four, five, or six layers of carbon in each stack were 2.2 cm thick. This is the thickness of the edge seal. The filter media did not exceed this thickness.

### 6.4 Qualitative Assessment

The quality of filters produced was very good, near final production quality. There were occasional weak spots at the end of the AFTP air ducts. Minor air bubbles (<1 mm diameter) were present throughout the edge seal. Major voids did occasionally exist, but this was due to periodic problems with the injection process. Typically, the edge sealant did not penetrate beyond the pinch point. In instances where there was penetration it was usually 1 or 2 mm beyond the pinch point and was not catastrophic to the filter element.

The filters are aesthetically satisfactory and clean. It is doubtful whether significant improvement could be made with the appearance of a filter element with this design.

The filters are not extremely flexible and could certainly not be folded. This is due to the bulk of the edge seal and material required because of the limited space. The filter is, however, not hard and is not expected to cause injury if impacted against the wearer (e.g., during a fall).

## 6.5 Optimization

### 6.5.1 Improvements

Within the size and material constraints, the filter element developed has been optimized. The primary design goal was to meet the 25 mmH<sub>2</sub>O design specification at the expense of not meeting aerosol filtration efficiency or gas life. Within the size claim given, the filtration materials cannot be configured to meet all of the design criteria.

The resources available for this project did not permit extensive changes to the filter design because the tooling design and fabrication are expensive. After producing over 100 filter elements and evaluating their performance, improvements to the design could be made. These improvements include:

- Redesign of the AFTP to reduce airflow resistance
- Inclusions of nonelectrostatic aerosol filtration medium
- Reduction in edge seal bulk and thickness.

The AFTP design selected contributes eight of the 25 mmH<sub>2</sub>O airflow resistance. The AFTP resistance can be lowered to 4 mmH<sub>2</sub>O by opening the ducts from semicircular to full circular. This was not done in this project because this reduces filter area and the tradeoff was not beneficial (see analysis in Section 5.4.1). The basic design of the AFTP is acceptable, but the next generation AFTP should be further optimized to reduce airflow resistance. The clamping ridge may be made smaller to increase the open area. The ducts that collect air from the manifold and lead to the mask should be redesigned. The cross sectional area of the duct can be increased by changing the geometry of the duct, without reducing filter area, from the current semicircle. This is expected to reduce the airflow

resistance by at least 2 mmH<sub>2</sub>O, enough to add another layer of carbon material or aerosol filtration material without increasing airflow resistance of the filter.

To ensure particle filtration capabilities, the inclusion of a nonelectrostatic aerosol filter medium is required. Electrostatic media are susceptible to adverse effects of high temperature, high humidity or moisture, and loss of efficiency with loading. The selection of Omega Web® over the Filtrete® was an attempt to move away from sensitive electrostatic material. Improved performance (lower airflow resistance of ~2 mmH<sub>2</sub>O and higher aerosol filtration efficiency may be enough to meet the specification) by use of Filtrete®. The Filtrete® medium was not selected because it is not amenable (in the form available to us) to high volume production. It was also susceptible to damage from the high temperature filter molding process.

The bulk and profile of the edge seal may be lowered. The encapsulation mold was designed conservatively to ensure adequate polymer to capture the filtration media. The design assumed that up to eight layers of carbon would be in each filter stack. If the stack contains fewer, then the profile should be lowered. The size of the cavity should be reevaluated to determine whether the amount of polymer can be reduced.

### **6.5.2 Area Effect**

The primary factor impacting the ability to design a filter that meets performance specifications is the size constraint. The materials cannot perform adequately to achieve required performance specifications within the area available. The impact that filter area has on the performance is assessed below. As an example, an analysis has been performed that assumes the length and width of the filter can each be increased by 0.5 in. The total filter cross sectional area (both sides) would then increase from 40 in.<sup>2</sup> to 49 in.<sup>2</sup> (255 cm<sup>2</sup> to 315 cm<sup>2</sup>). Other aspects of the AFTP remain the same. (The outer dimension of the filter would increase to 5 x 7 in.)

### 6.5.2.1 Aerosol Penetration

Increasing the area will have little effect regarding aerosol penetration. Aerosol penetration will decrease as the velocity decreases, but not enough to significantly impact performance within the velocity range studied. To decrease aerosol penetration, an additional layer of material is needed on each side of the filter. An additional layer of Omega Web® will increase the airflow resistance by about 2.0 mmH<sub>2</sub>O in the current filter design. Therefore, the impact of adding this layer is further discussed in the next section.

### 6.5.2.2 Airflow Resistance

The airflow resistance is highly dependent upon the available filter area. The results presented in Section 4.1 can be used to predict the effect of increasing filter area or addition of filter media. Although the results from Section 4.1 underestimated the airflow resistance in the filter, the results can be used to estimate filter performance.

Increasing the filter area from 255 cm<sup>2</sup> to 315 cm<sup>2</sup> will decrease the velocity through the filter media by the same proportion. A flow rate of 21.5 lpm through 80 cm<sup>2</sup> of material is equivalent to 85 lpm through 315 cm<sup>2</sup>. So, from Figure 1, this reduction in velocity causes a 20 percent reduction in airflow resistance through the material. (Although the data in Figure 1 underestimate actual performance in a filter, the relative reduction in resistance is assumed to hold.) On average, the airflow resistance through the filter media of the 4C-XX filters is 18 mmH<sub>2</sub>O (8 mmH<sub>2</sub>O is the contribution of the AFTP). The increase in area will then reduce the airflow resistance of the material to ~ 14 mmH<sub>2</sub>O. The airflow resistance of a 4C-XX filter would then be 22 mmH<sub>2</sub>O.

For filters with 315 cm<sup>2</sup>, each layer of carbon material is expected to increase resistance by ~ 2 mmH<sub>2</sub>O. Therefore, two additional layers of carbon material could be added and the resistance of the larger filter would be ~ 26 mmH<sub>2</sub>O. This result is confirmed using the current 6C-XX filters. The resistance of the media in those filters is 24 mmH<sub>2</sub>O and a 20 percent reduction would mean the resistance is 19 mmH<sub>2</sub>O. Adding the 8 mmH<sub>2</sub>O for the AFTP and the predicted resistance is 27 mmH<sub>2</sub>O. The addition of a single layer of Omega Web® to each side of the filter would increase resistance by ~ 1.5 mmH<sub>2</sub>O. So, a

single layer of Omega Web® and M-ASZM could be added to the filter and still meet the resistance specification. This approach would achieve the aerosol penetration specification.

#### 6.5.2.3 DMMP Gas Life

The increase of filter area by 60 cm<sup>2</sup> (255 cm<sup>2</sup> to 315 cm<sup>2</sup>) has to be multiplied by the number of layers of M-ASZM to obtain the increase in total area for adsorption. Thus, the increase of 240 cm<sup>2</sup> (four layers x 60 cm<sup>2</sup>) is nearly equivalent to an additional layer (255 cm<sup>2</sup>) in the current design. The 240 cm<sup>2</sup> increase in area of a four-layer carbon filter is expected to add ~16 min of DMMP gas life. This would increase the gas life to ~95 min for the larger filter.

From the airflow resistance analysis, it was shown that at least one layer of M-ASZM could be added to each side of the filter if the filter area is increased. Using Eq. (2), the predicted gas life of a single layer with  $S_F = 315 \text{ cm}^2$  is predicted to be 22 min. Therefore, a five-layer carbon filter should give the required 110 min gas life; a six-layer carbon filter would exceed the required life. Eq. (2) underestimated performance in the filter elements. So, using the filter results and the fact that available filter area is increased by ~24 percent, the gas life of a five-layer carbon filter should also increase by 24 percent or from 110 min to 135 min.

#### 6.5.2.4 CK Gas Life

The analysis for the effect of CK gas life is identical to that presented for DMMP gas life in Section 6.5.2.3. The increase in filter area of a four-layer carbon filter is expected to add ~5 min to the CK gas life. This would increase the gas life of a four carbon layer filter to ~27 min. An additional layer of carbon material in the larger filter would yield a filter with a ~35 min CK gas life. Because the five carbon layer filters had CK gas lives similar to the four carbon layer filters, the sixth carbon layer would be required to give the necessary CK gas life.

#### 6.5.2.5 AFTP

The above analysis assumed that the larger size was used to increase the open area for the filtration media. Alternatively, the 0.5 in. increase in filter width could be used to make the air duct cross section circular instead of semicircular. The filter length would still be increased by 0.5 in. The result would be a filter with available area of  $3.75 \times 5.75$  in. ( $43 \text{ in.}^2$ ) or  $9.5 \times 14.6$  cm ( $280 \text{ cm}^2$ ). Although the filter area increase is not as large, the AFTP design results indicate that the airflow resistance will be lowered from  $\sim 8 \text{ mmH}_2\text{O}$  to  $\sim 4 \text{ mmH}_2\text{O}$ .

Using the same analyses as above, an additional layer of Omega Web® and M-ASZM could be added and the predicted airflow resistance of the filter would be  $24 \text{ mmH}_2\text{O}$ . The addition of a sixth carbon layer would increase the predicted resistance to  $26 \text{ mmH}_2\text{O}$ . The sixth layer of carbon would be needed to assure the CK and DMMP gas lives are meet. In this alternative filter design, the predicted CK and DMMP gas lives are 40 and 140 min, respectively. This approach indicates better filter performance rather than strictly increasing area and not modifying the AFTP.

## **7.0 ELECTRONIC SYSTEMS**

In addition to preparing the demonstration electronic system, a secondary objective was to identify component and subsystem enhancements necessary for the final fielded RESPO 21 system. These recommendations, along with other improvements defined by ERDEC as the brassboard systems were evaluated, formed the basis of this follow-on development phase. This effort was broken down into six major tasks:

- Task 1. Communications Assist Subsystem Refinements
- Task 2. Miniature Blower Subsystem Refinements
- Task 3. Power Source Subsystem Refinements
- Task 4. Integration and Fabrication of Prototype System
- Task 5. Evaluation and Testing of Prototype System
- Task 6. Production of Prototype Units.

Each of these tasks is made up of various subtasks which formed the basis of the refinement effort for each subsystem.

### **7.1 Communications Assist Subsystem Refinements**

Refinements to the communications assist subsystem formed a substantial portion of this development effort. Refinement areas to be covered included feedback elimination, VOX circuit evaluation, noise filtering, volume adjust considerations, communications output compatibility, microphone compatibility, component selection analysis, and circuit miniaturization.

#### **7.1.1 Feedback Elimination**

For evaluation purposes early in the program, a preliminary communications package was assembled. This unit was used to identify potential feedback frequencies and associated parameters. Common feedback signals were found between 2 and 7 KHz. Efforts to filter single feedback frequencies revealed that other feedback paths were likely to form. Due to the wide potential feedback bandwidth, efforts involving signal phase mismatching

were also abandoned. The project team therefore evaluated AGC (automatic gain control) circuitry to actively block potential feedback loops. Two monitoring points were considered for tracking feedback signals, high level audio signals outside of the voiceband and power from the battery. After further evaluation and lack of good results tracking feedback by battery drain, efforts were directed towards the use of high level audio input signals to lower amplifier gain and eliminate potential feedback loops. Phase-Locked Loop (PLL), Voltage-Controlled Amplifier (VCA), and other ancillary circuit components were purchased and evaluated. Identification of feedback revolved around the use of PLL circuits which detect and lock onto the pure sinusoidal signals associated with feedback tones. Using PLL circuitry, feedback signals were found to be discernable from normal voice, which contains broadband frequency content.

It was determined that a proper voiceband includes frequencies of 350 to 3600 Hz (see noise filtering section for voiceband tests), but most of the voice content falls between 500 and 1500 Hz. Given that most of the potential feedback loops occur at frequencies greater than 2000 Hz, a feedback detection and control scheme which revolved around attenuating the high end of the normal voiceband frequencies where feedback usually occurs was developed. A final design was created which effectively detects and eliminates feedback with only subtle changes to the voice quality. A fourth order high pass filter was used along with a Maxim MAX291 controllable lowpass filter to create a switchable bandpass filter. The current filter has a normal passband of approximately 350 to 3600 Hz but changes to a passband of approximately 350 to 2000 Hz when feedback is detected, eliminating feedback signals ( $> 2000$  Hz). A CMOS 4046 phase-locked loop (PLL) circuit is used to detect feedback. Through filtering, the output of the PLL is converted to a logic signal which trips a one-shot timer upon detection of feedback. The timer automatically switches the bandpass filter into the feedback elimination mode and holds it there for a specified interval (currently 8 sec). This circuit was tested and found to detect and eliminate feedback with only a subtle temporary change to the voice transmission quality.

### **7.1.2 VOX Circuit**

The potential need for a voice-activated transmit capability for the communications assist subsystem was evaluated. A VOX circuit can allow enhanced battery life and eliminate background noise when the user is not speaking but can also cause a transmission delay at the beginning of speech. These trade-offs were evaluated to determine whether a VOX circuit should be designed into the prototype communications package.

Using spectral analysis software and equipment, work was performed in the area of analysis of human voice. This analysis was very helpful in limited characterization of voice and potential noise floors. The analysis showed that a VOX circuit threshold could likely be chosen which would allow system output only during speech. However, the time delays associated with VOX circuits proved to be somewhat cumbersome during conversation. Also, the use of a VOX circuit for elimination of local noise (i.e., blower noise) processed through the communications system does not provide any real advantage. Since the communications assist device is designed mainly for clarity and provides only minimal voice amplification, personnel within audible range will hear the local noise directly anyhow. The only potential advantage exhibited by a VOX circuit would therefore be for the use of field and crew radios which transmit out of the local audio range. However, since these interfaces include PTT (push-to-talk) already, the VOX again becomes useless. For these reasons, a VOX design for the communications assist subsystem was not implemented.

### **7.1.3 Noise Filtering**

One of the potential enhancements to the communications system involved further investigation and analysis of the audible noise generated by the airflow from the blower and other ambient noise sources.

Using spectral analysis software and equipment, work was performed in the area of analysis of human voice. Signals analyzed included voices recorded using the previous RESPO 21 system (with and without a blower) as well as voices from the radio and those of various members of the current project team. Examples of the analysis of voice and blower noise are given in Appendix E. This analysis was very helpful in limited characterization of

voice and potential blower noise. The analysis was also very helpful in the evaluation of potential system noise reduction.

Isolation of blower noise from early versions of the system indicates that it contains multiple peaks, some of which are located within the normal voice band. Potential filtering schemes that would minimize the amplification of blower noise while passing enough voice signal to provide good voice quality and clarity were performed. The new filter circuits designs included much steeper roll-off than the single pole filtering scheme used on the previous system. This provides better rejection of signals outside of the desired voice band. Due to variable blower speeds, uncertainty of the blower to be used, the potential presence of broadband blower noise, and the lack of a well-defined blower interface (plumbing) at the time that the communications filter design needed to be complete, it appeared likely that much of the blower noise reduction effort would need to be in the area of good acoustical design or adjustment to the blower subsystem and interface. Working with the new blower plumbing mock-up provided by ERDEC, it was found that the audible noise generated by airflow through the corrugated tubing varies greatly as the tubing is compressed or flexed. Isolation of blower noise from the previous system indicated that it contains multiple peaks with stronger peaks ranging around 2500 to 2700 Hz with a bandwidth of 300 to 500 Hz. Since the new blower system was to provide higher airflow than the previous system, it was anticipated that the strongest noise peaks would be pushed above the standard voiceband. After various filter designs were evaluated, a final design was completed using a fourth order high pass filter along with a Maxim MAX291 eighth order controllable lowpass filter to create a switchable bandpass filter. The final filter design has a normal passband of approximately 350 to 3600 Hz, but temporarily changes to a passband of approximately 350 to 2000 Hz when feedback is detected, eliminating feedback signals ( $> 2000$  Hz). This filtering scheme yields clear voice output and eliminates noise signals outside of the voiceband. An additional lowpass filter was added to the circuit with a cutoff frequency of about 50 KHz to eliminate high frequency noise created by feedthrough of timing signals generated for the MAX291 switched-capacitor filter. The final filter and amplifier design yields very good signal to noise ratios.

#### 7.1.4 Volume Adjust

The RESPO 21 brassboard communications system included a logarithmic full range volume adjust circuit. This allowed the user to set the volume between zero and a setting which is about twice as loud as unaided speech. For more repeatable control settings and to prevent inadvertent volume changes, a multi-position switch with positive user feedback ("click") was preferred. The volume adjust circuit was to be evaluated to determine which method, full range or switched, is most appropriate. The necessary number of settings (switch method) as well as the overall volume range was studied to identify and implement an optimal volume control design.

A variety of volume adjust systems were evaluated considering control, repeatability, ruggedness, size, and moisture resistance. It was indicated at the kick-off meeting that a rotating switch with on/off and two or three distinct volume positions was desirable. Several water-resistant candidate switches were identified which would be compatible with ongoing designs. An output amplifier with a voltage-controlled gain (Phillips TDA7056A) was initially considered but was eventually dropped as a candidate due to its sensitivity to the voltage at the control input. It was found that battery voltage dips associated with high source currents at high volume output settings caused the system to oscillate and added additional noise to the voice signal. A companion component (TDA7056), which is similar but provides a constant 40 dB gain, was evaluated and found to perform very well for this application. Volume control design then shifted to op-amp gain settings by switching in different series resistances to a simple inverting gain stage with a constant feedback resistance. This control circuit was designed to allow the use of various break-before-make switches without any associated "popping" sound during changing of switch position. The use of discrete resistors to set the output volume per each switch setting also provides adjustment flexibility. An appropriate waterproof Grayhill switch (Model 50N36-01-2-05N) was identified and ordered for the volume control circuit. The final volume control design includes five positions: off, low volume, medium volume, high volume, and field radio. The field radio switch setting allows the user to turn off the communications speaker output when transmitting through the field radio interface.

### 7.1.5 Communications Output Compatibility

One of the desired improvements for the prototype RESPO 21 communications units was to eliminate a separate field radio interface box. Therefore an output stage for the communications assist circuit, which would allow the system to directly interface to a representative field radio, was designed.

The Bendix/King LPI 5142 radio was identified as an appropriate demonstrator field radio. This radio is an enhanced commercial version of the PRC-127 military radio. Two radios, two ear mics, a rapid charger, and a service manual were ordered. Information was acquired from technical personnel at Bendix/King concerning the microphone input circuit impedance and normal signal levels so that an interface circuit between the communications unit and field radio could be designed while waiting for the radios to arrive. Once the radios were received, the design was completed and tested. The communications subsystem output was connected into the field radio through alteration of the standard interface cable and circuit such that the hand-held radio's PTT button and speaker could be used with an external signal source (RESPO 21 communications unit). The interface design was adjusted for appropriate volume levels and found to perform well with good reception on the receiving radio.

### 7.1.6 Microphone Compatibility

An interface cable was to be designed so that the mask microphone could be plugged directly into the microphone input in military crew radios. The cable was originally to be designed such that the mask microphone could be used in vehicles which normally use electret or dynamic microphones. The specific design however was set up for an interface unit which normally interfaces to dynamic microphones.

The Gentex model 3063 microphone was selected for use in the communications assist subsystem. Investigations showed that the normal crew helmet has an input connection from its standard dynamic boom microphone to the CVC control circuit. Plugging the mask microphone (with interface circuitry) directly into the control box allows the user to control PTT and intercom functions as normal. An in-line Fischer cable receptacle was identified

and ordered which is compatible with the microphone output plug. The signal from the crew helmet's dynamic microphone was analyzed to determine appropriate output levels. With a low voltage battery power, the electret microphone was analyzed and determined to have a higher output level. A simple resistive divider network was then designed to cause the electret output to be at the same level as the dynamic output. The batteries and interface circuit were put into a cable for two demonstrator units. These interface cables, via the in-line receptacles, accept the standard mask output cable termination plug (which normally connects to the microphone input receptacle on the communications subsystem), and provide a compatible output on the standard AstroCom connector that is currently used on the crew helmet. With this interface, a mask wearer can plug into the standard crew radio interface and use the mask microphone for all communication.

### **7.1.7 Component Selection Analysis**

The ancillary component evaluations that were performed during the brassboard phase of the RESPO 21 development were revisited during the prototype development effort to determine the potential for improvements in component choices. The microphone, speaker, connectors, and cables choices were scrutinized during this evaluation.

Various microphones, speakers, and connectors were evaluated for potential use in the communications subsystem. The microphone evaluation led to about three potential candidates, including the Gentex microphone that was used during the previous phase. The speaker evaluation included slim moisture-resistant speakers, including the mylar cone speakers. The most effort was put into the identification of new connectors which are moisture-resistant and sturdier than those used on the previous system. This led to the identification of four or five candidates. The Gentex model 3063 microphone was selected due to its small size and good output clarity. An ultraslim mylar speaker was also selected because of its moisture-resistance and small size. These speakers have been found to provide output volume and clarity which rivals paper cone speakers, which are several times as large. Early enclosure layouts indicated a need for a rear-mounted receptacle. This, coupled with excessive lead times and other issues, limited the choices to only a few. The leading candidate, and ultimately the set chosen for use, was the W.W. Fischer sealed connector pair

(SE102 and DBPE102 series). Initially, a retractile cable by AstroCom was desired, but this cable would be custom-made. A similar, but longer and thicker, retractile cable made by Belden (Type 9466) was identified and deemed to be a reasonable alternative to the AstroCom cable. The cables were ordered and received for evaluation. Further analysis indicated that these cables were too long and would be more appropriate if cut in half. These cables, which have three conductors (one shielded), were used for both the communications and blower units. The shielded conductor was used for the microphone output signal to the communications unit to minimize interference from external noise sources. The remaining two conductors connect power and ground to the electret microphone. The shield was connected with the ground conductor to the circuit board ground plane. The Belden cables mated well with the Fischer connectors and formed a much more robust system interconnect than that represented by earlier units.

### **7.1.8 Circuit Miniaturization**

Once the communications circuit was redesigned to include the additions and improvements outlined above, the circuit was analyzed to determine a layout that minimized its size. This included the utilization of surface mount technology for optimal size reduction.

While the communications circuit designs were in their early stages, little effort was placed into circuit miniaturization. Circuit design and component selection, however, included the consideration of parts minimization and surface mount availability. Also, where possible, parts were used which have military-approved replacements with the same or similar form, fit, and function. As the communications circuit design neared completion, work turned toward component packaging and circuit board layout issues. The goal was to fit the communication subsystem within the same basic package outline as that used for the blower subsystem. Because of the number of circuit components (over 100), the internal space constraints created by the battery, speaker, switch, and connectors, and the need for a low noise circuit layout, the printed communications circuit board design became fairly complex.

Once the layout for the communications PCB (printed circuit board) was completed, the appropriate design was sent out for board fabrication. The boards were completed and

returned to Battelle for component population. One board was populated and evaluated. The miniaturized circuit was found to have more noise on the virtual ground plane than the plugboard test circuit. This caused the feedback detect circuit to have some difficulty in locking onto loop signals. A  $1.0 \mu\text{F}$  capacitor was placed between the virtual ground and analog ground to eliminate the noise.

It should be noted that this circuit design could be even further miniaturized through an application specific integrated circuit (ASIC) design or the use of a Multi Chip Module (MCM) which forms much of the total circuit into one integrated circuit (chip). Miniaturization to that level was viewed as outside of the scope of this program but could be considered for future designs.

### **7.1.9 Performance Characteristics**

**7.1.9.1 Microphone.** The microphone of the communications circuit is a Gentex Model 3063 electret capacitor microphone. It has a frequency response of 100 to 5000 Hz, output impedance of  $\approx 3$  Kohms, supply voltage of 1.2 to 20 V, and nominal current drain of  $40 \mu\text{A}$ .

**7.1.9.2 Amplifier.** The amplifier circuit of the communications subsystem features a TDA7056 integrated mono audio power-amplifier, manufactured by Philips Semiconductors. The TDA7056 has a power rating of 3 W and a fixed voltage gain of 40 dB.

**7.1.9.3 Noise Reduction Filter.** Noise reduction filtering in the communications subsystem is accomplished with a fourth order, high pass, Chebyshev filter in series with an eighth order, low pass Chebyshev filter. The resulting band pass filter has a transmission range of approximately 350 to 3600 Hz, designed to pass voice frequencies, while eliminating blower and other background noise.

**7.1.9.4 Feedback Elimination Circuit.** The feedback elimination circuit of the communications subsystem controls feedback interference in the frequency range between

2000 to 3600 Hz, typically where feedback occurs in the RESPO 21 system. As feedback is encountered, the feedback elimination circuit immediately attenuates the high frequency signals, temporarily reducing the transmission range to 350 to 2000 Hz. The reduced transmission range is active for 8 sec and then the former frequency range, 350 to 3600 Hz, is reactivated.

**7.1.9.5 Volume Control.** Volume control is provided by a manual adjustment knob with three volume settings, low, medium, and high. A fourth control knob setting disconnects the speaker, enabling the field radio interface.

**7.1.9.6 Power Source.** Power for the communications subsystem is provided by a single Ultralife NEDA 1604LC nine volt, lithium battery. The Ultralife battery is made of a lithium manganese chemistry, rated at 1.2 Ah to 5.4 V at 900 ohms, and has a maximum discharge rate of 120 mA continuous.

Power consumption of the communications subsystem is designed to be minimal and was measured at approximately 0.4 to 1.3 W, 8.5 V at 45 to 150 mA.

Based upon the measured current draw by the communications subsystem and further analysis, these goals should be easily met with expected battery life at 20 plus hours at room temperature using the lithium batteries.

**7.1.9.7 Low Battery Warning Circuit.** The low battery warning circuit of the communications subsystem monitors the voltage level of the battery and activates an indicator when the battery voltage falls below approximately 5 V. The low battery LED was tested and comes on at 5.0 V and goes back off at 5.3 V (hysteresis effect).

The battery warning indicator is an ICL8211 LED, manufactured by Harris Semiconductor. It sinks 7 mA of current when the battery falls below the preset voltage level and remains activated continuously until the battery is replaced.

**7.1.9.8 Speaker.** The output speaker of the communications circuit is an MG Electronics Speaker Model MSC-299M. It is an 8 ohms, mylar speaker, with a power rating of 0.2 W continuous.

**7.1.9.9 Radio Interface.** The communications subsystem interfaces to a military field radio system which permits remote communication. The microphone of the communications subsystem is compatible with the military field radio system, and replaces the microphone of the field radio. The fourth setting on the communications volume control knob disconnects the speaker of the communications subsystem and enables the field radio interface. This prevents output interference between the communications subsystem and the field radio system.

## **7.2 Miniature Blower Subsystem Refinements**

Refinements to the miniature blower subsystem were predominantly in the area of control efficiency and design miniaturization. Areas to be covered included a blower/airflow study, design of an improved drive circuit, component selection analysis, and circuit miniaturization.

### **7.2.1 Blower/Airflow Study**

Micronel's Model V301MS-6V blower was chosen for the brassboard system. This study was to focus on the tradeoffs of increased air flow versus the expected life reduction associated with these larger blowers. Other blowers, including Micronel's brushless blowers, were also investigated as well as the feasibility of a custom blower design for this prototype development effort.

Various Micronel blowers were evaluated including the V301MS, V361MS, and V461LS. The V361 is a larger version of the V301 (1.2 versus 0.84 W) used in the earlier system. The V361 blower does not quite meet the design goals for air flow output against a pressure head, and furthermore, would not likely meet the running time goal. The V461LS was touted as Micronel's most efficient blower with a new high performance housing design. Few air flow data were available from the manufacturer. Airflow tests indicated that the V461LS blower delivers airflow commensurate with the V361 at about 65 percent of the energy consumption. The V461LS blower is shorter but wider than the V361 blower. It was also noted that all of the Micronel blowers show an operational temperature range of -20

to 65°C and would therefore have some difficulties at the -25°F (-31.7°C) temperature specified in the statement of work. Additional tests showed that the V361 blower drew over 1.6 W (270 mA at 6 V) when operated at zero pressure head. This blower came close to meeting the design goals for air flow versus pressure head only when overdriven at 8 to 9 V and would not meet the running time goal using the identified power source.

Blowers investigated include the V series blowers, the U series radial blowers, and Micronel's line of brushless blowers. A Micronel technical representative indicated that their model V641LS blower could meet the design requirements with the available power, and, if necessary, they could provide a custom blower with an operational temperature range lower than the normal -20 to 65°C. It was determined that the -20°C temperature limitation was acceptable and would not need to have custom blowers manufactured. Small, open-loop stepper motors can be used in blowers. It was found that these motors are not acceptable for this application due to their higher power requirements which could not be supported by the available power source. After a thorough evaluation, the most promising blowers to proceed with were the Micronel V461LS and the smaller V301MS.

### **7.2.2 Improved Blower Drive Circuit**

Since the blower used in the brassboard development was most likely to be operated near the batteries' output voltage, a low dropout linear voltage regulator was used. The linear design is relatively efficient when the regulator output is expected to be set close to the supply voltage minus the regulator dropout voltage. As it becomes necessary to run the blower at reduced voltage settings, the linear design becomes relatively inefficient. The prototype blower control system was to be redesigned around a switching regulator or pulse-width-modulated controller, yielding a circuit which is highly efficient at any blower voltage setting. This evaluation also included further evaluation of the need for variable blower speeds and determination of appropriate user settings and subsystem miniaturization considerations.

Various switching regulator circuits were evaluated as potential replacements for the linear regulator circuit utilized in the previous system. One circuit, designed around a Linear Technology buck-regulator (part number LT1072MJ8) was assembled and found to

perform favorably with efficiencies in the 80 to 90 percent range, depending on the output voltage. New information indicated that Linear Technology offered an improved efficiency device with a built-in low battery detection circuit. This component, along with two other recent releases, was also evaluated for the blower control subsystem. It was later discovered that these new parts were not yet commercially available and they were therefore abandoned. The circuit design that was being tested around an existing Linear Technology buck-regulator was therefore finalized and put into a breadboard system. This design was thoroughly tested with various blowers and found to perform very well.

### **7.2.3 Component Selection Analysis**

The ancillary component evaluations that were performed during the brassboard phase of the RESPO 21 development were revisited during the prototype development effort to determine the potential for improvements in component choices. For the blower control subsystem, these components included the connectors, switches, and cabling.

After some evaluations were performed, it appeared that the blower subsystem could suitably utilize the same connector and switch as that used for the communications subsystem. The only potential foreseen differences would be in the area of pin type and count, potential need for right angle versus straight mounting, and number of positions on the switch. The connectors chosen for the blower subsystem are the W.W. Fischer sealed connector pair (SE102 and DBPE102 series). The switch used by the blower subsystem is the Grayhill sealed switch model 50MP45-01-2-04N. The cable chosen was the Belden type 9466 retractile cable, also used for the communications subsystem. The blower, needing only power and ground, used only two of the three cable conductors. Power to the blower was run through the shielded conductor to minimize noise transmission. The shield for that conductor was run through the third pin of the Fischer connector and grounded at the circuit board.

#### **7.2.4 Circuit Miniaturization**

Once the blower control circuit was redesigned to include the additions and improvements outlined above, the circuit was analyzed to determine a layout which minimized its size. Although the blower control circuit was expected to be inherently small, miniaturization did include the use of surface mount technology for optimal size reduction. Also, due to minimal circuit complexity, much of the size reduction of the blower subsystem was to be achieved through custom packaging considerations.

While the blower circuit design was in its early stages, little effort was placed into circuit miniaturization. Circuit design and component selection, however, included the consideration of parts minimization and surface mount availability. Also, where possible, parts were used which have military-approved replacements with the same or similar form, fit, and function.

The design of the blower control board included the use of board-mounted flexible battery contacts so that the batteries could be pressed directly against the board for minimized connection spacing and easy battery replacement. Also, the rear-mount switch and connector were mounted directly to the board to maximize the efficient use of spaces within the enclosure. The board was designed with the appropriate shape and size to fit directly over the three batteries chosen for use.

Once the layout for the blower controller PCB (printed circuit board) was completed, the appropriate design was sent out for board fabrication. The boards were completed and returned to Battelle for component population. The blower controller printed circuit boards were tested and found to perform very well.

#### **7.2.5 Performance Characteristics**

**7.2.5.1 Blower.** Two unique blower subsystems were designed, each with a different size and capacity. The smaller capacity blower subsystem is designed to meet minimum package size requirements, while the larger capacity blower subsystem is designed to achieve maximum airflow requirements.

The smaller blower subsystem is designed with a Micronel V301MS blower. It has a power rating of 0.84 W, voltage rating of 6 V, and current rating of 140 mA. The output of the blower at a pressure drop of 30 mm H<sub>2</sub>O is unknown. Attempts to measure this output with a representative load provided varying results. Actual output levels will be determined when the final blower interface is designed at ERDEC.

The larger blower subsystem is designed with a Micronel V461LS blower. It has a power rating of 1.2 W, a voltage rating of 6 V, and a current rating of 200 mA. The output of this blower at a pressure drop of 30 mm H<sub>2</sub>O is also unknown as attempts to measure it with a representative load provided varying results. Micronel has however provided data sheets (see Appendix E) for the V461LS blower which indicate that it will deliver at least 2 CFM at 30 mm H<sub>2</sub>O.

**7.2.5.2 Airflow Control Circuit.** The airflow control circuit functions as a low dropout voltage regulator. It features an on/off control as well as the choice of three airflow/voltage levels. Airflow performance is dependent upon the blower size and voltage level:  $V_{out} = 4, 5, \text{ or } 6 \text{ V}$ , via a rotary switch. To verify circuit functionality, the three voltage outputs were measured for each unit and are given in Table 14.

**7.2.5.3 Low Battery Warning Circuit.** The low battery warning circuit of the blower subsystem monitors the voltage level of the blower subsystem battery pack and activates an indicator when the battery voltage falls below approximately 6 V. The low battery LED was tested and comes on at 6.0 V and goes back off at 6.2 V (hysteresis).

The battery warning indicator is an ICL8211 LED, manufactured by Harris Semiconductor. It draws 7 mA of current when the batteries fall below the preset voltage level and remains activated continuously until the battery is replaced.

Table 14. Voltage Output at Low, Medium, and High Air Flow Settings of the Blower Subsystems Produced

Blower Number	Blower Voltage Output Setting		
	Low (V)	Med (V)	High (V)
1	4.16	5.16	6.06
2	4.16	5.15	6.08
3	4.13	5.12	6.04
4	4.18	5.21	6.12
5	4.16	5.14	6.07
6	4.16	5.16	6.08
7	4.17	5.15	6.09
8	4.20	5.23	6.14
9	4.18	5.18	6.11
10	4.17	5.16	6.09
11	4.18	5.21	6.12
12	4.18	5.16	6.09
13	4.16	5.14	6.07
14	4.17	5.19	6.10
15	4.20	5.19	6.11
16	4.16	5.16	6.08
17	4.18	5.17	6.10
18	4.14	5.12	6.07
19	4.19	5.20	6.11
20	4.17	5.20	6.09
21	4.15	5.15	6.04
22	4.12	5.11	6.03
23	4.17	5.20	6.09
24	4.15	5.17	6.07

Table 14. (Continued)

Blower Number	Blower Voltage Output Setting		
	Low (V)	Med (V)	High (V)
25	4.13	5.15	6.07
26	4.12	5.14	6.03
27	4.19	5.19	6.12
28	4.16	5.14	6.07
29	4.17	5.20	6.15
30	4.17	5.15	6.08
31	4.16	5.17	6.09
32	4.16	5.16	6.07
33	4.19	5.18	6.12
34	4.15	5.17	6.05
35	4.14	5.16	6.05
36	4.18	5.20	6.10
37	4.16	5.19	6.08
38	4.17	5.17	6.10
39	4.17	5.17	6.09

**7.2.5.4 Drive Circuit Efficiency.** The blower subsystem is designed to achieve maximum drive circuit efficiency. A switching voltage regulator design was selected to achieve 85 percent drive circuit efficiency at the highest airflow level. Drive circuit efficiency is greater than 85 percent at the lower airflow levels.

## **7.3 Power Source Subsystem Refinements**

Evaluations of the power source subsystem included a battery study, evaluation of mission power requirements, and power source testing.

### **7.3.1 Battery Study**

Batteries for both the communications assist and miniature blower subsystems were evaluated. The main thrust of this evaluation was directed toward identifying a standard U.S. military battery suitable for implementation into the system.

Because of modularity issues and electrical noise generated by the blower control circuit, it was likely that the communications and blower subsystems would each have their own power source. However, an effort was to be made to utilize the same type of battery for both subsystems. Since the blower control circuit was likely be the limiting factor regarding battery life and associated mission durations, much of this effort involved developing an integrated power source design which will minimize blower control package growth. This effort included an attempt at identifying appropriate standard, military batteries for the blower and communications subsystems. The team was unable to identify a military battery that met the system needs. The battery evaluation led to two candidates: (1) the 9 V Ultralife lithium-manganese dioxide batteries used in the earlier system and (2) a line of 9 V lithium-thionyl chloride batteries (multiple manufacturers). The thionyl chloride batteries provide 1.6 Ah (versus 1.2 Ah for the Ultralife) but only provide about 7.0 to 7.4 V open circuit (versus 9.0 V for the Ultralife). Further review of the battery data sheets showed that the thionyl chloride batteries are strictly designed for low current applications with quickly decreasing amp-hour (Ah) ratings as current draw increases. The battery study therefore led back to the 9 V Ultralife lithium batteries for both the communications and blower subsystems.

### **7.3.2 Mission Power Considerations**

Along with the battery study, the operating conditions under which the power sources must function to help evaluate operational life expectancies were studied. Since battery life is directly related to temperature, especially for lithium type batteries, reasonable operational temperature extremes for the blower subsystem were to be investigated in an effort to minimize the size and/or number of batteries used. Operational considerations for the communications subsystem were to include determination of typical operating scenarios, such as average volume settings and speech duty cycles, to help determine peak and average power consumption.

At room temperature, measurements were taken of the final communications unit to indicate typical current draw. The unit draws 40 mA with no speech and 45 to 150 mA peak with low to high volume speech and volume settings. If the worst case were assumed so that the user would be talking loudly into the unit constantly, the battery would last 6 to 8 hr (using the 1.2 Ah rating given for the battery). Under circumstances where the user is only speaking part of the time the battery should last 20 to 25 hr (using a 45 mA average current draw).

At room temperature, measurements of current draw were also taken of the blower unit using both the large and small blowers. The large blower causes the blower control unit to draw 65 mA at the low setting, 108 mA at the medium setting, and 156 mA at the high setting. The small blower causes the blower control unit to draw 60 mA at the low setting, 96 mA at the medium setting, and 142 mA at the high setting. The blower control unit draws 8 mA with no blower attached at all settings. It should be noted that, since the final blower plumbing arrangement is yet to be determined, these tests were performed without the appropriate pressure on the intake and output side of the blower. The actual current draws will increase when the blowers operate against pressure.

### 7.3.3 Power Source Testing

Power for the blower subsystem is provided by three Ultralife NEDA 1604LC nine volt, lithium batteries. The Ultralife battery is made of a lithium manganese chemistry, rated at 1.2 Ah to 5.4 V at 900 ohms, and has a maximum discharge rate of 120 mA continuous.

Power consumption of the blower subsystem is dependent upon the blower size and the selected voltage level. Power consumption levels are provided in Table 15.

Table 15. Power Consumption of Blowers as a Function of Blower Setting

Blower	Blower Setting (V)	Current Draw (mA)	Power (W)
V301MS, 0.84 W	4	60	0.24
	5	96	0.48
	6	142	0.85
V461LS, 1.2 W	4	65	0.26
	5	108	0.54
	6	156	0.94

Battery life of the blower subsystem is largely determined by the blower size and the airflow level at which it is operated, i.e., low, medium, high. When the smaller capacity blower subsystem, V301MS, is operated at the high voltage level, 6 V, the required battery lives should be achieved (see Table 3).

The batteries that were chosen for system implementation were to be tested to verify peak current and useful life expectations. One blower control unit was run on the high setting with the larger blower to determine battery life expectancy. The output voltage to the blower was checked at least hourly while the batteries were drained. The output voltage remained at 5.99 V for over 14 hr of operation and then decayed. The output voltage remained above 4.0 V (low setting output value) until after 19 hr of operation. It was also noted that the low battery indicator had come on after 17 hr of operation and that the output voltage began to drop more rapidly at about this time. This indicates that the low battery

threshold was chosen at an appropriate voltage to indicate that the batteries should be replaced.

Battery life of the blower subsystem will degrade from these specifications with use of the larger capacity blower subsystem. The larger blower was run with fresh batteries at room temperature to determine the battery life with no plumbing connected to the blower. The test results are shown in Table 16. It is estimated that the blower will draw close to 30 percent more current when it is under pressure. No representative tests were done to verify voltage versus time as the final blower interface is yet to be defined. From a purely mathematical standpoint, using the lithium batteries, the data indicate that the blower power source should deliver a full 6.0 V at the high setting for over 11 hr and should provide at least 5.0 V to the blower for over 13 hr. It must be realized, however, that the total energy delivery rating for a given battery is not constant versus current draw such that the higher current draw associated with the loaded blowers may cause further (although relatively small) reduction in the output capability.

## **7.4 Integration and Fabrication of Prototype System**

The integration and fabrication task included custom packaging considerations and design, package evaluation and testing, and system consolidation.

### **7.4.1 Custom Packaging Considerations and Design**

The RESPO 21 brassboard design included the use of off-the-shelf enclosures for both the communications and blower subsystems. This approach led to some inefficiencies regarding package sizes. For the prototype development, a short search for appropriate off-the-shelf enclosures was conducted. If nothing suitable was identified, custom packaging was to be designed and manufactured for this development effort.

A search for appropriate off-the-shelf packages for the communications and blower subsystems and produced no suitable items. Custom packaging was therefore required. After some layout work had begun, it was found that it would be very difficult to achieve the desired 6.5 in<sup>3</sup> package size with any normal package shape. In the case of the blower

Table 16. Battery Life at Room Temperature as a Function of Continuous Operating Time in a V461LS Blower

Run Time (hr)	Measured Voltage at Blower (V)
1	5.99
2	5.99
3	5.99
4	5.99
5	5.99
6	5.99
7	5.99
8	5.99
9	5.99
10	5.99
11	5.99
12	5.99
13	5.99
14	5.99
15	5.82
16	5.65
17	5.30
18	4.68
19	4.09
20	3.62
21	3.10

subsystem, the three Ultralife batteries occupy ~ 67 percent of the space and nearly half of the weight allotted.

To minimize package size and to facilitate battery change-out, a snap-on bottom was designed for the blower control package. This package was designed so that the completed blower circuit (with mounted switch, connector, and battery contacts) would fit into the very top portion, allowing the switch and connector to fit through preplaced holes. A guide plate, which fits over the board's battery contacts, was also included to prevent the batteries from being placed in reverse polarity. Once a layout design for the blower enclosure was completed, a stereolithography model was fabricated for further evaluation.

A cost-benefit analysis was performed to determine the most economical way to produce enclosures. Because a conductive, fiber-filled polycarbonate in a variety of colors was available and little post-production processing would be required, injection molding was selected.

As the tooling for injection-molded communications and blower enclosures matured to near completion, an appropriate polycarbonate material was specified and ordered. This material is olive-drab polycarbonate and is impregnated with stainless steel fibers for improved shielding capability. The material was received and transferred to the tool maker. Additional design work for the cases, such as a speaker hole pattern and lettering for the control surfaces, continued and were transferred to the tool maker for implementation before final enclosure runs. When the tooling was completed, some initial blower cases were run for evaluation using some leftover black polycarbonate material (identical to ours except for color). These cases were evaluated before cases were fabricated with the olive-drab polycarbonate. After initial evaluation, final communications and blower cases were run.

The RESPO 21 System is likely to experience outdoor industrial temperature extremes in shipment, storage, service and operation. The electronic circuitry was designed with industrial and/or military grade components which, at the minimum, can withstand temperature extremes of 0 to +70°C.

#### **7.4.2 Package Evaluation and Testing**

The packages to be used, custom or off-the-shelf, were to be evaluated and tested to verify that all of the components would fit into the enclosures. The ruggedness of the packages was also to be evaluated as well as their ability to seal to prevent excessive water permeation.

The first part of the package evaluation included comparing the populated communications and blower boards to the drawings to verify that they would fit into the enclosures properly. Once custom cases began to be received, a more thorough evaluation was performed. Early results indicated that the cases would perform as expected. The snap-fit was found to hold very well and the completed blower circuit boards fit nicely into the blower cases. The communications board and components also fit into the communications case as expected. An appropriate rubber padding material was identified and placed into the bottom of the blower assemblies. In general, the custom enclosure evaluation has shown that the cases are rugged, compact, and easy to use (ease of use includes switch and connector specifications). The enclosures themselves are water resistant in that sealed switches and connectors have been utilized for both the communications and blower units and a mylar cone speaker was utilized in the communications unit. As expected, the communications and blower packages are slightly larger than goal at approximately 8.5 in<sup>3</sup> but are of a form and fit that is reasonable. Both the communications and blower unit came in well under the weight goal.

#### **7.4.3 Subsystem and System Integration**

The completed communications and blower control circuit boards were to be integrated into their respective packages along with all of the necessary ancillary components and power sources for each subsystem. The basic functionality of the communications and blower control subsystems was then verified. The subsystems would be integrated together, along with a protective bib, air intake filter, and multilayer mask, to form the RESPO 21 advanced individual protective system. The bib, filter, mask, and much of the physical

interface were provided to Battelle by ERDEC and were not designed as part of this prototype development effort.

The main areas of full system integration were the microphone throughput on the mask and the communications and blower interface cables. ERDEC provided a custom receptacle to pass the microphone signals through the mask. A three-pin connector for the microphone cable, which would attach to the mask voicemitter throughput receptacle being provided at ERDEC, was designed. A similar connector was designed for the inside of the mask which includes a mount for the microphone. A stereolithography model of the connector and microphone mount was made and sent to Schmit Prototypes for quotes on molded urethane parts. The parts were made and shipped to Battelle for final fabrication.

Fabrication of the custom connector and cable which connects the communications unit to the mask throughput first included mating the retractile cable to the Fischer connector which connects to the communications unit. The other end of the cable was then fit into the custom connector by soldering to the three pins, forming and gluing the connector halves around the pins, and applying epoxy to the cable entry point to provide strain relief.

The internal microphone connector and mount was formed out of four pieces: two connector halves, an elbow, and a microphone holder arm. These units were fabricated by connector wires between the microphone and connector pins, fastening the microphone into its holder with the wires run through the holder and elbow, and forming and gluing the connector halves around the three pins. The elbow and microphone holder were then adjusted appropriately and glued to form a single piece connector/microphone holder which plugs into the inside of the mask throughput receptacle.

The blower interface cables were first formed by connecting the blower retractile cable to the Fischer connector which connects to the blower control unit receptacle. The next step was to connect the other end of the cable to the blower motor wires and add heat shrink and epoxy for sealing and strain relief.

### 7.5 Production of Prototype Units

Once the initial prototype units were evaluated, tested, and found to be acceptable, 34 prototype communications systems and 39 blower systems were to be assembled. Each

system includes a mask microphone, a communications assist unit, a miniature blower, a blower control unit, and connecting hardware. Masks and bibs for these systems will be provided by ERDEC.

As an entire system includes the use of close to 200 components. Once many of the parts needed to build blower and communications subsystems were received, parts kits began to be put together for individual units to improve the efficiency of system production. The first step in the production of prototypes was the placement of surface mount components on the communications and blower circuit boards. This was followed by the placement of any through-hole components as well as the attaching of the battery contacts to the blower circuits. The board-mounted switch and connector were then attached to the blower boards. The boards could then be functionally evaluated by mocking up the appropriate interface. The communications boards have a switch, two connectors, a speaker, and a battery cable that are separate (wired in). These components were prewired and then attached to the communications boards. The communications boards could then be functionally evaluated by mocking up the appropriate interface. At this point the circuits were ready to be integrated into the enclosures.

The blower circuits were placed directly into their cases so that the switch and connector protrude through their respective holes. After being secured by tightening the external nuts onto the switch and connector, the blower unit battery terminal covers were placed in the case and glued in. This seals off any further access to the blower circuit. The final assembly of the blower unit involved simply dropping in three Ultralife batteries and connecting the snap-on bottom lid. The blower units themselves were then made complete by attaching the knob to the control switch.

The communications circuits were much more difficult to place into their cases as they have several parts which are not rigidly attached. The circuits had to be carefully guided into a slot in the case while keeping the switch and connectors aligned with their respective holes and the speaker aligned with its bracket. After the switch and connectors are guided through their respective holes, they are fastened down with external nuts. Once the circuit is in place, and additional plate holds the unit together and separates the circuit from its tethered battery. Connecting the battery and attaching the snap-on bottom lid and the control knob completes the assembly.

Both the communications and blower subsystems required the assembly of external cables and connectors for use. The communications unit interface includes a retractile cable, with a standard W.W. Fischer connector for connection to the actual unit at one end, and the custom interface mask connector at the other end. Internal to the mask is an additional custom connector which holds the microphone. Two special cables have also been made for connection of the communication unit's field radio output to the Bendix/King LPI 5142 radio. The blower unit interface is simply a retractile cable with a standard W.W. Fischer connector on one end and one of two Micronel blowers (Model V461LS or V301MS) attached to the other end.

A photograph of the final blower system controller and communication system are given in Figure 7. Additional photographs and details of the design are given in Appendix E. Those details include mechanical drawings, electronic schematics, and manufacturer data of selected components.

## **7.6 Evaluation and Testing of Prototype System**

Evaluation and testing was performed on the initial prototype system prior to the development of prototype units. Testing was performed on the communications and miniature blower subsystems, as well as the power source. Basic functionality tests were performed at Battelle, before hardware delivery, while comprehensive tests on the integrated system will be performed at ERDEC once the appropriate hardware is delivered and integrated. Performed tests regarding power has been presented in Sections 7.1 and 7.2. The mass of the blower and communication subsystems produced are given in Table 17.

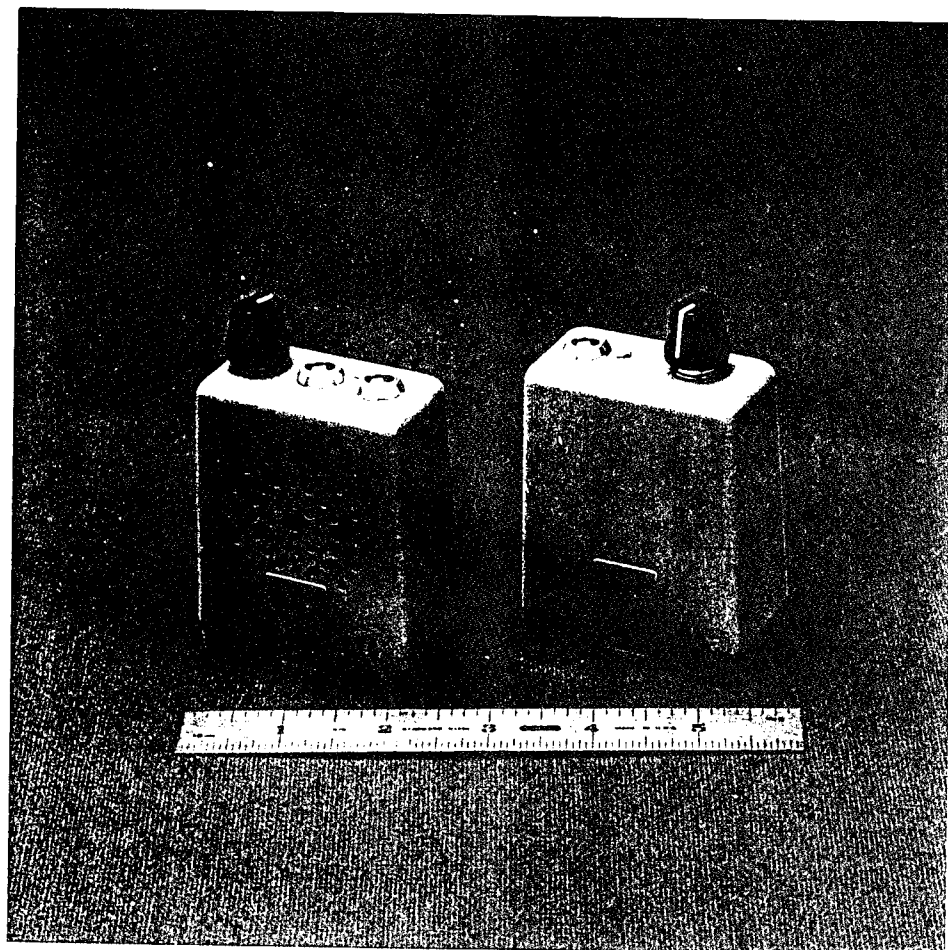


Figure 7. Photograph of Communications (left) and Blower Controller Systems

Table 17. Weight of Communications and Blower Subsystems

Communications Unit	Weight, g	Blower Unit	Weight, g
1	150.9	1	188.8
2	151.4	2	188.8
3	151.7	3	189.3
4	150.6	4	188.5
5	151.4	5	190.5
6	151.6	6	188.6
7	150.9	7	189.1
8	149.5	8	189.3
9	152.3	9	188.8
10	151.4	10	189.8
11	151.2	11	189.0
12	151.0	12	189.0
13	149.6	13	189.2
14	150.5	14	189.2
15	152.1	15	188.8
16	150.8	16	189.1
17	150.2	17	189.6
18	151.1	18	190.8
19	151.2	19	189.6
20	151.2	20	190.1
21	151.1	21	189.5
22	150.1	22	190.4
23	149.6	23	189.0
24	150.8	24	190.3
25	151.2	25	188.5
26	151.2	26	189.5

Table 17. (Continued)

Communications Unit	Weight, g	Blower Unit	Weight, g
27	151.6	27	190.8
28	151.4	28	189.2
29	150.7	29	190.1
30	149.9	30	189.0
31	152.7	31	190.1
32	151.4	32	189.3
33	151.7	33	189.1
34	151.2	34	189.1
		35	188.9
		36	189.1
		37	189.9
		38	189.5
		39	190.0

### 7.6.1 Communications Subsystem

The projected voice output of the communications subsystem were evaluated at the speaker and at the radio interface output. These outputs will be evaluated with the integrated system at ERDEC and tested for voice quality, volume, noise and interference levels, and presence of feedback, with and without the blower running. Power consumption evaluations of the communications subsystem were also performed. The communications circuit's low battery detect circuit was also to be tested to verify the alarm threshold.

The communications units were evaluated prior to shipment to verify that three distinct volume settings (low, medium, and high) were noted. The units were tested to verify that they would lock onto and eliminate appropriate feedback signals. The units were also connected to the field radio interface to verify that they would provide an appropriate signal

to be transmitted between the representative field radios. The communications units were weighed and showed a range of 149 to 152 g. The low battery threshold was also checked and was determined to come on at 5.0 V and go off at 5.3 V (built-in hysteresis).

The major dimensions of the communications subsystem case are 2.87 x 2.39 x 1.37 in. The overall volume of the communications case is 8.5 in<sup>3</sup>. The weight of the communications units ranges between 149 and 152 g. The communications mask interface cable weighs 42.7 g and the microphone connector/holder weighs 4.3 g.

### **7.6.2 Miniature Blower Subsystem**

The blower subsystem will be evaluated to determine its overall effectiveness in aiding breathing and eliminating moisture buildup at each of the control settings. The audible noise created by the blower and associated airflow will be evaluated directly and as it is amplified by the communications subsystem to validate the results of the noise reduction effort. The airflow out of the blower will also be studied to verify that it does not cause excessive drying of the eyes at the higher flow settings. These tests will be performed by ERDEC staff with the integrated RESPO 21 system. Power consumption evaluations of the miniature blower subsystem were performed at Battelle. The blower control circuit includes a low battery detect circuit which was tested at Battelle to verify the alarm threshold.

The blower units were evaluated prior to shipment to verify the output voltage at each of the three power settings. Each unit was also run with a large blower to verify good battery contact and power control. The blower units were weighed and showed a range of 188 to 190 g. The low battery threshold was also checked and was determined to come on at 6.0 V and go off at 6.2 V (built-in hysteresis).

The major dimensions of the blower subsystem case are also 2.87 x 2.39 x 1.37 in. The overall volume of the blower case is 8.5 in.<sup>3</sup>. The weight of the blower units ranges between 188 and 190 g. The large blower with its cable weighs 99.2 g. The small blower and cable weighs 71.9 g.

## **8.0 CONCLUSIONS AND RECOMMENDATIONS**

### **8.1 Filter Elements**

Sample media were successfully evaluated and used to develop a RESPO 21 filter design concept. Filter design concepts were evaluated, molds fabricated, and filter elements produced. Performance evaluation tests of media were used to specify a filter design concept and predict its performance. A novel AFTP was conceived, designed, and fabricated that permitted air to be transported from the center of a two-sided filter to ducts that lead to the respirator. A mold was fabricated and a polyurethane polymer selected to produce the AFTP. A second mold was designed to encapsulate the filtration media and AFTP with a polymer edge seal, thereby forming the filter element. The polyurethane polymer selected for the edge seal was soft and flexible and adhered to the filtration media and AFTP. Performance evaluations of the filters were conducted to determine whether the required specifications were met. Although all design specifications were not met, the filter design concept conceived and executed is a viable and promising concept for RESPO 21.

Within the size constraints and the filtration media currently available, the design specifications established in Table 1 cannot be met. Improvements in both aerosol filtration and gas adsorption media are required. The aerosol filtration efficiency and sorptive capacity of the media must be increased, while maintaining or lowering the airflow resistance.

It is recommended that the filter design established in this study be retained for continued development. Modifications to the design should be pursued to lower the airflow resistance of the AFTP by changing the geometry of the air duct. The size of the filter needs to be increased. Increasing both the length and width by about 0.5 in. should be adequate for the current design concept and filter media to meet performance specifications.

A nonelectrostatic aerosol filtration medium should be identified for use to avoid temperature and relative humidity concerns associated with the electrostatic media. If filter development continues with the use of an electrostatic material, then its performance after exposure to high temperature ( $> 150^{\circ}\text{F}$ ) and its performance during humid conditions or during heavy particulate loading must be demonstrated. The carbon medium should be optimized to give the ideal particle size and mass loading with the lowest pressure drop.

## 8.2 Electronic Systems

The objective of this effort was to develop and implement design enhancements to the brassboard systems that were delivered to ERDEC at the end of the previous phase of the RESPO 21 program. This improved system design also led to the development of prototype units for delivery to ERDEC for further evaluation. The Battelle project team was successful in the design of prototype subsystems which meet or come close to meeting the design goals called out in the statement of work. Achieved improvements to the communications unit design included the addition of feedback elimination, improved noise filtering, improved volume control, improved output capability, improved ruggedness and moisture rejection, and miniaturization. Achieved improvements to the blower unit design included a more efficient drive circuit, improved ruggedness and moisture rejection, and miniaturization.

As expected, further improvements that could be made to the design (outside of the scope of this program) were identified during the course of this effort. The final communications circuits provided an output that was a little more noisy than expected based on the breadboard circuit analysis. Much of this noise is caused by the complex signal cross-talk and characteristics of a high density printed circuit board. Further analysis of the layout of this circuit would yield an improved noise immunity and a better signal to noise ratio. It was also noted that the threshold at which the circuit detects feedback was higher than anticipated and varied from circuit to circuit. Better circuit layout and the use of lower tolerance components, as well as minor adjustments of some of the component values, should provide a feedback detection with very little audible feedback.

The blower subsystem design was much simpler and did meet most of the expectations concerning efficiency and control. The enclosures for the communications and blower units could be improved upon through some basic mechanical adjustments. The main potential benefit to the enclosures would be improved sealing. Without significant effort, it is felt that the units could be made waterproof instead of just water-resistant. The ruggedness, size, and weight of the units did however meet with the basic expectations formed early in the design process.

## 9.0 REFERENCES

1. Hofacre, K.C., Kuhlman, M.R., and Bothe, C.L., "Evaluation and Optimization of a Flexible Filtration System for Respiratory Protection System 21," U.S. Army CRDEC Final Report, Contract No. DLA900-86-C-2045, February, 1992.
2. Hofacre, K. C., Markham, R. L., and Northrup, V. M., "Evaluation and Optimization of a Flexible Filtration System for Respiratory Protection System 21," U.S. Army ERDEC Final Report, Contract No. DLA900-86-C-2045, August, 1993.
3. Corey Grove, ERDEC, 1992. Personal communication between Corey Grove, Kent Hofacre, and Richard Markham, Battelle, August 25, 1992.
4. American Society for Testing Materials, ASTM F778-88, "Gas Flow Resistance Testing of Filtration Media," 1916 Race Street, Philadelphia, PA 19103.
5. American Society for Testing Materials, ASTM F1215-89, "Determining the Initial Efficiency of A Flat Sheet Filter Medium in an Air Flow Using Latex Spheres," 1916 Race Street, Philadelphia, PA 19103.
6. CRDEC Purchase Description, Canister, Chemical-Biological, C2; EA-C-1322C Amendment 6; 6 March 1990.
7. Bagley, Frank D. et al., *Simulant Review and Selection (DOD-1)*, Interim Report U.S. Army Dugway Proving Ground, September, 1977.
8. U.S. Government, 1983 "Military Specification, Filter Element Set, Charcoal-Biological Mask, M13A2", Amendment 1 (September, 1986), MIL-F-51425 (EA).
9. Warriner, S., 3M Occupational Health and Environmental Safety Division, 1993. Written communication to Kent Hofacre, Battelle, November 15, 1993.
10. Kuhlman, M. R. and Ramamurthi, M., "Evaluation of a Low Profile Filtration System (LPFS) for Marine Corps Lightweight Assault Mask," U.S. Army ERDEC Final Report, Contract No. DLA900-86-C-2045, July, 1992.
11. Haller, R. B. and Roberts, C. C., "Development of New Design Configurations of C18 Gas Aerosol Filter Material," U.S. Army Edgewood Arsenal Final Report, Contract No. DAAA15-67-C-0196, Mine Safety Appliances, August, 1969.
12. Markham, R.L., Battelle Memorial Institute, 1993. Written correspondence to Corey Grove, ERDEC, October 29, 1993.
13. Markham, R.L., Battelle Memorial Institute, 1993. Written correspondence to Corey Grove, ERDEC, November 17, 1993.

## **APPENDIX A**

### **FILTER DESIGN CONCEPT GENERATION**

- A-1. Edge Sealant Materials**
- A-2. Transition/Spacer Pieces**

## APPENDIX A-1

### MATERIALS FOR FILTER SEAL

A team of polymer materials scientists and engineers met to discuss the materials requirements for the edge seal for the RESPO 21 filter and to propose candidate materials. The major problems concern the processability of the seal materials at temperatures no higher than 160°F. This temperature limitation results from the use of an electrostatic material for aerosol filtration. Temperatures above 160°F may begin to degrade the electrostatic charges on the filtration medium, rendering it incapable of removing the aerosol.

The following are descriptions of the ideas that were proposed during the session:

- (1) Make the substrate electrostatic after molding the seal on the filter. (Not possible.)
- (2) Since contact of the filter media with the hot mold is only at the pinch next to the edge seal, it may be possible to mold at temperatures over 160°F while protecting the filter media from exposure of higher temperature. One approach may be to cut out the mold so that the interior is open and the filter media does not touch the hot mold.
- (3) Use reaction injection molding (RIM) Materials from DSM in Cleveland.
- (4) Use a heat shrink material for the edge seal. May fabricate the heat shrink part and at 250°C and then shrink it at 50 to 70°C (above the Tg). Look for materials that can be oriented but have a Tg below 160°F (71°C).
- (5) Inject a monomer mixture and polymerize in the mold. An example might be methyl methacrylate in butyl methacrylate. Add a diacrylate to cross link. Use benzoyl peroxide plus an accelerator for a fast cure. May not need to heat the mold. Could add fillers or fibers for reinforcement. Perhaps there is soft version of dioctyl methacrylate. Beware of residual monomer that may be toxic.
- (6) Use a system similar to the "Bondo" used to repair auto dents - styrene polyester - but use butyl acrylate to obtain a soft material.
- (7) In the monomer approach, substitute low molecular weight oligomers. The viscosity would be higher and therefore the material would not pass through the filter media into the interior of the filter. Also, the exotherm would be lower.

- (8) Dip the edges in an appropriate liquid and cure the liquid with electron beam (EB) or ultraviolet (UV) light.
- (9) Use the resin transfer molding (RTM) materials without the glass reinforcement. GenCorp may have some that are rubbery. Look in Battelle's multiclient report on reactive processing for sources of RTM resins.
- (10) Look in the Battelle report on Plastics Molds for suitable materials for the edge seal.
- (11) Look in hardware stores for sealants that may be appropriate.
- (12) Try polyvinyl acetate.
- (13) Use a heat sealing material.
- (14) Identify a suitable material that can be cured with microwave radiation.
- (15) Interleaf the filter media layers with "picture frames" of a suitable rubber that could be heated under pressure to impregnate the media layers and then cure to form a full seal around the edges. This may allow the use of a harder material for the edge seal since the thin sealed area would no longer be the contact point when the wearer of the filter would do a belly flop.
- (16) Combine idea 15 with the use of a heat shrink material to form the cover over the edge.
- (17) Add a foam cover over the hard edge in idea 15.
- (18) Make a foam edge seal and then heat treat the outer surface to make a skin to prevent permeation by agent.
- (19) Question--does the material have to have low durometer of the geometry provides a thinner edge seal?
- (20) Shell now has a plasticized Kraton that should have a much lower viscosity so that it may be suitable for injecting around the filter edges.
- (21) Tin catalysts sometimes have a volatile product that may be unacceptable in the respiratory system.
- (22) Try a nylon/silicone blend.
- (23) Letter press materials are UV curable and may be suitable.
- (24) Evans has mercapto compounds that could be used in the system.

- (25) Grace makes polymers with allyl end caps that are UV cured for lithography. Could we use a peroxide?
- (26) Use castor-oil based epoxy (aliphatic); use tetrafunctional mercapto.
- (27) Unsaturated polyester long oil alkyd are rubbery. This is old technology.
- (28) Make the mold from a polyolefin like poly(4-methyl pentene). then cure can be effected with microwave. Maybe could use the new syndiotactic polystyrene (Tg of 270°F).
- (29) Use plastisols (plasticized PVC).

## APPENDIX A-2

### TRANSITION/SPACER PIECES

- (1) Look at the cross sectional area first of the edge of the transition piece. Consider that this is a tube and that this will be the controlling factor for the air intake through the areas "opened" by the tube. Thus the "openings" to the "tubes" must be equal. Then one must control the cross section of the tubes to obtain the air flow coming from the farthest parts of the filter.
- (2) Make the spacer pieces thicker at the outside of the filter in the far areas (corners) so that the cross section provides flow to offset the greater distance. Thus, the spacer will be thinner in the middle than on the edges. Can this be done without adding too much thickness to the total filter?
- (3) Should we look at including a part of the spacer within the compressed area so that we get a more stable filter, but, more importantly, get an easier manufacturing because of stabilization of the stack of filter media?
- (4) In considering the most direct approach to using the greatest percent of the available area of filter, the side placements of the transitions may be best. Calculate the area achievable using a simple radius from the opening and assuming equal flow from all directions.
- (5) In considering molding the transitions in one piece with the spacer, the top placement of the transitions may allow a molding of a single piece. The parting line of the mold may be placed to obtain a "pin" for the center of the transition piece. Perhaps a three part mold could be made and would be simple enough to fit our present budget.
- (6) What material is available from which to mold the transition/spacer that will adhere naturally to the seal material?
- (7) Do we have any selection of seal materials to enhance the adhesion?
- (8) What surface treatment would assist in obtaining the adhesion to the seal material?
- (9) Can we design a part to give a physical attachment of the transition to the seal material?

(10) If connect with a 0.5-in. diameter hose, need cross section of transition to be at least that area  
2.5 X 0.080 in.  
1.6 X 0.125 in.

(11) The funnel shaped part would have to narrow as it approaches the entry from the filter. This is not a moldable design. Find a way to mold.  
  
Mold it open and use a post-molding heat-forming process to flatten the opening.  
  
Use a metal piece that could be flattened by pressure. This may have some advantage in achieving an adhesion to the seal.

(12) If the transitions will both be at the top, the two connections can be molded together.

(13) Design a means of mechanically connecting two molded parts—the funnel and the spacer.

(14) How can we design a spacer so that a very high percentage of the air does not come directly from the area very close to the transition?

(15) Would a design be better at directing flow from areas away from the transition if the thickness is greater near the transition?

(16) If we assume that the flow into the transition is relatively parallel and perpendicular to the edge of the transition, how do we design the shape of the channel to get flow also from the far areas? This would appear to be difficult since we will not have much variation in thickness of the spacer.

(17) In order to project a shape for the conveying channels, consider pressure drop as directly related to cross sectional area, but consider that the larger areas have less pressure drop and therefore will pull with less force on the top and bottom (filter media) surfaces of the channels. This would seem to indicate that the channels must decrease in size with distance from the transition. However, we must consider also that there is a maximum pressure drop that will allow enough flow to meet the design specification for the filter. Will this limit us from taking this approach?

(18) Should we focus on getting the parallel flow described in 15 above? Can this be induced by making additional exit points for the transition, i.e., several funnels feeding into the two main hose connections.

## **APPENDIX B**

### **MATERIAL SUPPLIERS**

## **APPENDIX B**

### **MATERIAL SUPPLIERS**

#### **Edge Seal Material Suppliers**

F-40, F-60, F-70  
BJB Enterprises, Inc.  
13912 Nautilus Drive  
Garden Grove, California. 92643  
(714) 554-4640  
Contact: Mr. Terry McGinnis

Dow Corning Silicone 3110, 3112, and Sylgard 186  
Brownell Electro  
895 Sivert Dr.  
Woodale, IL 60191  
(412) 221-0074

TC 640, TC 660  
Conap  
1405 Buffalo St.  
Olean, NY 14760  
(716) 372-9650  
Contact: Mr. Bob Keenan  
Facsimile (716) 372-1594

PolyTek  
P.O. Box 384  
Lebanon, NJ 08833  
(908) 534-5990  
Contact: Mr. Angus Macauley

GE RTV 630  
Rudolph Brothers  
960 W. Walnut St.  
Canal Winchester, OH 43110  
(614) 833-0707  
Contact: Mr. Rick Rudolph

Smooth On  
10000 Valley Rd.  
Gillette, NJ 07933  
(908) 647-5800  
Contact: Mr. Rick Huck

## **Spacer Material Suppliers**

### **Style S/027**

Pittsfield Weaving Co., Inc.  
1 Fayette, NH 03263  
(603) 435-8301  
Contact Mr. Jan Cysarz  
(207) 876-3485

(Spacer material used in final filter design)

Lumite Style 60617000  
Synthetic Industries  
Lumite Division  
P.O. Box 977  
Gainesville, GA 30503  
(404) 532-9756  
Contact: Ms. Hilda Burke

## **Static Mixer Suppliers**

John W. Blair Co.  
P.O. Box 192  
Westerville, OH 43081  
(614) 882-6431  
Contact: Mr. Bob Slavens

TAN160-632 1/4 X 32 Static Mixer  
100 X 100 ml Cartridges  
TS526S Manual Dispensing Gun  
Locking Nut

## **APPENDIX C**

### **ENGINEERING DRAWINGS OF FILTER PARTS AND MOLDS**

- C-1. Schematic of AFTP**
- C-2. Schematic of Encapsulation Mold**

**Figure C-1.** Schematic of AFTP

**Figure C-2.** Schematic of Encapsulation Mold

## **APPENDIX D**

### **FILTER FABRICATION PROCEDURES**

**D-1. Procedure for Molding the Air-Flow Transition Piece (AFTP)**

**D-2. Procedure for Encapsulating the Filter Stacks and AFTP**

## APPENDIX D-1

### PROCEDURE FOR MOLDING THE AIR-FLOW TRANSITION PIECE (AFTP)

The air flow transition piece (AFTP) is designed to convey filtered air from the space between the two filter stacks in the RESPO 21 filter to the two tubes leading to the face mask with a minimum restriction in flow. Stacks of filter media are placed on each side of the AFTP and the system is encapsulated to produce a sealed filter element.

The attached drawing provides the details of the design of the AFTP (also called the filter frame). An aluminum mold was designed and fabricated to produce this part. The mold consists of removable parts including "pin blocks" that form the holes in the frame between the space between the filter stacks and the manifold that conveys the filtered air to the connection to the tubes leading to the mask. "Long pins" are also used in the molding to form the manifold. The pins on the pin blocks are inserted in holes in the long pin as the mold is assembled.

- Clean entire mold with acetone. Remove all flash and trimmings of sealant from the previous molding.
- Apply soap suds to the long pins and pin block.
  - Spray 20% soap solution into hand.
  - Swirl the soap vigorously with a brush until large, wet bubbles are formed.
  - Use an excess of soap.
  - Put parts into the vacuum chamber to evaporate water.
- Spray silicone mold release into air vent on top of mold.
- Spray silicone mold release on pressure adapter and 3/8-T x 1/4-MPT fitting.
- Assemble mold.
  - Pin block and long pins are numbered--all the numbers must line up in the assembly.
  - Place pin block-long pin assembly into the numbered cavity in mold; use plastic and rubber mallet to tap it into place. Do not force the parts together; mold could be damaged.
  - After the assembly is in place, use brass rod and rubber mallet to ensure the pins are tightly fitted in the long pins.
  - Place the other half of the mold carefully on top of the half with the pin blocks in place.

- Close mold by lightly tapping on the top surface of the mold. To avoid misalignment, tap on the edges of each of the four sides in succession.
- Using scissors, cut the tip of the static mixer off at the line on the end of the mixer.
- Put plastic nut, brass nut, 3/8-inch ferrule on static mixer.
- Place mold in center of press.

**NOTE:** The press should have been preheated for at least 30 min at 150°F. Allow at least 30 min to reach and hold at that temperature to assure that the mold reaches the desired temperature.

- Raise pressure on the mold to about 7 tons.
- Pour SP-180 Parts A and B into injection cartridge.
  - Add each part to a separate chamber to a depth of 2 inches in the 100-ml cartridge.
  - The volumes of Parts A and B must be within 5% of one another.
  - Purge both of the SP-180 containers with argon when finished to help reduce premature curing of the materials.
- Put plastic nut, brass nut, 3/8-inch ferrule on static mixer.
- Using scissors, cut the tip of the static mixer off at the line on the end of the mixer.
- Attach static mixer to 3/8T and 1/4-MPT fitting on the mold; tighten until snug. Do not overtighten.
- Place cartridge in injector.
- Attach static mixer to cartridge with plastic nut.
- Inject the materials quickly. No more than 5 to 7 sec is desirable because the cure will proceed rapidly once the Parts A and B are mixed.
- Maintain temperature for 15 min in press.
- Remove mold from press without cooling.
- Disassemble mold immediately.

- Pry mold halves apart using the brass tool in the slots at the parting line of the mold. Be careful that the AFTP is not torn due to sticking to the mold or other deformation of the part.
- Using the brass rod and a rubber or plastic mallet, tap on the pin blocks through the holes in the outside of the mold. The AFTP will come out with the pin blocks and the long pins still inserted in the part.
- Carefully remove the pin blocks. This requires loosening the pins from the long pins by carefully rocking the pin block and long pin.
- Carefully remove the long pins. This will require some twisting. There is danger of tearing the AFTP if this twisting is done too vigorously.

■ Cure the demolded part for 4 hr at 150°F in oven

**NOTE:** At the end of each production day, shake the containers of Parts A and B of SP-180. This will assure that the black pigments are well mixed. By shaking only at the end of the day, there will be sufficient time for the air bubbles to dissipate before the materials must be used the next day.

## APPENDIX D-2

### PROCEDURE FOR ENCAPSULATING THE FILTER STACKS AND AFTP

The filter is assembled by encapsulating the two filter stacks and the air-flow transition piece (AFTP) with the spacer between the stacks. The filter stacks comprise the prescribed number of layers of carbon-impregnated fabric between a layer of aerosol filtration media on the top and on the bottom. The electrostatic aerosol filtration media will not withstand elevated temperature. Therefore, it is imperative that the filter stack not be subjected to temperatures above 150°F.

The encapsulation mold is designed to assure that the encapsulating sealant covers and impregnates the edges of the filter stack but does not penetrate into the active area of the filter. In addition, the encapsulant must assure a seal around the edges of the filter stacks and the AFTP against penetration of unfiltered air.

The attached drawing provides details of the encapsulating mold.

Filter stacks are prepared by assembling the prescribed number of layers of filter media and top and bottom layers of electrostatic material followed by cutting with a specially designed and sized die to the desired dimensions. Spacers that will be placed between the filter stacks will also be precut.

- Clean entire mold with acetone. Remove all flash and trimmings of encapsulant from the previous molding.
- Spray brass fittings with silicone.
- Center one filter stack on bottom half of mold. **NOTE:** Top half of the mold has the government inventory control number.
- Insert long pins into AFTP. Pins are numbered; numbers should be visible when the long pins are properly installed.
- Lay the AFTP over filter stack making sure the stack is within the tabs on the sides of the frame part of the AFTP.
- Place spacer inside AFTP.
- Place another filter stack on top of the spacer making sure that the stack is within the tabs on the sides of the frame of the AFTP.
- Place brass fittings into mold.

- Carefully place the top half of the mold on top of the filter stack. Align the mold by placing the holes in the top of the mold over the guide pins in the bottom of the mold.
- Close the mold by carefully tapping on the top surface of the mold with a rubber or plastic mallet. Tap each of the four sides in succession to avoid misalignment. Do not force the mold closed.
- Place the mold in the center of the press.

**NOTE:** The press should have been preheated for at least 30 min at 150°F. Allow at least 30 min to reach and hold at that temperature to assure that the mold reaches the desired temperature.

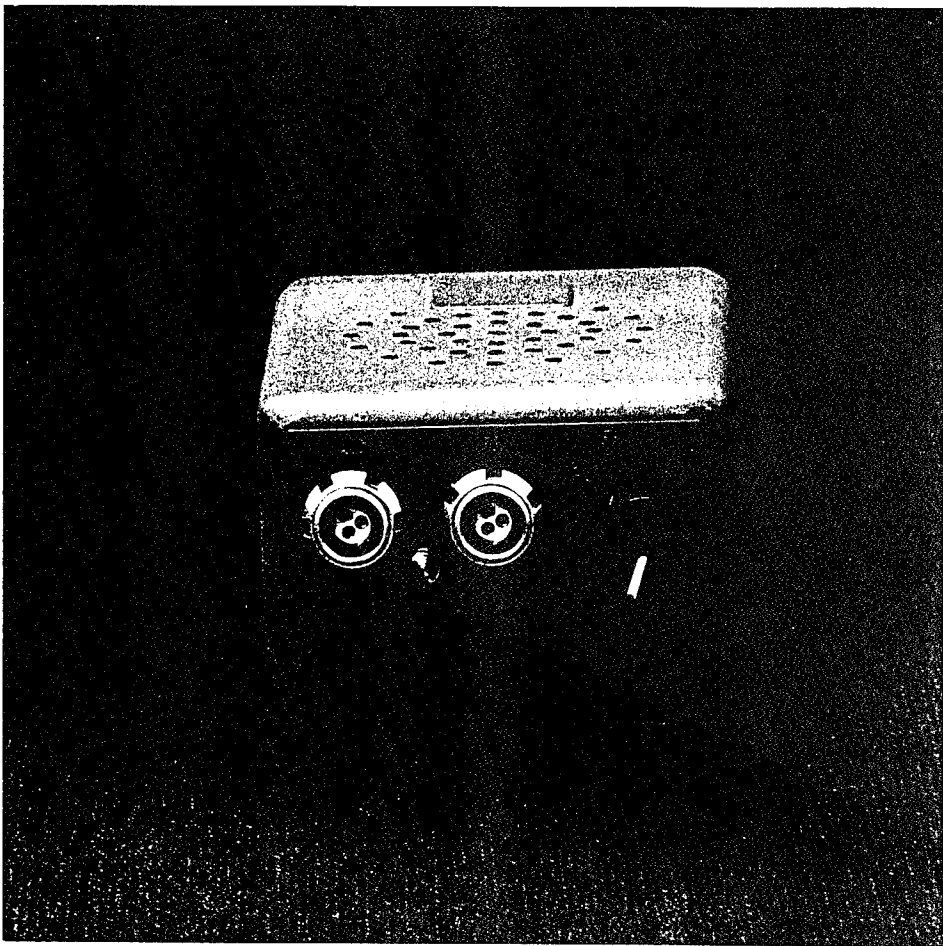
- Raise pressure on the mold to about 7 tons.
- Pour F-70 Parts A and B (containing 2% by weight of black pigment) into injection cartridge.
  - Add each part to a separate chamber to a depth of 1-3/4 inches in the 100-ml cartridge.
  - The volumes of Parts A and B must be within 5% of one another.
  - Purge both of the F-70 containers with argon when finished to help reduce premature curing of the materials.
- Put plastic nut, brass nut, 3/8-in. ferrule on static mixer.
- Using scissors, cut the tip of the static mixer off at the line on the end of the mixer.
- Attach static mixer to 3/8T and 1/4-MPT fitting; tighten until snug. Do not overtighten.
- Place cartridge in injector.
- Attach static mixer to cartridge with plastic nut.
- Inject the encapsulant slowly, taking 20 to 30 sec to fill the mold.
- Maintain temperature for 15 min in press.
- Remove mold from press without cooling.

- Disassemble mold immediately.
  - Pry mold halves apart with brass tool in the slots at the parting line of the mold. Be careful that the filter is not torn due to sticking to the mold or other deformation of the part.
  - Carefully lift the encapsulated filter from the mold.
  - Carefully remove the long pins from the tubes.
- Post-cure the filter at room temperature for at least one week.
- Place filter in vacuum chamber for at least 48 hr to remove any unreacted monomer

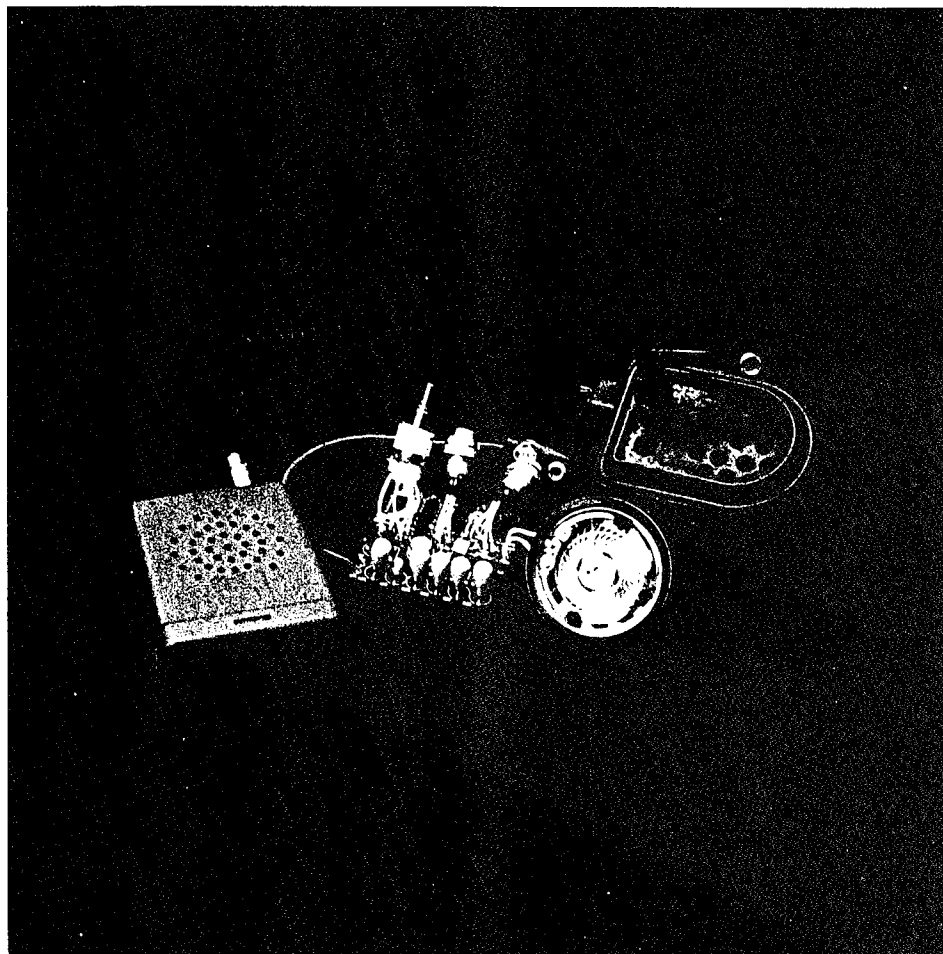
**NOTE:** At the end of each production day, shake the containers of Parts A and B of F-70. This will assure that the black pigments are well mixed. By shaking only at the end of the day, there will be sufficient time for the air bubbles to dissipate before the materials must be used the next day.

## **APPENDIX E**

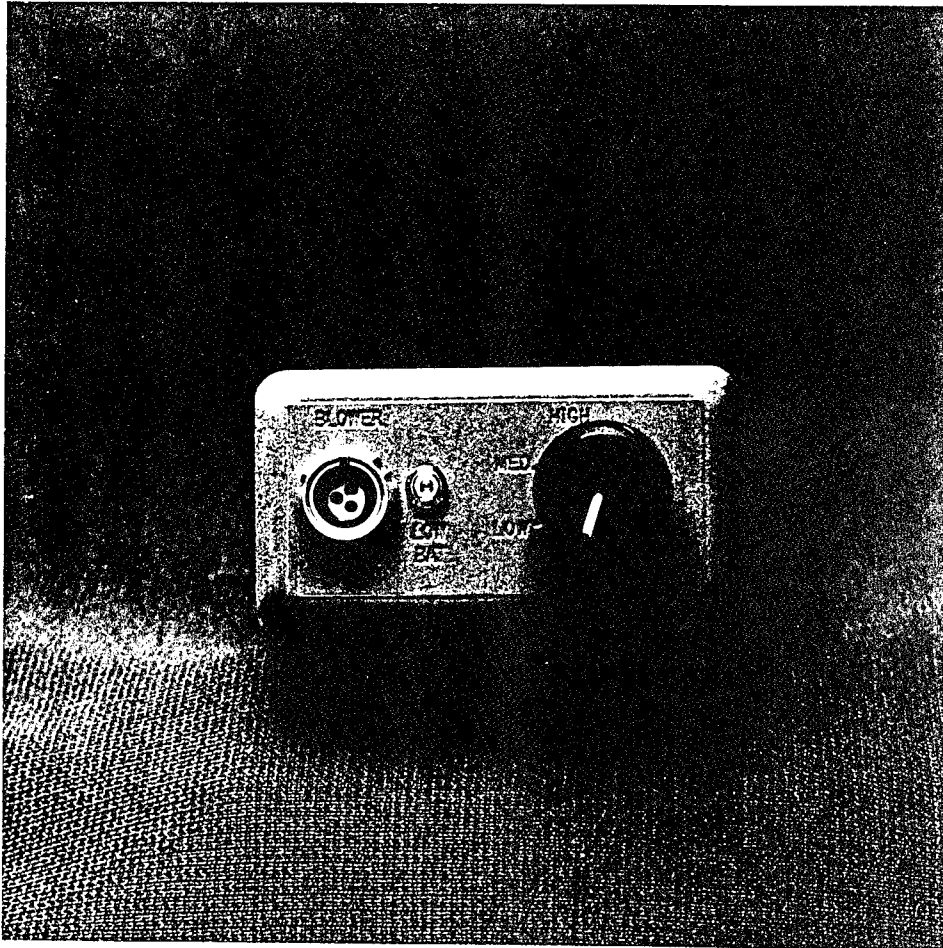
**MECHANICAL DRAWINGS, ELECTRONIC SCHEMATICS, AND  
PERFORMANCE DATA OF ELECTRONIC SUBSYSTEMS**



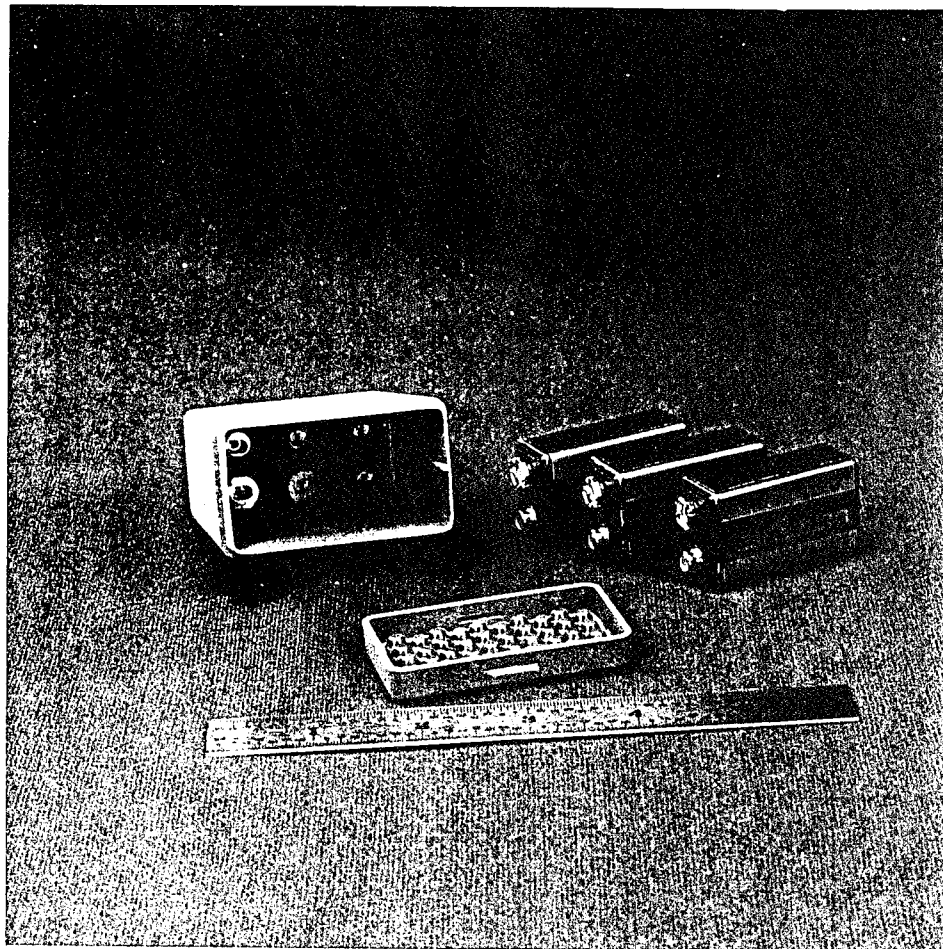
TOP VIEW OF COMMUNICATIONS UNIT



COMMUNICATIONS UNIT WITH INTERNAL PARTS, CABLE, AND INTERFACE



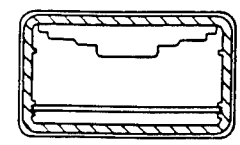
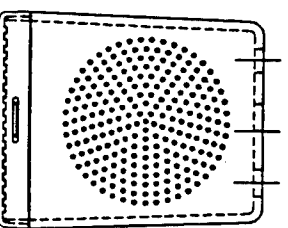
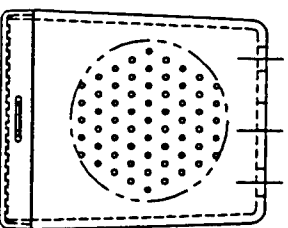
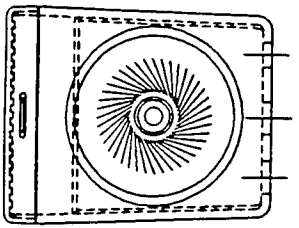
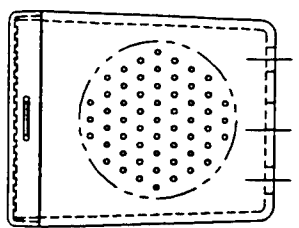
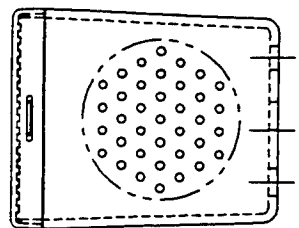
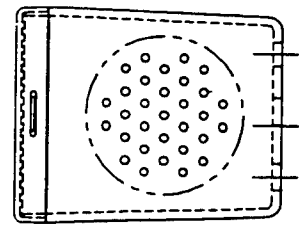
TOP VIEW OF BLOWER UNIT



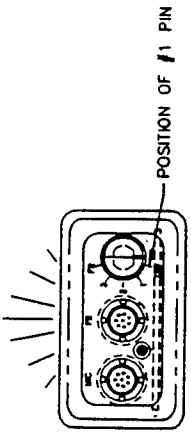
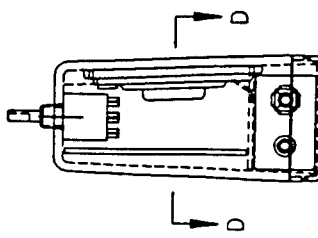
OPEN BLOWER UNIT SHOWING BATTERY BAY

NAME: SPEAKER CASE

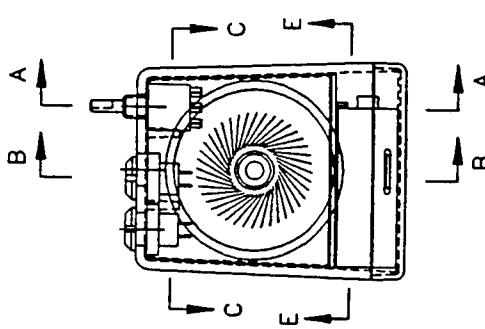
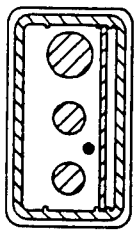
FILE: 401.DWG  
SCALE: 1/1



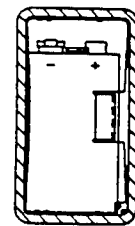
SECTION D-D



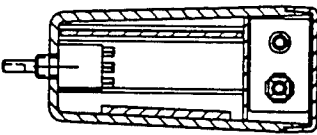
SECTION C-C



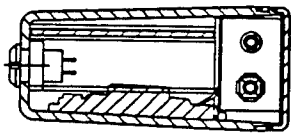
SECTION E-E



SECTION A-A



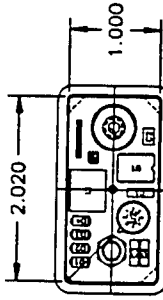
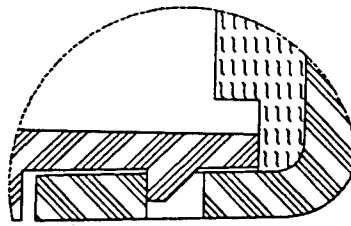
SECTION B-B



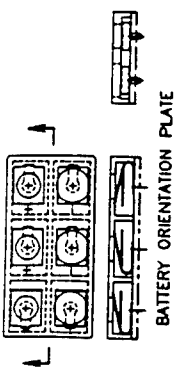
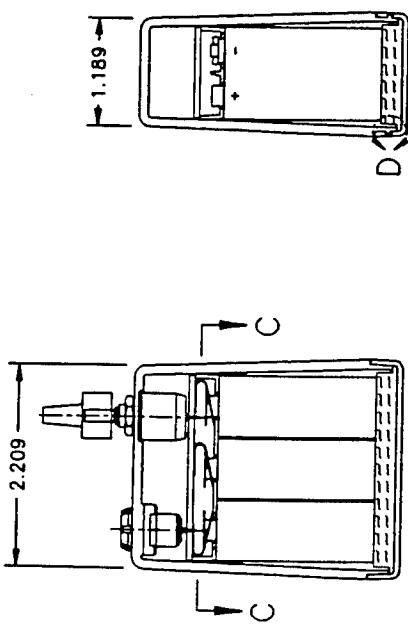
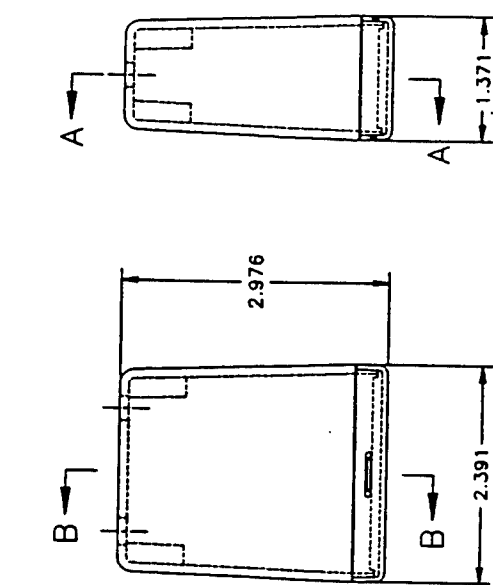
NAME: BLOWER BATTERY CASE

FILE: 400.DWG  
SCALE: 1/1

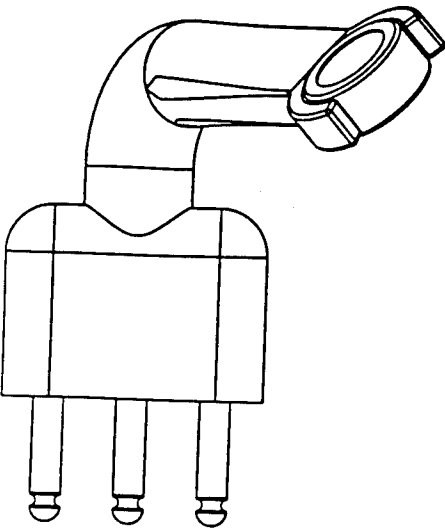
VIEW D  
SCALE: 10/1



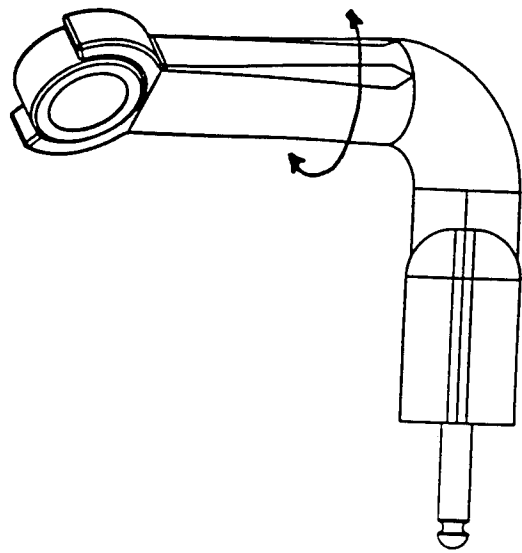
SECTION A-A SECTION B-B



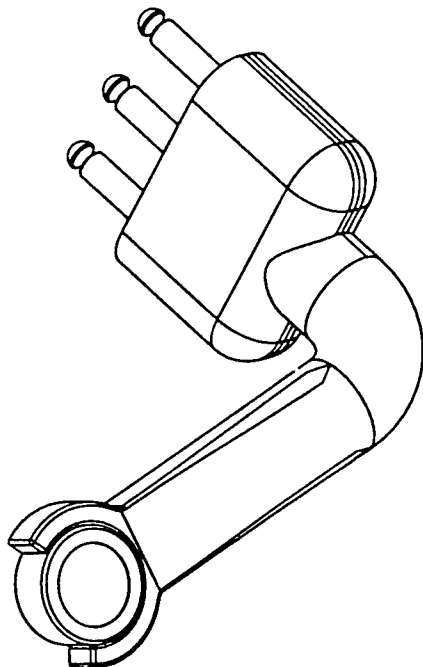
BATTERY ORIENTATION PLATE



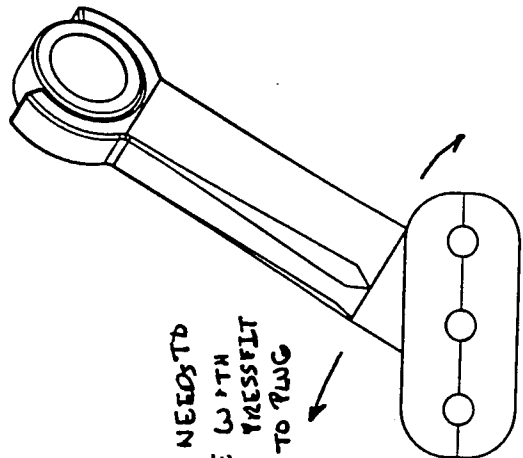
MICROPHONE EXT.  
TUBE NEEDS TO  
ROTATE WITH  
LIGHT PRESS FIT  
W.R.T. ELBOW



→  
ELBOW FIT SHOULD  
NOT SPREAD PLUG

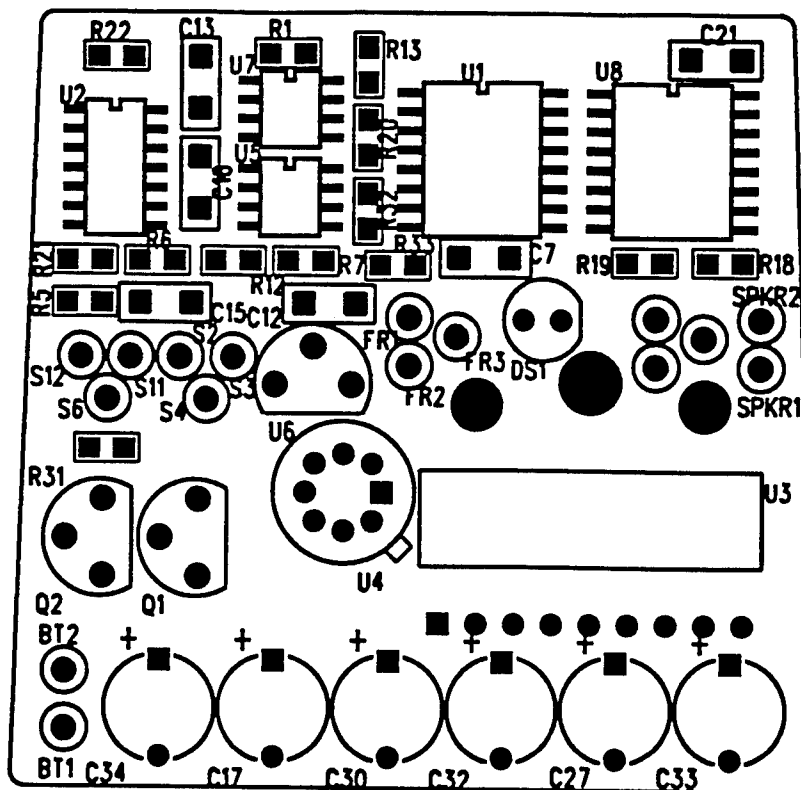


ELBOW NEEDS TO  
ROTATE WITH  
LIGHT PRESS FIT  
PLUG TO PLUG



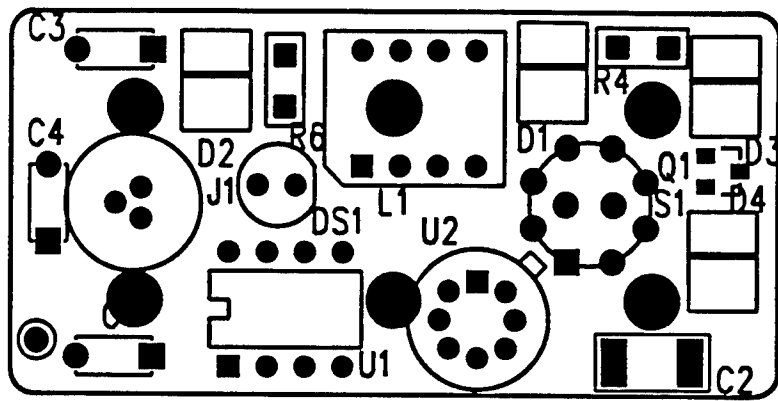


## COMPONENT SIDE SILKSCREEN





## COMPONENT SIDE SILKSCREEN



**GENTEX**  
CORPORATION

3060 SERIES ELECTRET ELEMENT

CANCELLER  
FLAT FREQUENCY RESPONSE

MODEL NO. 3063

P/N 100208

FREQUENCY RESPONSE: 100 Hz TO 5KHz

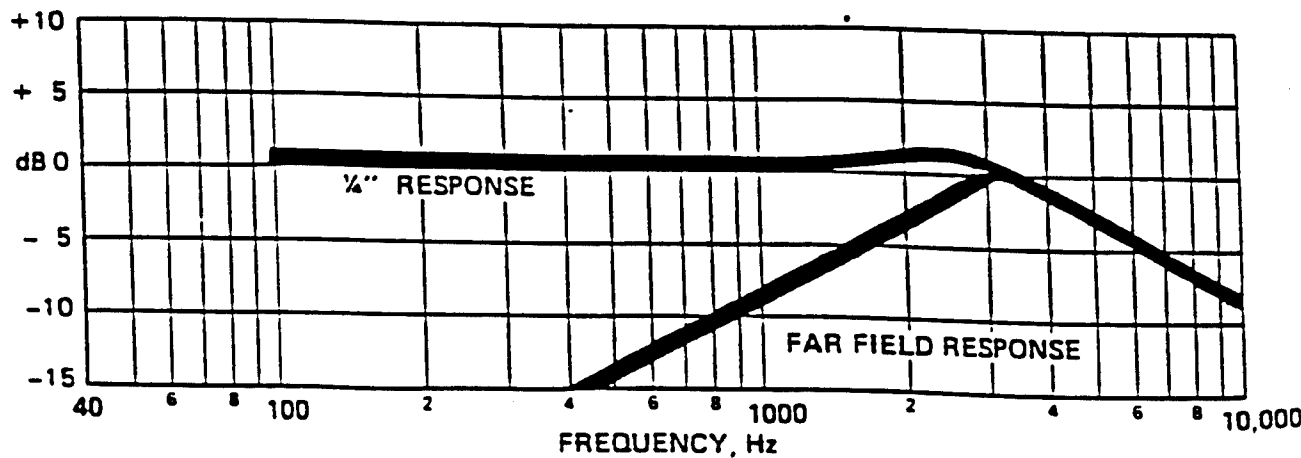
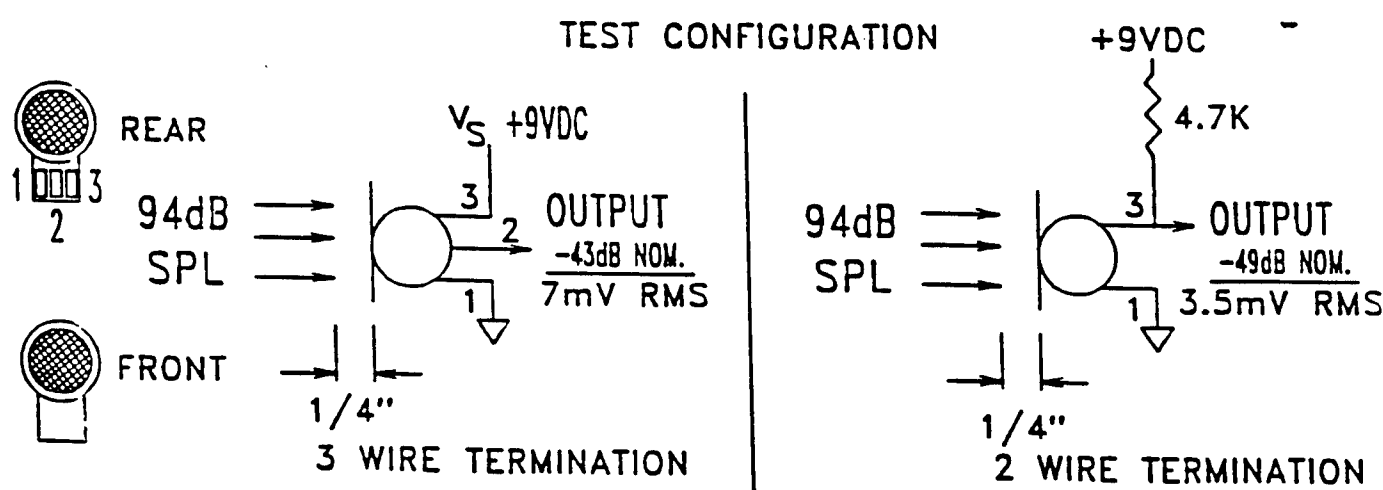
SENSITIVITY: -43dB +/-4dB re 1V/Pa @ 1KHz @ 1/4" 3 WIRE TEST

SUPPLY VOLTAGE: 1.2 VOLTS MIN.  
20 VOLTS MAX.

NOMINAL CURRENT: 40 $\mu$ A | 75  $\mu$ A MAX. |  $T_a=25^\circ C$   
| 15  $\mu$ A MIN. |

DIMENSIONS : O.D. 0.312"      THICKNESS 0.150"

TERMINATION : SOLDER PADS      APPROX. .06" X .04"



NOTES.  
1. INTERPRET DRAWING PER DOD-STD-100.  
2. INTERPRET DIMENSIONS AND TOLERANCES PER ANSI Y14.5.  
3. INCLINE ANGLE TO BE  $Z$  UNLESS OTHERWISE SPECIFIED.  
4. INCLINE TILTS TO BE  $\theta$  UNLESS OTHERWISE SPECIFIED.  
5. WALL THICKNESS TO BE  $A$  UNLESS OTHERWISE SPECIFIED.  
6. ALL OUTSIDE SURFACES EXCEPT THE TOP FACE WHICH CONTAINS THE LETTERING MARKINGS.

POSITION MARKINGS AS SHOWN, REFER TO VIEW C FOR LETTER SPECIFICATIONS.  
10 OF NATURALI FEATURES BY THE ELECTRO-DISCHARGE MACHINING (EDM) PROCESS.

THUMB PAD STARTS AT THE  
CORNER AND DRAFTS UP AT 0.5

A technical drawing of a semi-circular arch. The vertical height is labeled as .36. A horizontal dimension line indicates a width of .103. An angle of 45 degrees is shown at the base of the arch. A label 'AT THE' points to the left side of the arch.

This technical drawing shows a rectangular component with two circular features. The top circle has a diameter of .356 THRU and is labeled 'OF PART' with a leader line. The bottom circle has a diameter of .049 and is also labeled 'OF PART' with a leader line. There are several other markings: 'OFF' at the top right, 'ON' at the bottom left, 'UP' at the bottom center, and 'DOWN' at the top center. A line extends from the bottom right corner of the rectangle to a dimension of .171 THRU.

**VIEW C**  
POSITION MARKINGS TO BE AS SHOWN  
WITH .060 HIGH LETTERS AND .015  
DEEP. NOTE ORIENTATION OF FLATS  
IN THE HOLE TO MARKINGS.

**VIEW A**  
SCALE: 10'/1  
TYPICAL 2 PLACES

SECTION B-B

		BLOWER CASE	
		79986	403
		2/1	1 OF 1

1

2

3

4

D C B A

**REVISIONS**

ZONE REV	DESCRIPTION	DATE	APPROVED
----------	-------------	------	----------

**NOTES:**

- INTERPRET DRAWING PER DOD-STD-100.
- INTERPRET DIMENSIONS AND TOLERANCES PER ANSI Y14.5.
- DRAFT ANGLE TO BE 2° UNLESS OTHERWISE SPECIFIED.
- INSIDE FILLETS TO BE R .031 UNLESS OTHERWISE SPECIFIED.
- WALL THICKNESS TO BE .050 UNLESS OTHERWISE SPECIFIED.

**A → [ ]**

**B → [ ]**

**C → [ ]**

**D → [ ]**

**SECTION A-A**

**POLYCARBONATE**

QTY	ITEM NO.	NAME	IDENTIFYING NO.	MANUFACTURER	SPECIFICATION	REVISION
1	404			Battelle	MLX	1

**PARTS LIST**

COMPUTER FILE NO.	ITEM NO.	NAME	CONTRACT NO.	DATE
			DF 33-00-22	

UNLESS OTHERWISE SPECIFIED  
DIMENSIONS ARE IN INCHES  
FRACTIONS OR DECIMALS  
K= .01 IN. 1/2 IN.  
ANGLES  
DO NOT SCALE DRAWING

**MATERIALS & PROCESSES**

MANUFACTURING PROCESS	QUALITY ASSURANCE	PART NO.	REV.	REV.	REV.

**ADDITIONAL APPROVALS**

DATE	APPROVAL	NO.	TYPE	APPLIED TO	REMOVED ON	REMOVED BY	REMOVED DATE

**4**

**3**

**2**

**1**

**REV. 1 OF 1**

**4**

**3**

**2**

**1**

**NOTES:**

1. INTERPRET DRAWING PER DOD-STD-100.
2. INTERPRET DIMENSIONS AND TOLERANCES PER ANSI Y.14.5.
3. DRAFT ANGLE TO BE  $2^{\circ}$  UNLESS OTHERWISE SPECIFIED.
4. WALL THICKNESS TO BE .043 UNLESS OTHERWISE SPECIFIED.
5. INSIDE FILLETS TO BE R.020 UNLESS OTHERWISE SPECIFIED.

1

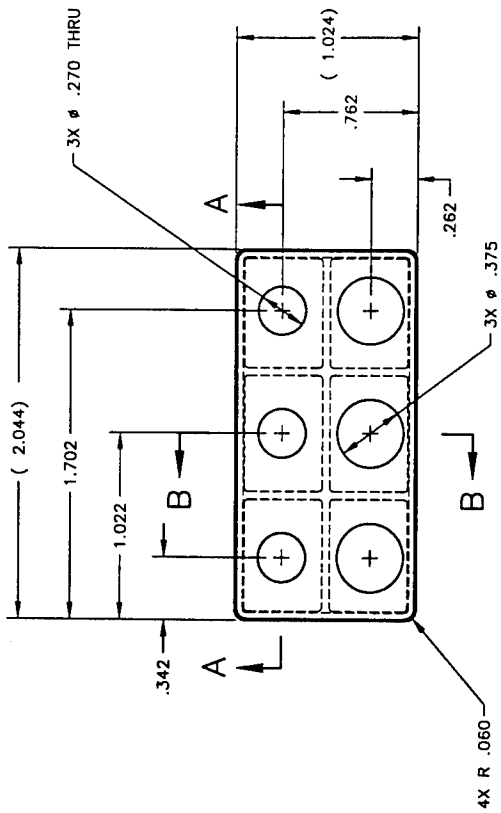
6

DIVISION NO.

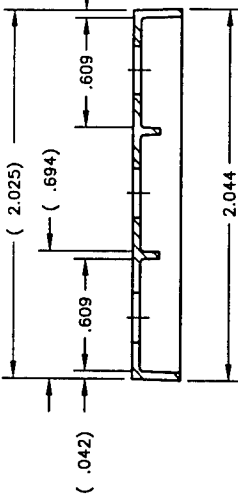
REV.

1

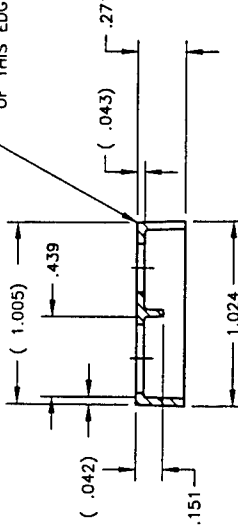
ZONE	REV	DESCRIPTION	DATE	APPROVED
REVISIONS				



SECTION A-A



SECTION B-B



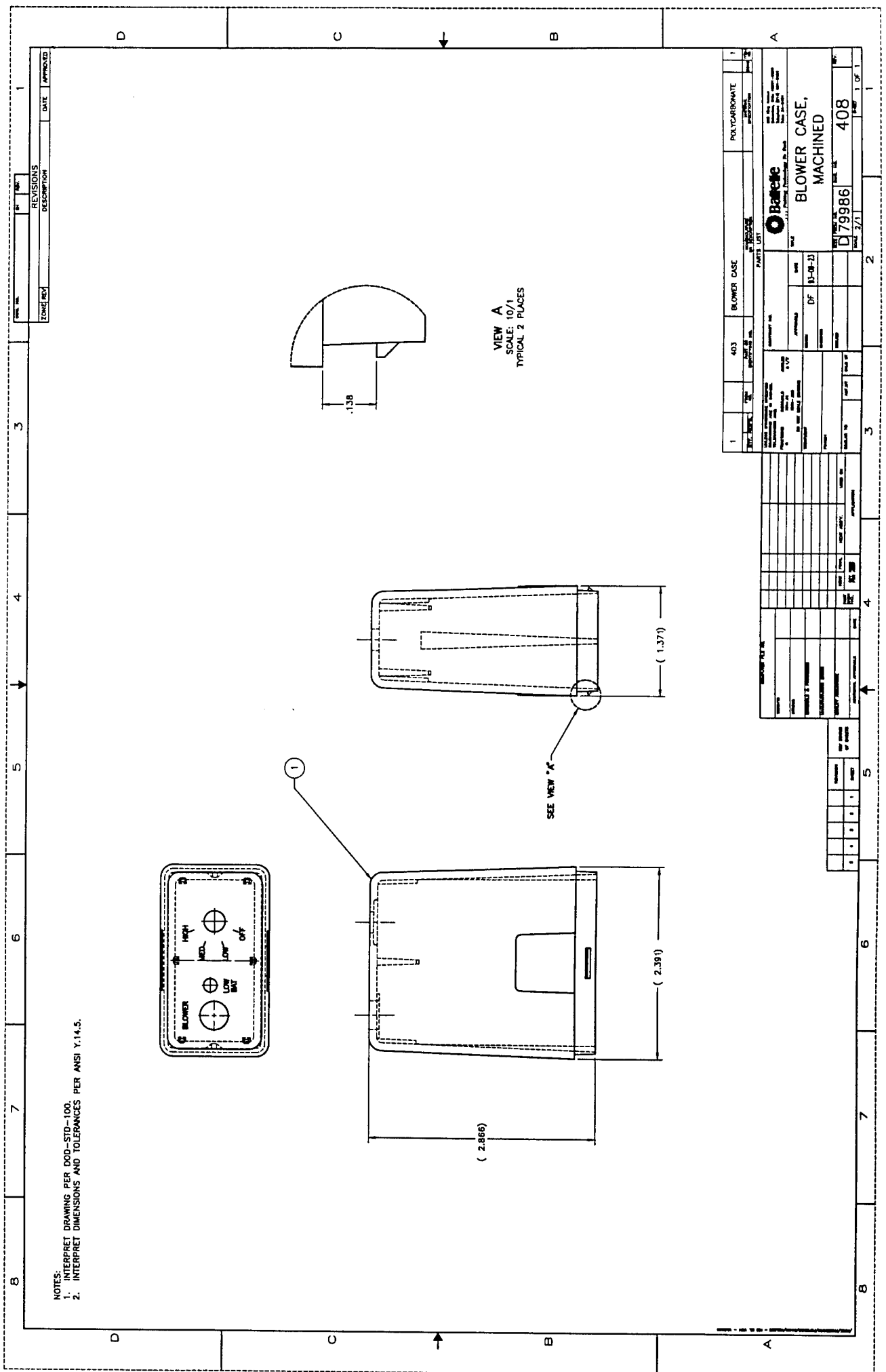
- SHARP TO R .010 ALL  
AROUND PERIMETER  
OF THIS EDGE

		PART NO.		NAME		ITEM NO.	
		PRINT OR IDENTIFICATION NO.		MANUFACTURER'S OR DESCRIPTION		SPECIFICATION	
		406		Batterie COVER PLATE		POLYCARBONATE	
CITY, STATE		PCU, IDENTIFICATION NO.		MANUFACTURER'S OR DESCRIPTION		ITEM NO.	
UNLESS OTHERWISE SPECIFIED, ALL DIMENSIONS ARE IN INCHES.		CONTRACT NO.		DATE		REV.	
FRACTIONS OF AN INCHES ARE TO BE DIVIDED BY 16.		DIMENSIONAL TOLERANCES		53-09-29		1	
DO NOT SCALE DRAWING		DRAWN		DF		1	
TREATMENT		CHECKED		C 75986		406	
FINISH		TESTED		C 75986		1	
SIMILAR TO		ACT W/ CHG		C 75986		1	
		SCALE 2:1		C 75986		1	
		SCALE 1:1		C 75986		1	
		SCALE 1:2		C 75986		1	
		SCALE 1:4		C 75986		1	
		SCALE 1:8		C 75986		1	
		SCALE 1:16		C 75986		1	
		SCALE 1:32		C 75986		1	
		SCALE 1:64		C 75986		1	
		SCALE 1:128		C 75986		1	
		SCALE 1:256		C 75986		1	
		SCALE 1:512		C 75986		1	
		SCALE 1:1024		C 75986		1	
		SCALE 1:2048		C 75986		1	
		SCALE 1:4096		C 75986		1	
		SCALE 1:8192		C 75986		1	
		SCALE 1:16384		C 75986		1	
		SCALE 1:32768		C 75986		1	
		SCALE 1:65536		C 75986		1	
		SCALE 1:131072		C 75986		1	
		SCALE 1:262144		C 75986		1	
		SCALE 1:524288		C 75986		1	
		SCALE 1:1048576		C 75986		1	
		SCALE 1:2097152		C 75986		1	
		SCALE 1:4194304		C 75986		1	
		SCALE 1:8388608		C 75986		1	
		SCALE 1:16777216		C 75986		1	
		SCALE 1:33554432		C 75986		1	
		SCALE 1:67108864		C 75986		1	
		SCALE 1:134217728		C 75986		1	
		SCALE 1:268435456		C 75986		1	
		SCALE 1:536870912		C 75986		1	
		SCALE 1:1073741824		C 75986		1	
		SCALE 1:2147483648		C 75986		1	
		SCALE 1:4294967296		C 75986		1	
		SCALE 1:8589934592		C 75986		1	
		SCALE 1:17179869184		C 75986		1	
		SCALE 1:34359738368		C 75986		1	
		SCALE 1:68719476736		C 75986		1	
		SCALE 1:137438953472		C 75986		1	
		SCALE 1:274877906944		C 75986		1	
		SCALE 1:549755813888		C 75986		1	
		SCALE 1:1099511627776		C 75986		1	
		SCALE 1:2199023255552		C 75986		1	
		SCALE 1:4398046511104		C 75986		1	
		SCALE 1:8796093022208		C 75986		1	
		SCALE 1:17592186044416		C 75986		1	
		SCALE 1:35184372088832		C 75986		1	
		SCALE 1:70368744177664		C 75986		1	
		SCALE 1:14073748835532		C 75986		1	
		SCALE 1:28147497671064		C 75986		1	
		SCALE 1:56294995342128		C 75986		1	
		SCALE 1:112589990684256		C 75986		1	
		SCALE 1:225179981368512		C 75986		1	
		SCALE 1:450359962737024		C 75986		1	
		SCALE 1:900719925474048		C 75986		1	
		SCALE 1:1801439850948096		C 75986		1	
		SCALE 1:3602879701896192		C 75986		1	
		SCALE 1:7205759403792384		C 75986		1	
		SCALE 1:14411518807584768		C 75986		1	
		SCALE 1:28823037615169536		C 75986		1	
		SCALE 1:57646075230339072		C 75986		1	
		SCALE 1:115292150460678144		C 75986		1	
		SCALE 1:230584300921356288		C 75986		1	
		SCALE 1:461168601842712576		C 75986		1	
		SCALE 1:922337203685425152		C 75986		1	
		SCALE 1:1844674407370850304		C 75986		1	
		SCALE 1:3689348814741700608		C 75986		1	
		SCALE 1:7378697629483401216		C 75986		1	
		SCALE 1:14757395258966802432		C 75986		1	
		SCALE 1:29514790517933604864		C 75986		1	
		SCALE 1:59029581035867209728		C 75986		1	
		SCALE 1:11805916207173441944		C 75986		1	
		SCALE 1:23611832414346883888		C 75986		1	
		SCALE 1:47223664828693767776		C 75986		1	
		SCALE 1:94447329657387535552		C 75986		1	
		SCALE 1:18889465931477507104		C 75986		1	
		SCALE 1:37778931862955014208		C 75986		1	
		SCALE 1:75557863725910028416		C 75986		1	
		SCALE 1:15111572745820056832		C 75986		1	
		SCALE 1:30223145491640113664		C 75986		1	
		SCALE 1:60446290983280227328		C 75986		1	
		SCALE 1:12089258196656045456		C 75986		1	
		SCALE 1:24178516393312090912		C 75986		1	
		SCALE 1:48357032786624181824		C 75986		1	
		SCALE 1:96714065573248363648		C 75986		1	
		SCALE 1:193428131146496727296		C 75986		1	
		SCALE 1:386856262292993454592		C 75986		1	
		SCALE 1:773712524585986909184		C 75986		1	
		SCALE 1:1547425049171973818368		C 75986		1	
		SCALE 1:3094850098343947636736		C 75986		1	
		SCALE 1:6189700196687895273472		C 75986		1	
		SCALE 1:12379400393375790546944		C 75986		1	
		SCALE 1:24758800786751581093888		C 75986		1	
		SCALE 1:49517601573503162187776		C 75986		1	
		SCALE 1:99035203147006324375552		C 75986		1	
		SCALE 1:19807040629401264875112		C 75986		1	
		SCALE 1:39614081258802529750224		C 75986		1	
		SCALE 1:79228162517605059500448		C 75986		1	
		SCALE 1:15845632535201011900896		C 75986		1	
		SCALE 1:31691265070402023801792		C 75986		1	
		SCALE 1:63382530140804047603584		C 75986		1	
		SCALE 1:126765060281608093207168		C 75986		1	
		SCALE 1:253530120563216186414336		C 75986		1	
		SCALE 1:507060241126432372828672		C 75986		1	
		SCALE 1:101412048245286674565744		C 75986		1	
		SCALE 1:202824096490573349131488		C 75986		1	
		SCALE 1:405648192981146698262976		C 75986		1	
		SCALE 1:811296385962293396525952		C 75986		1	
		SCALE 1:162259277192458679051904		C 75986		1	
		SCALE 1:324518554384917358103808		C 75986		1	
		SCALE 1:649037108769834716207616		C 75986		1	
		SCALE 1:1298074217539669432415232		C 75986		1	
		SCALE 1:2596148435079338864830464		C 75986		1	
		SCALE 1:5192296870158677729660928		C 75986		1	
		SCALE 1:10384593740317355459321856		C 75986		1	
		SCALE 1:20769187480634710918643712		C 75986		1	
		SCALE 1:41538374961269421837287424		C 75986		1	
		SCALE 1:83076749922538843674574848		C 75986		1	
		SCALE 1:16615349984577768749014968		C 75986		1	
		SCALE 1:33230699969155537498029936		C 75986		1	
		SCALE 1:66461399938311074996059872		C 75986		1	
		SCALE 1:13292279966662214992019768		C 75986		1	
		SCALE 1:26584559933324429984039536		C 75986		1	
		SCALE 1:53169119866648859968079072		C 75986		1	
		SCALE 1:10633823973339771936018544		C 75986		1	
		SCALE 1:21267647946679543872037088		C 75986		1	
		SCALE 1:42535295893359087744074176		C 75986		1	
		SCALE 1:85070591786718175488148352		C 75986		1	
		SCALE 1:17014118357343635097629664		C 75986		1	
		SCALE 1:34028236714687270195259328		C 75986		1	
		SCALE 1:68056473429374540390518656		C 75986		1	
		SCALE 1:13611294685858988079103712		C 75986		1	
		SCALE 1:27222589371717976158207424		C 75986		1	
		SCALE 1:54445178743435952316414848		C 75986		1	
		SCALE 1:10889037748687970463289696		C 75986		1	
		SCALE 1:21778075497375940926579392		C 75986		1	
		SCALE 1:43556150994751881853158784		C 75986		1	
		SCALE 1:87112301989503763706317568		C 75986		1	
		SCALE 1:17422460397850752741265136		C 75986		1	
		SCALE 1:34844920795701505482530272		C 75986		1	
		SCALE 1:69689841591403010965060544		C 75986		1	
		SCALE 1:13937968318280602193012108		C 75986		1	
		SCALE 1:27875936636561204386024216		C 75986		1	
		SCALE 1:55751873273122408772048432		C 75986		1	
		SCALE 1:11150374654624417544096864		C 75986		1	
		SCALE 1:22300749309248835088193728		C 75986		1	
		SCALE 1:44601498618497670176387456		C 75986		1	
		SCALE 1:89202997236995340352774912		C 75986		1	
		SCALE 1:17840599447398668070554924		C 75986		1	
		SCALE 1:35681198894797336141109848		C 75986		1	
		SCALE 1:71362397789594672282219696		C 75986		1	
		SCALE 1:14272479557918934456443936		C 75986		1	
		SCALE 1:28544959115837868912887872		C 75986		1	
		SCALE 1:57089918231675737825775744		C 75986		1	
		SCALE 1:11417983646351547565151548		C 75986		1	
		SCALE 1:22835967292703095130303096		C 75986		1	
		SCALE 1:45671934585406190260606192		C 75986		1	
		SCALE 1:91343869170812380521212384		C 75986		1	
		SCALE 1:18268773834162676104242672		C 75986		1	
		SCALE 1:36537547668325352208485344		C 75986		1	
		SCALE 1:73075095336650704416965688		C 75986		1	
		SCALE 1:14615019067330140883331376		C 75986		1	
		SCALE 1:29230038134660281766662752		C 75986		1	
		SCALE 1:58460076269320563533325504		C 75986		1	
		SCALE 1:11692015258640126706651008		C 75986		1	
		SCALE 1:23384030517280253403302016		C 75986		1	
		SCALE 1:46768061034560506806604032		C 75986		1	
		SCALE 1:93536122069121013613208064		C 75986		1	
		SCALE 1:18707224413824202722616128		C 75986		1	
		SCALE 1:37414448827648405445232256		C 75986		1	
		SCALE 1:74828897655296810890464512		C 75986		1	
		SCALE 1:14965779531059362178092904		C 75986		1	
		SCALE 1:29931559062118724356185808		C 75986		1	
		SCALE 1:59863118124237448712371616		C 75986		1	
		SCALE 1:11972623624847489542473324		C 75986		1	
		SCALE 1:23945247249694979084946648		C 75986		1	
		SCALE 1:47890494499389958169893296					

COMPUTER FILE NO.	UNLESS OTHERWISE SPECIFIED DATA SHEETS ARE IN INCHES AND FRACTIONAL INCHES ARE IN THOUSANDS OF AN INCH		
WEIGHTS	PRINTED ON ONE SIDE OF PAPER ONLY		
THICKS	DO NOT DRAW TO SCALE		
MATERIALS & PROCESSES	DRAWINGS ARE NOT DRAWN TO SCALE		
MANUFACTURING DATA	DRAWINGS ARE NOT DRAWN TO SCALE		
QUALITY ASSURANCE	DRAWINGS ARE NOT DRAWN TO SCALE		

1





NOTES:  
1. INTERPRET DRAWING PER DOD-STD-100.  
2. INTERPRET DIMENSIONS AND TOLERANCES PER ANSI Y.14.5.

**NOTES:**

1

6

1

DWQ NO.

2

4

REVISIONS		DESCRIPTION	DATE	APPROVED
ZONE	REV			

1  
2  
3  
4

A

A blank rectangular frame with rounded corners, resembling a page border.

A

A technical drawing of a rectangular component. The total width is labeled as 2.391. The total height is labeled as .355. A central slot has a width of .95. A side gap of .50 is indicated from the center of the slot to the right edge. The drawing uses solid lines for main features and dashed lines for internal boundaries.

R .031)

SECTION A-A

1	404	PART OR IDENTIFYING NO.	BLOWER CASE CAP	DESCRIPTION	POLYCARBONATE	1	ITEM NO.
UNLESS OTHERWISE SPECIFIED DIMENSIONS ARE IN INCHES FRACTIONAL DECIMALS ANGLES DO NOT SCALE DRAWING TOLERANCE	CONTRACT NO.	DATE APPROVED	APPROVALS	DATE	TITLE	REV.	
	X-51	DF	03-09-21	C	REV. NO.	409	SHEET 1 OF 1
	9/12			9986			
PRINTED	RELEASER TO	ACT W	DATE	SCALE 2/1			

1

2

3

4

1

ZONE/REV.	DESCRIPTION	DATE	APPROVED
		11-11-70	14-07-78
B-1-A	ADDED 2X .050 DIMENSION		
B-1-A	ADDED CENTER LINE "...." NOTE		
B-1-A	ADDED .005 DIMENSION		
B-1-A	ADDED .005 DIMENSION		
C-7	ADDED HOLE TO HOLE "...." NOTE		
C-8	ADDED LOW BAT MARKING		
C-8	ADDED BAT 6		

NOTES:  
1. INTERRUPTED DRAWING PER DOD-STD-100.  
2. INTERIOR DIMENSIONS AND TOLERANCES PER ANSI Y14.5.  
3. DRAFT ANGLE TO BE 1° UNLESS OTHERWISE SPECIFIED.  
4. INSIDE FILLETS TO BE R 0.12 UNLESS OTHERWISE SPECIFIED.  
5. WALL THICKNESS TO BE 0.12 UNLESS OTHERWISE SPECIFIED.  
6. ALL OUTSIDE SURFACES EXCEPT THE TOP FACE WHICH DISCHARGE MAY BE NATURALLY TEXTURED BY THE ELECTRO-DISCHARGE MACHINING PROCESS.

- 5. WALL THICKNESS TO BE .100 UNLESS OTHERWISE SPECIFIED.
- 6. ALL OUTSIDE SURFACES EXCEPT THE TOP FACE (WHICH CONTAINS THE LETTERING MARKINGS) TO BE NATURALLY TEXTURED BY THE ELECTRO-DISCHARGE MACHINING (EDM) PROCESS.

THUMB PAD STARTS AT TOP  
CORNER AND DRAFTS UP AT 0

- POSITION MARKINGS AS SHOWN. REFER TO VIEW "B" FOR LETTER SPECIFICATIONS

1.000.  
HOLE TO HOLE DIMENSION  
CENTRE LINE OF PART

The technical drawing shows a rectangular part with a central vertical slot. The top edge has a height of .375 inches, divided by a center line into two 2x .1875 sections. The bottom edge has a height of .260 inches, divided by a center line into two 2x .130 sections. A horizontal dimension of .250 is shown across the top of the slot. On the left side, there are two vertical slots, each labeled with a depth of (.100). The overall width of the part is .866 inches. A note on the right side reads "SEE VIEW B".

VIEW D  
SCALE: 4' /  
TYPICAL 2 PLACES

SECTION C-C

A technical drawing showing a cross-section of a stepped bearing shoulder. The shoulder has a total height of .5. The top surface is inclined at 45.0 degrees. The bottom surface has a thickness of .103.

VIEW A  
SCALE: 4'  
TYPICAL 2 PLACES

POSITION MARKINGS TO BE AS SHOWN  
WITH .060 HIGH LETTERS AND .015  
DEEP. NOTE ORIENTATION OF FLATS  
IN THE HOLE TO MARKINGS.

A technical drawing of a cylindrical component. It features a shoulder at the top with a height of .050. A slot is cut into the side of the cylinder, extending from the shoulder down to a diameter of .700. The bottom of the cylinder has a diameter of 2X .070. The overall height of the part is 2.07.

SEE VIEW 1

SCALE: 4/1  
TYPICAL 2 PLACES

.694 →

2X .340

2X .585

SECTION E-E

8  
7  
6  
5  
4  
3  
2  
1  
0

NOTES:  
1. INTERPRET DRAWING PER DOD-STD-100.  
2. INTERPRET DIMENSIONS AND TOLERANCES PER ANSI Y14.5.  
3. DRAFT ANGLE TO BE 2° UNLESS OTHERWISE SPECIFIED.

1

2

3

4

□

5

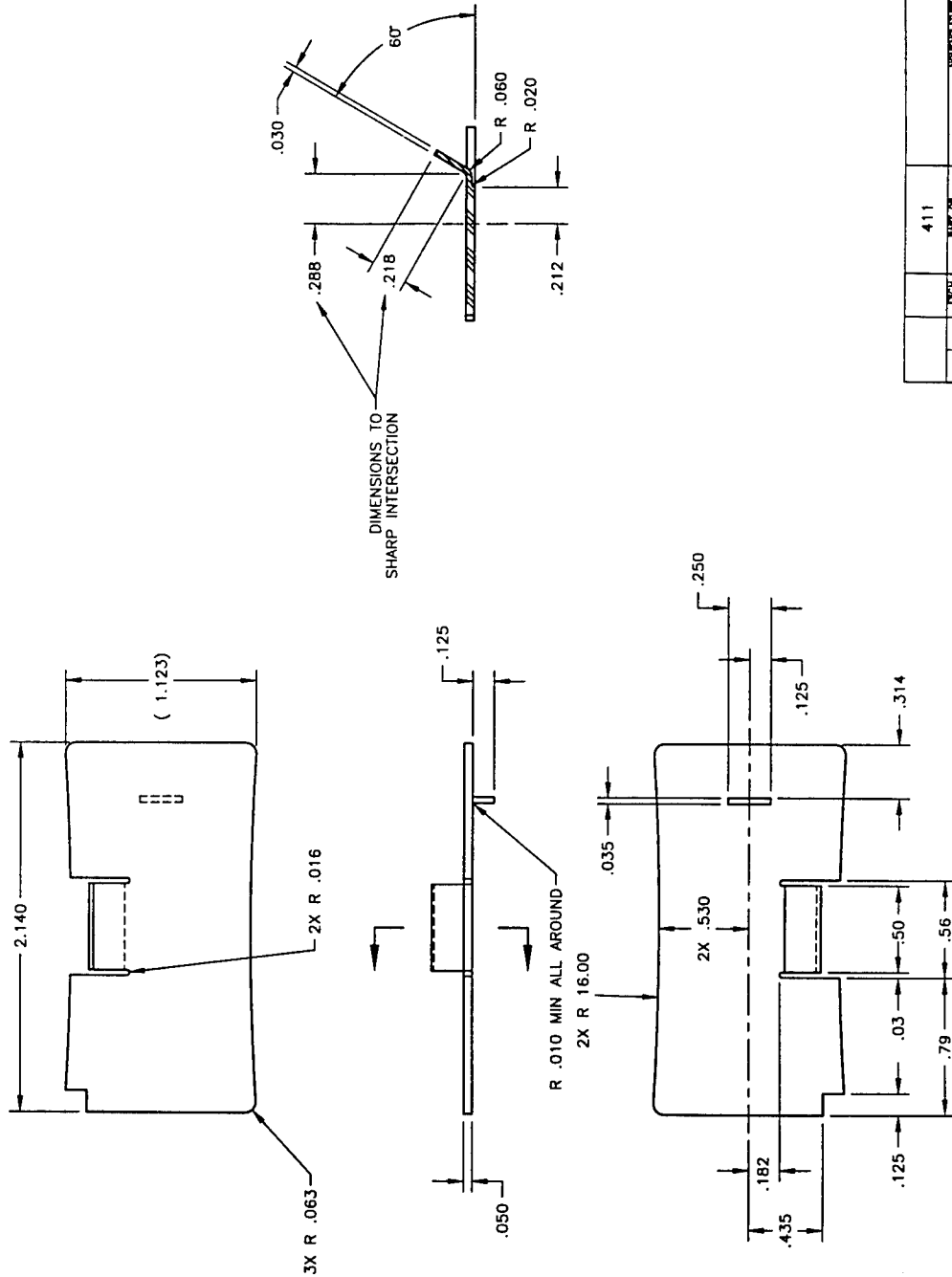
1

DVD

2

1

6



NOTES

**NOTES:**

1. INTERPRET DRAWING PER DOD-STD-100.
2. INTERPRET DIMENSIONS AND TOLERANCES PER ANSI Y14.5.

**VIEW A**  
SCALE:  $4\frac{1}{2}$   
TYPICAL 2 PLACES

**SECTION B-B**

**SECTION C-C**

**VIEW D**

**APPENDIX**

PART LIST		MATERIAL		QUANTITY	
1	412	1	POLYCARBONATE	1	1
2	SEE VIEW A	2	ALUMINUM	1	1
3	SEE VIEW B	1	STAINLESS STEEL	1	1
4	SEE VIEW C	1	STAINLESS STEEL	1	1
5	SEE VIEW D	1	STAINLESS STEEL	1	1

**COMMUNICATION CASE, MACHINING**

PART LIST		MATERIAL		QUANTITY	
1	412	1	POLYCARBONATE	1	1
2	79986	1	ALUMINUM	1	1
3	79986	1	STAINLESS STEEL	1	1
4	79986	1	STAINLESS STEEL	1	1
5	79986	1	STAINLESS STEEL	1	1

NOTES:  
1. INTERPRET DRAWING PER DOD-STD-100.  
2. INTERPRET DIMENSIONS AND TOLERANCES PER ANSI Y.14.5.  
3. REMOVE ALL BURRS AND SHARP EDGES.

□

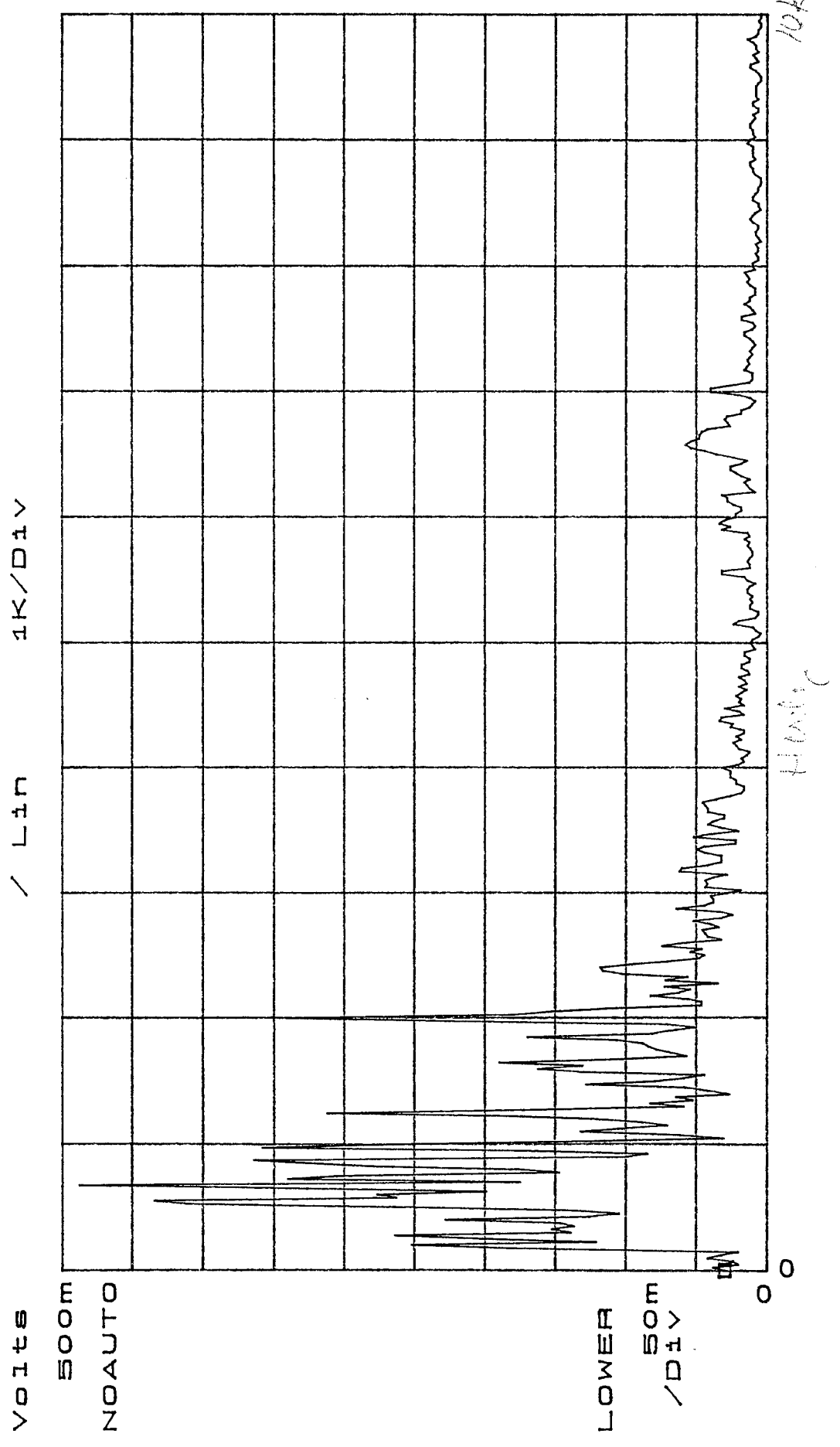
۳

1

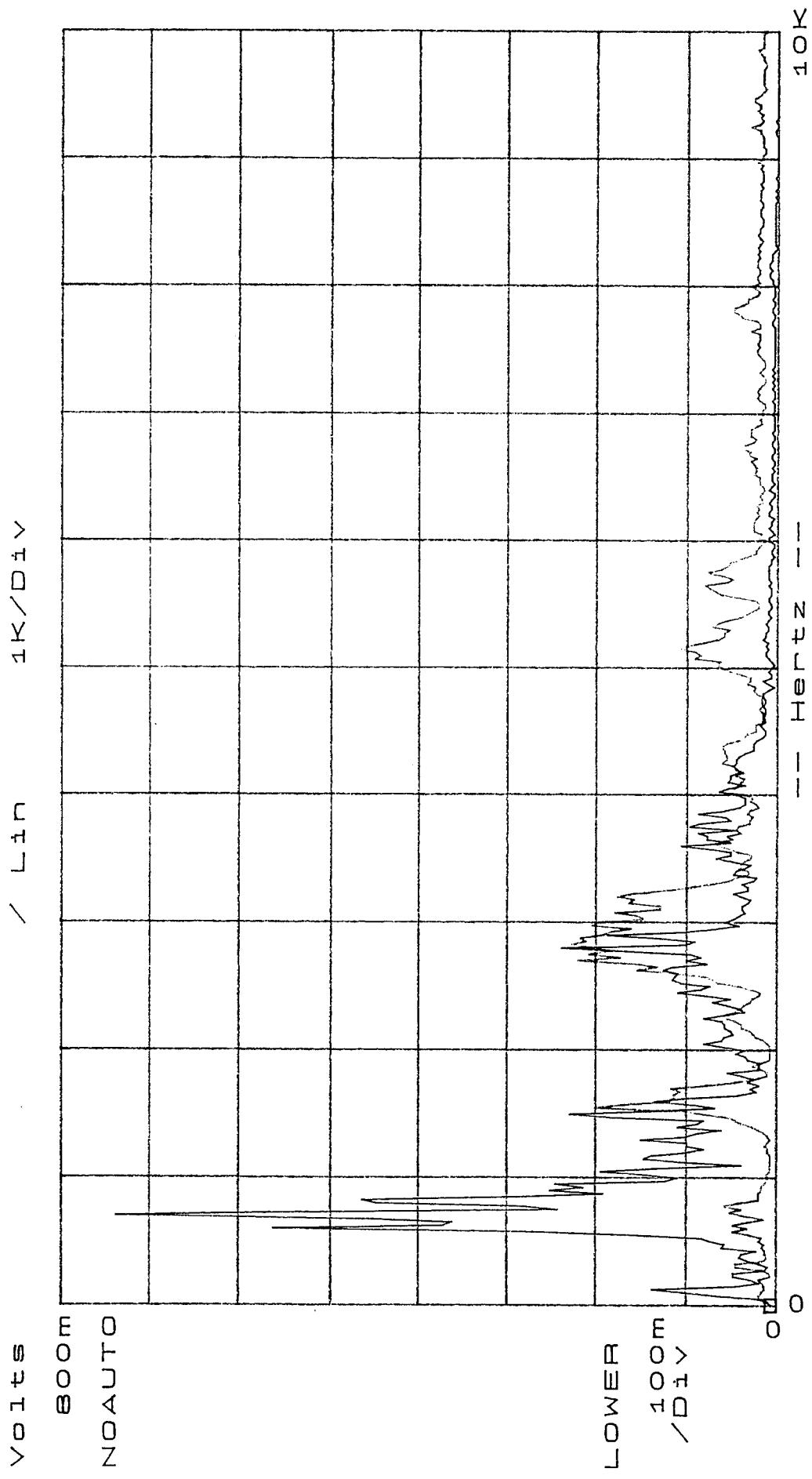
1

-

4

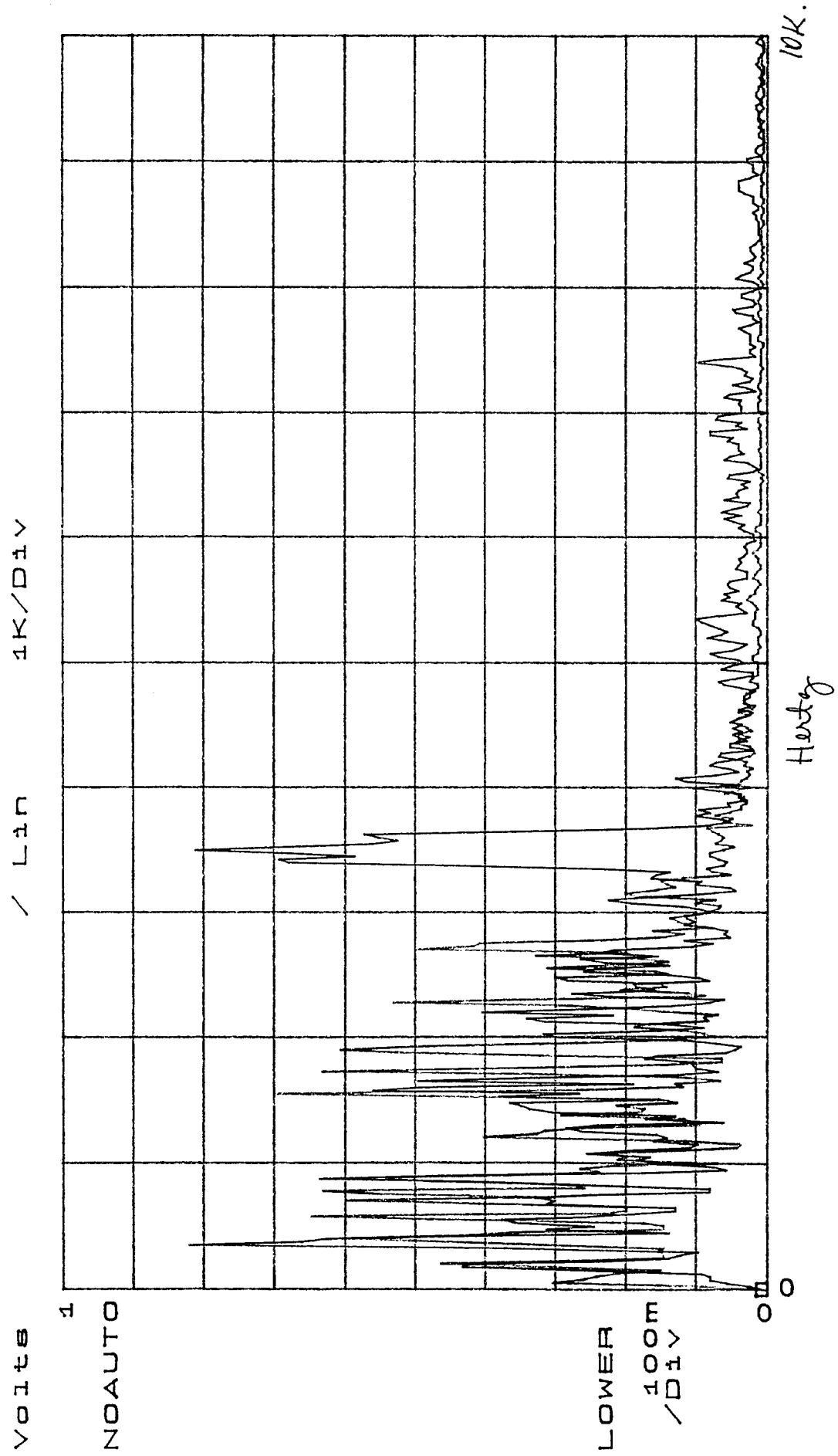


Spillman, John Andrew, 1870-1940. *John Andrew Spillman*. 1900.



St. Louis, Mo., Blank,  
House made of stone & wood.  
L. no 20

W. H. D. 1900



Block: Voice vowel-s.  
 Ro: Voice fulbnd.

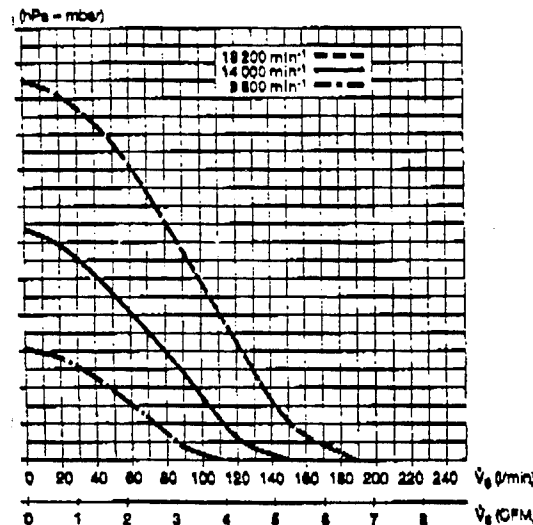
All from C. H. W. H. 1964  
 Fig. 10

2 of 2

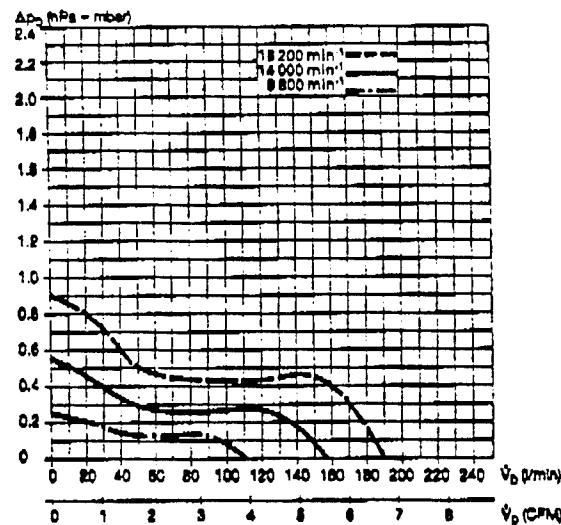
**Technical data**

nominal voltage  
 nominal current max.  
 nominal power input  
 oil current  
 speed typically  
 flow rate SUCTION  
 flow rate PRESSURE  
 static pressure difference, SUCTION  
 static pressure difference, PRESSURE  
 expected life  
 acoustic emission level S/D  
 ambient temperature range  
 slight  
 strings

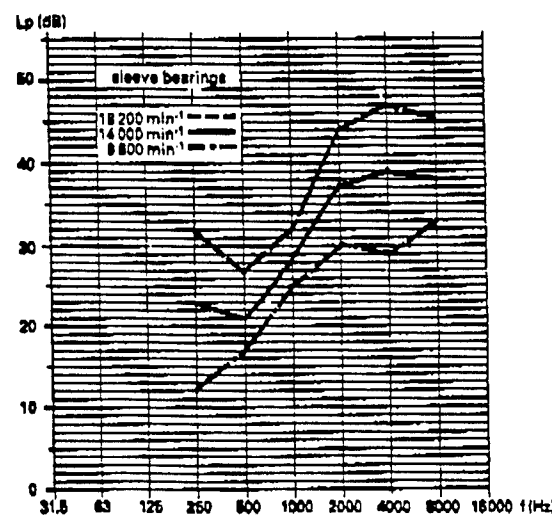
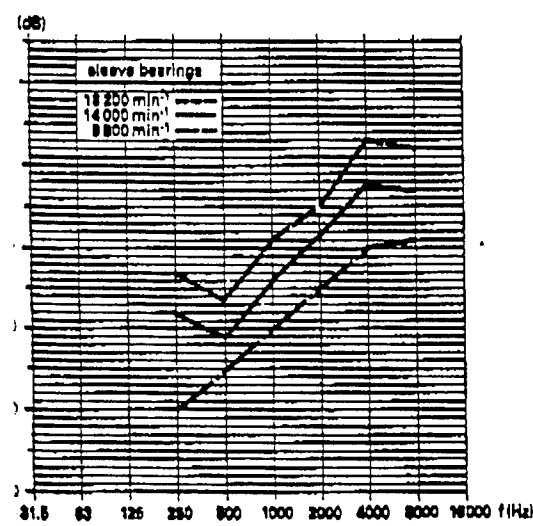
$U_N$	12	24	V
$I_N$	70	35	mA
$P_N$	0.84	0.84	W
$I_H$	740	370	mA
$n$	14 000	14 000	$\text{min}^{-1}$
$\dot{V}_S$	150	150	$\text{l/min}$
$\dot{V}_D$	155	155	$\text{l/min}$
$\Delta p_S$	125	125	Pa
$\Delta p_D$	55	55	Pa
$t$	3000	3000	h 15,000
LpA	41/45	41/45	dB(A)
T	-20 ... +65		°C
m	35		g
Sleeve bearings			

**Inflow performance graphs**

V301-V304



V305-V309

**Acoustic emission graphs**

## Technical data

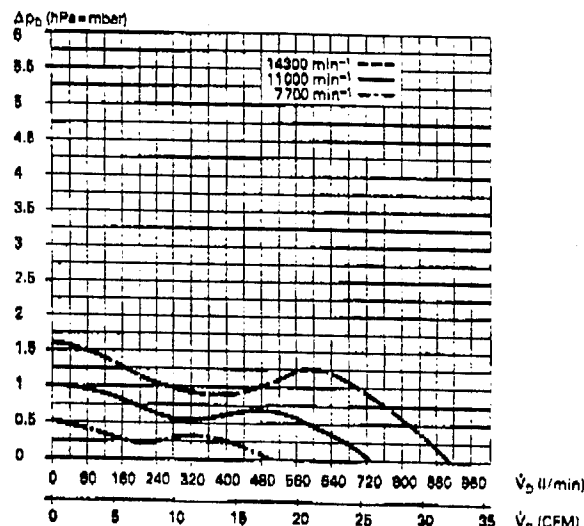
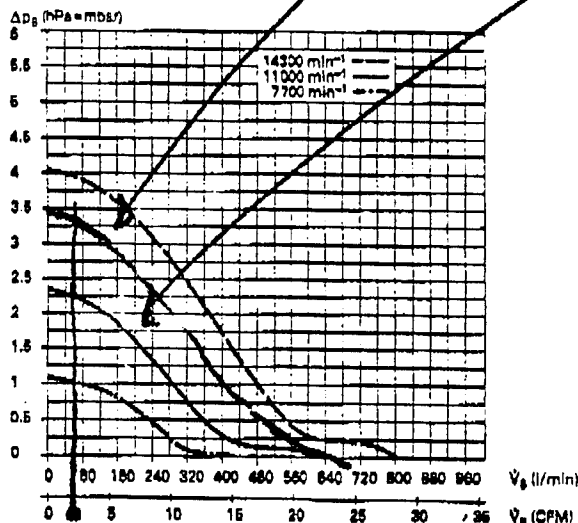
Nominal voltage  
 Nominal current max.  
 Nominal power input  
 Stall current  
 Speed typically  
 Flow rate SUCTION  
 Flow rate PRESSURE  
 Static pressure difference, SUCTION  
 Static pressure difference, PRESSURE  
 Expected life  
 Acoustic emission level S/D  
 Ambient temperature range  
 Weight  
 Bearings

$U_N$	12	24	V
$I_N$	330	150	mA
$P_N$	3.96	3.60	W
$I_{stall}$	7.70	3	A
n	11 000	11 000	$\text{min}^{-1}$
$\dot{V}_s$	610	610	l/min
$\dot{V}_p$	720	720	l/min
$\Delta p_s$	225	225	Pa
$\Delta p_p$	100	100	Pa
t	15 000	15 000	h
LpA	55/58	55/58	dB(A)
T	-20 ... +65		$^{\circ}\text{C}$
m	180		g
	Ball bearings		

V4614-6 C6J

V4614-6J. C4.8J

## Airflow performance graphs



## Acoustic emission graphs

